TÉCNICO LISBOA

Single-cell quantification of the abundance of plasma membrane MDR transporter Tpo3 from fluorescence imaging in *Saccharomyces cerevisiae*

Lara Cardoso Pereira Batista da Costa

Thesis to obtain the Master of Science Degree in

Biological Engineering

Supervisors: Professor João Miguel Raposo Sanches
Professor Doctor Isabel Maria de Sá-Correia Leite de Almeida

Examination Committee

Chairperson: Professor Gabriel António Amaro Monteiro
Supervisors: Professor João Miguel Raposo Sanches
Member of Committee: Doctor Joana Filipa Fernandes Guerreiro

November 2016

“In order to succeed, your desire for success should be greater than your fear of failure.”

Albert Einstein

Acknowledgments

First and foremost, I would like to thank my supervisors Profs. João Miguel Sanches and Isabel Sá-Correia, for the opportunity of joining this project, and for all the guidance, motivation and support given to me throughout the entire development of this thesis.

I would further like to thank Joana Guerreiro for the valuable biological data that served as starting point and basis for the project and for the availability to clarify doubts during this project.

Additionally, I would like to thank Tânia Mestre for the help regarding the profiling algorithm and its respective code.

A special thank you to my mother for all the advices and support throughout all my life.

Finally, a special and sincere thank you to all those who support me in this journey.

Abstract

The experimental model and cell factory *Saccharomyces cerevisiae* was used in this study to better understand the mechanisms underlying adaptation and tolerance to acetic acid, a widely used food preservative and an important inhibitor in many industrial fermentation processes. Besides the adaptive responses to acetic acid stress in yeast, the transcriptional activation of the gene encoding the plasma membrane transporter involved in multidrug/multixenobiotic resistance (MDR/MXR) Tpo3 is in special focus in this thesis. This activation is mediated by the transcription factor Haa1, which contributes to reduce the intracellular concentration of acetate accumulated upon acetic acid exposure. The role of Hrk1 protein is also important in order to provide protection against acetic acid through the reduction of intracellular acetate concentration, Hrk1 protein was proposed to be a protein kinase that has been implicated in the activation of the plasma membrane H^+ -ATPase (Pma1) in response to glucose metabolism, belonging to a family of kinases dedicated to the regulation of plasma membrane transporters. The aim of this work is to perform a single-cell quantification of Tpo3 expression from fluorescence microscopy images. The abundance of Tpo3 protein at the plasma membrane of yeast cells is evaluated using a GFP-tagged version of this transporter inserted into yeast genome and expressed in the *wild-type* strain in an *HAA1* deletion mutant, in an *HRK1* deletion mutant in weak acid stressing conditions.

A processing pipeline was designed and the corresponding software application was implemented for this analysis where the green intensity in specific selected cells is quantified along the radial axis of the cells (from the center to the plasma membrane). The profile representing the spatial distribution of the protein in the intra-cellular space of each cell is obtained after normalizing and averaging the extracted profiles anchored at the centers for different orientations. This normalization procedure aims at dealing with the different sizes and eccentricities of the cells within the population.

The radial-based protein expression profile obtained with the proposed method is computed for several selected cells in four time points, 0, 1, 2 and 4 hours (during the latency period), for the parental, *haa1*△ cells and *hrk1*△ cells exposed to an inhibitory sub-lethal concentration of acetic acid (50 mM, at pH 4.0). The results obtained confirm the predicted plasma membrane localization of this transporter and evidence a steady increase in Tpo3 abundance in the plasma membrane in the presence of acetic acid when compared with the control condition, an activation that is strongly reduced when *HAA1* is deleted, as suggested before.

Keywords

Saccharomyces cerevisiae, adaptation and tolerance to acetic acid, plasma membrane transporter, fluorescence microscopy images, processing pipeline

Resumo

O modelo experimental e a fábrica celular *Saccharomyces cerevisiae* foi utilizado neste estudo para melhor compreender os mecanismos subjacentes à adaptação e tolerância ao ácido acético, um conservante de alimentos amplamente utilizado e um inibidor importante em muitos processos de fermentação industrial. Uma das respostas adaptativas ao stress ao ácido acético em levedura é a activação da transcrição do gene que codifica o transportador de membrana plasmática envolvido na resistência a multidrogas (MDR / MXR) Tpo3, que tem especial atenção nesta tese. Esta activação é mediada pelo factor de transcrição Haa1, o que contribui para reduzir a concentração intracelular de acetato por exposição acumulada ao ácido acético. O papel da proteína Hrk1 também é importante, porque confere protecção contra o ácido acético através da redução da concentração de acetato intracelular, a proteína Hrk1 é considerada uma proteína-cinase que está envolvida na activação da H + -ATPase (Pma1) em resposta ao metabolismo da glicose, que pertence a uma família de cinases específicas para a regulação de transportadores da membrana de plasmática. O objetivo deste trabalho é realizar uma quantificação de uma única célula de expressão Tpo3 a partir de imagens de microscopia de fluorescência. A abundância de proteína Tpo3 na membrana plasmática de células de levedura é avaliada por ligação da proteína GFP a este transportador e de seguida inserido no genoma da levedura e expresso na estirpe de tipo selvagem num mutante *HAA1* de eliminação e num mutante *HRK1* de eliminação em situação de stress com ácido acético.

Foi desenvolvido uma pipeline de processamento e a aplicação de software específico para esta análise, onde a intensidade da cor verde em células especificamente selecionadas é quantificada ao longo do eixo radial das células (a partir do centro para a membrana plasmática). O perfil que representa a distribuição espacial da proteína no espaço intracelular de cada célula é obtido após a normalização e a média dos perfis extraídos nos centros de orientações diferentes. Este procedimento de normalização visa lidar com os diferentes tamanhos e excentricidades das células dentro da população.

O perfil de expressão proteico é obtida com o método proposto e calculado para várias células selecionadas em quatro pontos temporais, 0, 1, 2 e 4 horas (durante o período de latência), para as células parentais, células *haa1*△ e células *hrk1*△ expostas a uma concentração inibitória sub-letal de ácido acético (50 mM, a pH 4,0). Os resultados obtidos confirmam a localização prevista para este transportador e evidencia um aumento constante de Tpo3 na membrana plasmática na presença de ácido acético, quando comparado com a condição de controle, esta ativação é fortemente reduzida quando *HAA1* é suprimido, como sugerido antes.

Palavras-Chave

Saccharomyces cerevisiae, adaptação e tolerância ao ácido acético, transportador da membrana plasmática, imagens de microscopia de fluorescência, pipeline de processamento

Contents

List of Tables

List of Figures

Abbreviations

ATP Adenosine triphosphate

ABC ATP – binding cassette

Aqr1p Aqr1 protein

Azr1p Azr1 protein

Aifp Aif protein

CWP Cell wall protein

CMI Cytoplasm Mean Intensity

DNA Deoxyribonucleic acid

Fps1p Fps1 protein

FM Fluorescence Microscopy

GPI Glycosylphosphatidylinositol

GAAC General amino-acid control

GUI Graphical User Interface

Haa1 p Haa1 protein

Hrk1 p Hrk1 protein

KanMX Kanamycin MX

MDR Multidrug resistance

MXR Multixenobiotic resistance

MFS Major Facilitator Superfamily

MMI Membrane Maximum Intensity

MW Mann-Whitney U test

MWW Mann-Whitney-Wilcoxon U test

Msn2p Msn2 protein

Msn4p Msn4 protein

OD Optical density

Pma1p Plasma membrane H^+- ATPase

PM Plasma membrane

pH_i intracellular pH

PCD Programmed cell death

Pdr12p Pdr12 protein

ROS Reactive oxygen species

Rim101p Rim101 protein

RD Radial profile

RDP Radial profile

RDM Radial map

S. Cerevisiae *Saccharomyces cerevisiae*

SGD *Saccharomyces* genome database

STD Standard deviation

Tpo2p Tpo2 protein

Tpo3p Tpo3 protein

TF Transcription factor

TOR Target-of-rapamycin

WT Wild-type

War1p War1 protein

YEASTRACT Yeast search for transcriptional regulators and consensus tracking

1

Introduction

1.1. Motivation

Weak acids are widely used in the food and chemical industries, in agriculture, and in medicine. Weak acids have a huge potential in many areas, in the food industry they are used to control microbial growth, while in the chemical industry these molecules can be used, as raw materials, for the synthesis of a wide range of products, like plastics, cosmetics and pharmaceuticals as well as, replacing petrochemicals that have a more negative environmental impact. It is crucial to understanding the mechanisms underlying the adaptive response and resistance to these weak acids in order to design more efficient weak acid-based food preservation strategies and more robust industrial yeast strains.

In this work we are studying the behave of *S. cerevisiae* in the presence and absence of acetic acid. This yeast has proven to be an invaluable model eukaryote to study the cytotoxic effects and the cellular responses to weak acids, this yeast is a powerful model system to increase our understanding of the effects and targets of drugs and of underlying resistance mechanisms on more complex organisms. [1], [2]. The aim of this study is analyse the role of the transcription factor Haa1 protein, and the role of *HRK1* gene in *TPO3* gene expression, all involved in *Saccharomyces Cerevisiae* resistance to acetic acid.

The acetic acid form change, in a growth medium with a pH equal or below its pKa the undissociated form of this acid prevails (RCOOH). This undissociated form of acetic acid enters the yeast cells by simple diffusion through the plasma membrane lipid bilayer and dissociates in the near-neutral cytosol leading to the accumulation of protons and acetate in the cell interior. This has some repercussions, the acid acetic induces the intracellular acidification leading to inhibition of cell metabolic activity, the dissipation of plasma membrane electrochemical gradient. The recovery of intracellular pH in stressed cells is achieved by the activity of plasma membrane H^+-ATPase (PM-H^+-ATPase) Pma1p, which couples ATP hydrolysis to proton expression, the expression of the plasma membrane multidrug resistance transporters of the major facilitator superfamily Tpo2 protein, Tpo3 protein, Aqr1 protein and Azr1 protein, that confers resistance to acetic acid and they are through to mediate the active expulsion of acetate. It is well known that *TPO2*, *TPO3* genes are transcriptionally activated in response to acetic acid under the dependence of the transcriptional activator Haa1 protein, which is crucial in acetic acid resistance. [3]

The expression of *HAA1* has a major impact on the alterations occurring in yeast genomic expression during the early adaptive response to acetic acid, the Haa1 protein is required for the transcriptional regulation of approximately 80% of the acid-responsive genes. The Haa1 protein -regulated genes could be separated into two classes, the first class includes 64 genes whose acetic acid-induced transcriptional activation was fully dependent on Haa1 protein, the second class includes 21 genes whose acetic acid-induced transcriptional activation was only partially dependent on Haa1 protein. The Haa1 protein -dependent genes encode proteins belonging to many classes such as “Transcription factors”, “Multidrug resistance transporters”, “Cell wall”, “Lipid metabolism”, “Regulation of carbohydrate metabolism”, “Protein folding”, “Carbohydrate metabolism”, “Amino acid metabolism”, “Nuclei acid processing”. It was demonstrated that the *HRK1* gene was also important in yeast

resistance against acetic acid, it is a protein kinase belonging to a family of kinases dedicated to the regulation of plasma membrane transporters in the

activation of the plasma membrane H^+-ATPase (Pma1p) in response to glucose metabolism, in order to reduce the intracellular acetate concentration. [2] [3]

In this work, the development of software to measure the amount of Tpo3 protein, is crucial to better understand the role of Haa1 protein and Hrk1 protein in Tpo3 membrane transporter in yeast stressed cells with acetic acid.

1.2. Thesis Outline

This dissertation is organized into five main chapters. Chapter 2 provides a literature survey on the mechanisms of adaptation and tolerance to acetic acid in yeast, with special focus on the species with biological and industrial interest in this work, *Saccharomyces cerevisiae*. In Chapter 3 the materials and methods used in this work are described, beginning with the image acquisition protocol, followed by the image processing pipeline and finally by the description of computational methods applied to obtain the radial profile images. In Chapter 4, the obtained results concerning the previously mentioned are displayed, regard to profiles and features extracted. A widespread discussion of the obtained results is performed. Finally, in Chapter 5 an overall conclusion of the developed work is done.

1.3. Original Contributions

This dissertation contribution begins with the characterization and quantification of Tpo3 protein in the wild-type strain and *haa1Δ* and *hrk1Δ* mutants strains, and its distribution at cellular level, namely at the cell membrane.

In addition, a Graphical User Interface was implemented in *Matlab* ® where a user can manually select relevant points of study in an image. This interface allows a specialist to select the representative cells of an image, excluding from the analysis all negative cells that worse the results. This GUI is useful in bioimaging.

Another original aspect of this work is the development of radial profiles, anchored in nuclei centers, to characterize protein distribution at intra-cellular level.

This work provides: a full description of the images processing; an analysis of the Tpo3 distribution within the cell and a statistical analysis of some selected features to perceive the quantitative differences between *WT* cell line and the mutant cell lines.

This work resulted in:

- A poster presentation with the title *Single-cell quantification of the expression of plasma membrane MDR transporter Tpo3 from fluorescence imaging*., 6th edition of the Conference on Physiology of Yeasts and Filamentous Fungi, Lisbon, July 2016.

2

Biological Background

2.1. Adaptation and tolerance to acetic acid in *Saccharomyces cerevisiae*

The following sections describe the role of the acetic acid as growth inhibitor as well as yeast acetic acid tolerance as cause of food spoilage.

2.1.1. Acetic acid as a growth inhibitor

Short-chain weak organic acids are potent inhibitors of microbial growth and are widely applied as preservatives in food and beverages. Acetic Acid has many applications to prevent growth of spoilage microbes, being used mainly in the preservation of acidic products such as soft drinks, pickles and sauces. At low pH, acetic acid occurs predominantly in the undissociated form, which has relatively high membrane permeability. After entry into the cell via passive diffusion, the higher pH of the cytosol causes dissociation of the acid, thus acidifying the cell ad triggering the ATP-dependent efflux of protons. Membrane disruption and enzyme inhibition have been proposed as possible mechanisms of anion toxicity. Furthermore, acetate has been implicated in the induction of apoptosis. This weak acid is also a by-product of *Saccharomyces cerevisiae* alcoholic fermentation. High concentrations of ethanol, acetic acid and other toxic metabolites of yeast metabolism may contribute to fermentation arrest and non-feedstock substrate in industrial biotechnology, high concentrations of acetic acid have been suggested to be a causative of incomplete fermentation, this acid can reduce the growth and fermentation activity of *Saccharomyces cerevisiae*, and incomplete ferments can contain a high concentration of acetic acid. [1] [3] [4] [5]

Acetic acid is also present in lignocellulosic hydrolysates, a highly interesting non-feedstock substrate in industrial technology, considered an important alternative for a sustainable production of bioethanol and other chemicals, it was demonstrated that acetic acid is one of the most important inhibitors present in lignocellulosic hydrolysates that are used as substrates in the production of second generation bioethanol. [6]

2.1.2. Acetic Acid Tolerance and Food Spoilage

Yeasts are a group of microorganisms with an enormous impact on food and beverage production. Scientific and technological understanding of their roles in this production began to emerge in the mid-1800s, starting with pioneering studies of Pasteur in France and Hansen in Denmark on the microbiology of beer and wine fermentations. There are two different approaches to describe and understand the role of yeasts in food and beverage production. One approach focus on the commodity and technology of its processing (e.g. wine production, fermentation of bakery products).

A second approach is to focus on the yeasts themselves, and their cellular and molecular responses to environmental influences, in this work we focus on both approaches.
On the positive side, there is increasing interest in using yeasts as novel probiotic and biocontrol agents, and for the nutrient fortification of food. On the negative side, food-associated yeasts could be an under-estimated source of infections and other adverse health responses in humans. [7], [8]

Yeast spoilage is very predictable, typically yeasts will grow and spoil in low-pH food, products with high sugar (e.g. more than 10% w/v) or high salt (more than 5% NaCl) content, and products preserved with weak organic acids (e.g. acetic, sorbic, benzoic) are prone to yeast spoilage. Some others products are also very susceptible to spoil such as: fruit, fruit juices, sugar and flavours syrups, confectionery products, alcoholic beverages, carbonated beverages, vegetable salads with acid dressings, salt- and acid-based sauces, fermented dairy products and fermented or cured (salted) meat products. A list of the most commonly found food spoilage yeasts is provided in **Table 2.1.1**. The metabolic activity of these organisms have a significant impact and develop several changes in the properties of food products. [7]

Table 2.1.1 – Examples of the most frequently isolated contaminating yeasts. Adapted from [7].

Contaminating yeasts	Products affected
Cryptococcus, Rhodotorula spp.	Frozen meat, poultry, seafood and products stored for lengthy periods
Thermosyntropha lipolytica	High-fat, low-water-activity commodities (e.g. margarine and butter)
Zygosaccharomyces rouxii	Very high sugar products
Debaryomyces hansenii	Salted meat products
Zygosaccharomyces bailii	Products preserved with weak organic acids

The yeast *Saccharomyces cerevisiae* has been exploited as an exceptional model organism to study adaptive responses to different stresses induced by chemical compounds. This yeast is a widely used eukaryotic model for molecular and cellular biology studies. This unicellular non-pathogenic microorganism is a robust and inexpensive experimental tool, simple to genetically manipulate, possesses a remarkable level of functional conservation with higher eukaryotes, and its genome has been extensively annotated with functional information. This yeast has been used to pioneer the development of several post-genomic experimental approaches and computational tools, allowing the easy implementation of genome-wide analyses and the availability of a wide range of experimental tools and biological material. The *Saccharomyces cerevisiae* has been at the forefront of post-genomic research, a web database resource is available, providing the ***S**accharomyces* **G**enome **D**atabase (SGD), the major community resource for gene, genomic and protein information in yeast and the web database, YEASTRACT (**Y**east **S**earch for **T**ranscriptional **R**egulators **and C**onsensus **T**racking), a

curated repository of regulatory associations between transcription factors (TF) and target genes. [9], [10]

Based on this, the mechanisms underlying adaptation and response to organic acids, in acetic acid in particular, have been much better characterized in S. Cerevisiae than other eukaryotics.

2.2. Molecular mechanisms of adaptation and tolerance to acetic acid – *Saccharomyces Cerevisiae*

The following sections describe the molecular mechanisms of adaptation and tolerance to acetic acid developed by *Saccharomyces Cerevisiae*.

2.2.1. Toxicity induced by acetic acid – Intracellular acidification

Acetic acid is an inhibitor of yeast growth. At the external pH below the acetic acid pK_a value (4.76), the lipophilic undissociated form of the acid (CH_3COOH) predominates and is able to permeate the plasma membrane by simple diffusion, it has been studied that acetic acid can also enter the cells by facilitated diffusion, mediated by the aquaglyceroporin Fps1p, a protein involved in the transport of glycerol. Once inside the cell, more specifically in the cytosol, the release of protons (H^+) and the acetate anion (CH_3COO^-) occurs. This process is schematically represented in **Figure 2.2.1**. These ions are not able to cross the hydrophobic lipid plasma membrane bilayer and accumulate in the cell interior, causing intracellular acidification. This accumulation leads to negative effects in the yeasts cells, like decreasing of the internal pH, destabilizing of the lipid organization, function of cellular membranes, increasing of oxidative stress and decreasing of the DNA and RNA synthesis rate, as well as inhibit metabolic activity. As a consequence of the inhibitory concentration of acetic acid, the cell population enters into a period of growth latency, named the lag phase. During this lag phase, the reduction of cell viability occurs. [1], [11].

Saccharomyces Cerevisiae developed some strategies to adapt and recover from acetic acid exposure, the mechanism and molecular responses are detailed in the following sections.

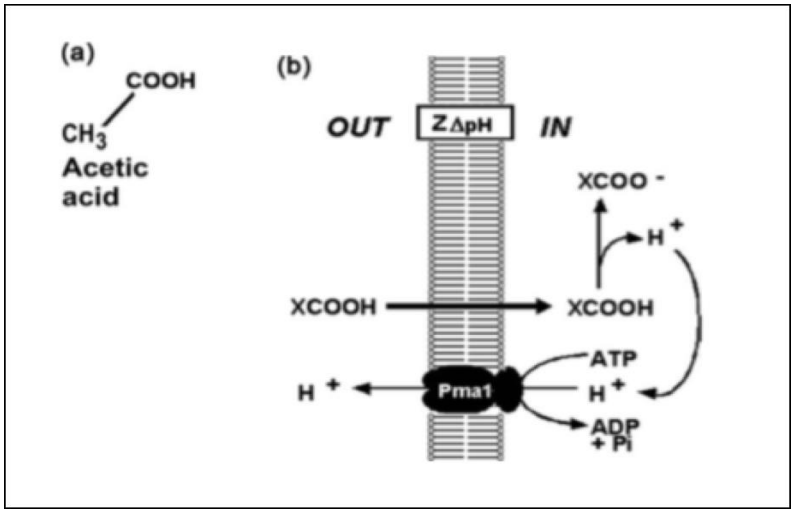

Figure 2.2.1 - (a) Scheme of the chemical structure of acetic acid (weak acid). The acetic acid has a pk_a value of 4.75. **(b)** The usual concept of how the weak acids act on cells. If the undissociated acid (XCOOH) is freely permeable to the membrane, its concentration inside and outside the cell will be governed by the pH on either side of the membrane and the dissociation constant of the acid. A higher pH in the cytosol will cause a substantial fraction of this acid to dissociate to the membrane-impermeant anion ($XCOO^-$), leading to intracellular accumulation of this anion. An electrochemical potential difference ($Z\Delta pH$) is maintained across the yeast plasma membrane, largely through a plasma membrane H+-ATPase (Pma1p)-catalysed proton extrusion. Adapted from *[11]*

2.2.2. Adaptive response leading to pH recovery

Saccharomyces cerevisiae has developed several molecular responses to adapt to stress caused by acetic acid, in order to maintain the internal pH within physiologic values, the cells increase the activity of the plasma membrane H^+-ATPase, Pma1p, which couples ATP hydrolysis to proton extrusion as represented in **Figure 2.2.2**. This protein can also be present in the vacuolar membrane (V-ATPase) and it is crucial for the internal pH homeostasis, in these particular conditions contributes to the recovery of cytosolic pH and counteract the acid-induced dissipation of the transmembrane potential across the vacuolar membrane. [1], [12]

It has been found that cytosolic pH and V-ATPase are both under the influence of glucose or other fermentable carbon sources, and it was found that the regulation of cytosolic pH is mediated by energy metabolism, the inactivation of pyruvate kinase, which is responsible for a large part of the ATP production of yeast in glucose media, is sufficient to reduce cytosolic pH. Moreover, K^+ ions play a crucial role in cytosolic pH regulation. Sensitive to changes in membrane potential, Pma1p responds with an increment in the proton pumping to the exterior of the cell, which is observed as an additional cytosolic alkalinisation after potassium uptake by yeast cells. In addition, K^+ ions are also involved in stimulation of energetic metabolism of yeast cells, favouring the bicarbonate ion concentration in the cytosol and, therefore, Pma1p activity. [1], [13]

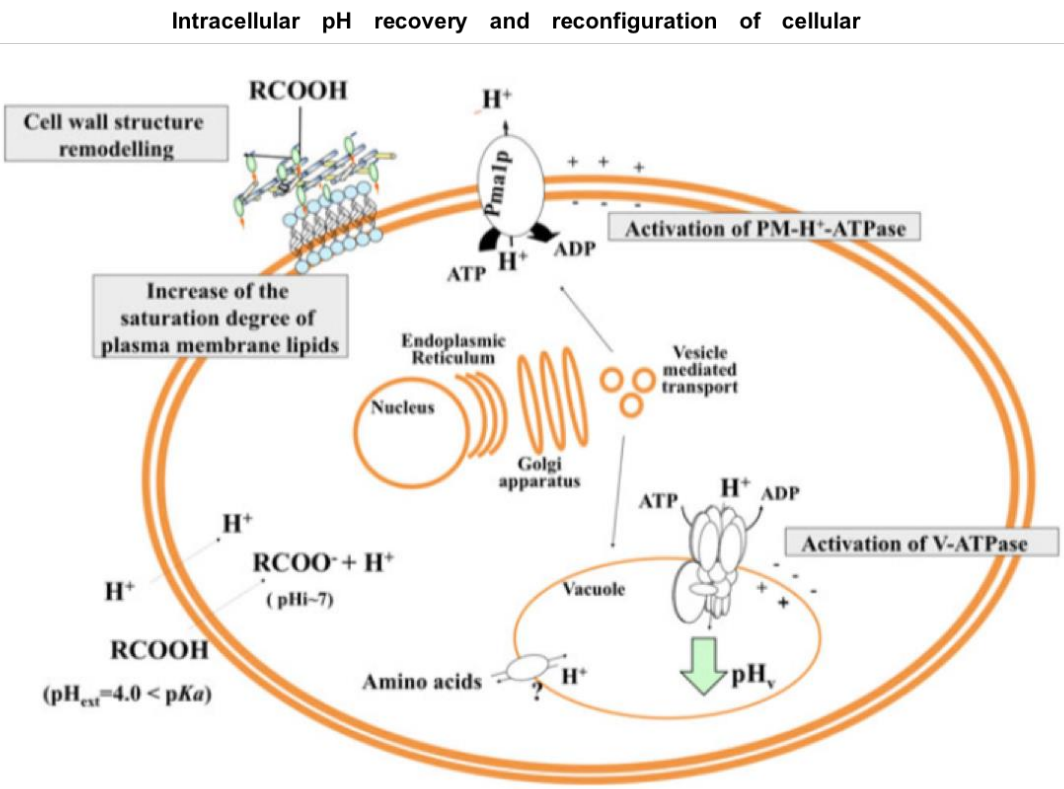

Figure 2.2.2 – Schematic model for the adaptive response of Saccharomyces cerevisiae to acetic acid-induced stress. Stimulation of the activity of H^+-ATPase present in the plasma and vacuolar membranes contributes to the recovery of internal pH to normal values for cell. The reconfiguration of cell wall structure and plasma membrane lipid composition may reduce the diffusion rate of undissociated weak acid and reduce weak acid-induced plasma membrane damage. Extracted from *[1]*.

2.2.3. Response to intracellular accumulation of acetic acid counter-ion – Multidrug resistance transporters

During the acetic acid dissociation, the acetate anion (CH_3COO^-) accumulates in the yeast cytosol, this accumulation in the cell interior may lead to an increase in turgor pressor, oxidative stress, protein aggregation, lipid peroxidation, inhibition of membrane trafficking, and perturbation of plasma and vacuolar membranes spatial organization. To counteract this phenomenon, *Saccharomyces cerevisiae* use specific membrane transporters, which are able to remove the acetate from the intracellular medium. The transporters involved in this process belong to two big families, the ATP-binding cassette (ABC) Superfamily or to the Major Facilitator Superfamily (MFS), which are involved in Multidrug Resistance (MDR) in yeasts.

The expression of the genes *AQR1*, *TPO2*, *TPO3* are strongly involved in the active extrusion of acetate anion from the intracellular to the extracellular environment. The *HAA1* genes are also involved in the reduction of the intracellular concentration of acetate, being the effect exerted by Haa1 protein much more evident than the one associated to the expression of its target gene *TPO3*.[1], [14], [15].

2.2.4. Remodelling of the cellular envelope to limit the diffusional entry of the acid

The active expulsion of acetic acid anions from the cell interior would be energetically expensive and worthless if the undissociated acid could reenter the cells at a similar rate, so, the restriction of the passive diffusion to prevent the re-entrance of the undissociated form of acetic acid should be an essential step in *Saccharomyces cerevisiae* adaptation to acetic acid. A mechanism presumed to reduce the diffusion rate of weak acids is the reinforcement of cell wall structure to reducing cell envelope permeability, and in consequence decreasing the weak acid diffusion across the cell. This mechanism was first described to occur in response to the acetic herbicide 2,4-D, mediated by the glycosylphosphatidylinositol cell wall protein Spi1p, and it was demonstrated extended to reduce weak acid food preservatives. [1], [16].

The SPI1 gene encodes a member of the glycosylphosphatidylinositol (GPI)-anchored cell wall protein (CWP) family. It has been observed that SPI1 gene is required for a more rapid adaptation to weak acid in stressed cells and was also demonstrated that the elimination of the SPI1 gene led to an increase in the duration of the period of latency, and this increase was correlated with the lipophilicity of the weak acid. The expression of SPI1 was shown play a role in adaptation and cell wall resistance in cells exposed in acetic acid, more interestingly with SPI1 transcription being activated in dependence of the transcription factor Haa1 under these particular stress conditions. [16].

Another relevant piece of evidence is the degradation of aquaglyceroporin Fps1. This protein is presumed to be involved in the facilitated diffusion of acetic acid into the cells. It appears that in *Saccharomyces cerevisiae* cells in the presence of acetic acid its activated Hog1 pathway, which generates endocytosis and degradation of the Fps1 aquaglyceroporin, in these stressed cells the loss of Fps1 protein is important for the acquisition of resistance to acetic acid, due to the elimination of the channel for the passive diffusional entry of this acid into the cells. [17]

2.2.5. Response to energy and nutrient limitation

In response to stress caused by acetic acid, *Saccharomyces cerevisiae* developed some resistance strategies to counteract the nutrient limitation. The TOR (Target-of-Rapamycin) pathway, a regulatory system dedicated to the yeast response to nutrient starvation was suggested to be activated in response to acetic acid. [1] In [18] it was demonstrated that acetic acid causes severe intracellular amino-acid starvation, involving the general amino-acid control (GAAC) system as well as the TOR pathway. Moreover, the alteration of carbohydrate metabolism is also a feature of weak acid-stressed yeast cells, as suggested by the upregulation of a number of genes and proteins encoding enzymes of glycolysis and of the Krebs cycle in response to acetic acid. [18] These strategies are relevant to compensate the severe depletion of ATP as well as the activation of processes such as the PM-H^+-ATPase, V-H^+-ATPase and ABC drug pumps. A large number of genes in ATP synthesis were identified as determinants of resistance to weak acids, in particular to acetic acid. The expression of genes related

to the uptake of potassium, calcium, iron and zinc are also important in tolerance to acetic acid stress. [1]

2.2.6. Acetic acid as an induced of programmed cell death

The yeast *Saccharomyces cerevisiae* is able to undergo cell death with an apoptotic phenotype upon induction by several stimuli, including acetic acid. High concentrations of acetic acid are able to induce *Saccharomyces cerevisiae* to an apoptotic or a necrotic death process, which is dependent on the acid concentration. In yeast apoptosis, genes involved in cell cycle-regulation, DNA-repair, oxidative stress response, mitochondrial functions and, though to a lesser extent, cell-surface rearrangement, were found to be differentially regulated during this process. [18] An exposure of *Saccharomyces cerevisiae* to 20-200 mM acetic acid for 200 min at pH 3 results in a programmed cell death (PCD) process with an apoptotic phenotype that is dependent on mitochondria. Moreover, the plasma membrane and mitochondria are both targeted by acetic acid in *S. cerevisiae* and as mentioned above, can induce a PCD process which shares common features with an apoptotic phenotype (reviewed in [19]). The **Figure 2.2.3** shows the main processes of PCD that occurs in stressed cells of *Saccharomyces cerevisiae*.

The process developed by acetic acid extreme stress, PCD, has specifically apoptotic hallmarks such as: chromatin condensation along the nuclear envelope; exposure of phosphatidylserine on the surface of the cytoplasmic membrane; occurrence of internucleosoma DNA fragmentation; cytochrome c from the mitochondria to the cytosol; production of mitochondrial reactive species (ROS). Mitochondria play a major part in the PCD process due to the production of reactive oxygen species (ROS) and the release of different proteins into the cytosol including cytochrome C – a soluble protein bound to the outer face of the inner mitochondrial membrane, its release is associated with an interruption of the normal electron flow at the complex III site of the respiratory chain. The release of cytochrome C to the cytosol drives the assembly of the mitochondrial apoptosome that activates caspases, cytochrome C can act both as an electron donor and a ROS scavenger. [20] [21] [22] In response to acetic acid, the mitochondria becomes permeabilized and that facilitates the release of lethal factors to the cell like cytochrome C and yeast AIF, both contributing to the death process. Mitochondrial degradation has been shown to occur in a number of systems following apoptosis induction and usually involves an autophagic process, but in yeast that mechanism is not fully understood. It has been hypothesized that, mitochondrial degradation might be controlled by the vacuolar protease Pep4. This protein was found to be translocated to the cytosol, after partial permeabilization of the vacuolar membrane, in cells undergoing acetic acid-induced PCD with an apoptotic phenotype. The role of Pep4 seems to be a protective one, since a *pep4Δ* strain showed increased susceptibility to acetic acid, while an overexpression strain exhibited higher resistance to acetic acid-induced PCD. [23]

Another phenomenon that occurs in cell death is the production of ROS and occurs 15 minutes after cell exposure to acetic acid. It seems the production of hydrogen peroxide occurs in the early response to the acid stress and the production of superoxide anions is only a later stage of the process, after hydrogen peroxide levels had already decreased. [24]

In conclusion, it is well known that the non-dissociated form of the acid enters the cell and dissociates, if the extracellular pH is lower than the intracellular pH this will lead to the accumulation of acetate and to the acidification of the intracellular environment. The effects of this stress include the inhibition of amino acid uptake and carbohydrate metabolism. In a later stage, acetic acid affects mitochondria function and dynamics triggering the release to the cytosol of mitochondria resident apoptogenic molecules such as cytochrome C and Aifp, leading to DNA fragmentation. In this process the partial permeabilization of the vacuolar membrane and release of Pep4p also occurs, which could lead directly or indirectly to proteolytic degradation of mitochondria.

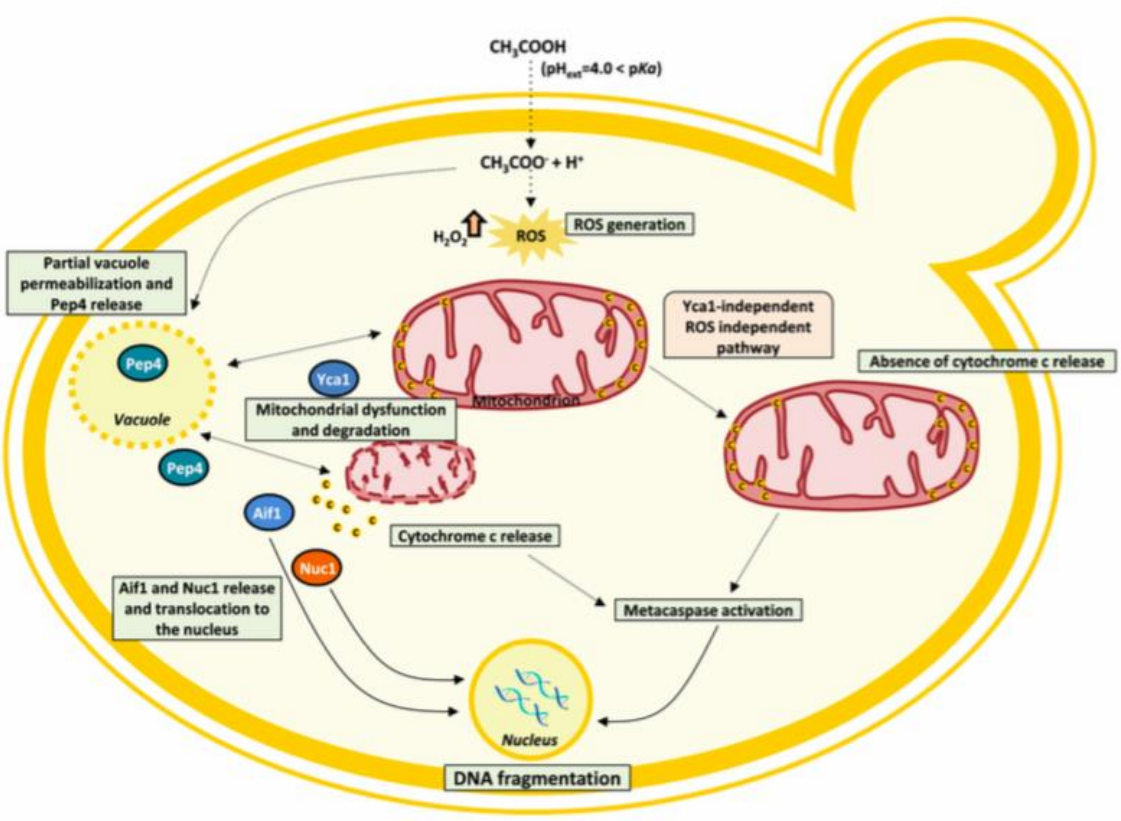

Figure 2.2.3 – Current knowledge on targets and pathways underlying PCD induced by acetic acid in Saccharomyces cerevisiae. Adapted from *[21]*.

2.3. Transcriptional regulatory networks involved in acetic acid tolerance - *Saccharomyces Cerevisiae*

The following sections describe the transcriptional regulatory networks of *Saccharomyces cerevisiae* involved in acetic acid tolerance, with a highlight in the role of regulon Haa1 protein and in Tpo3 protein over this process.

2.3.1. The main regulatory pathways involved in weak acids response

Saccharomyces cerevisiae has many specific resistance responses to weak acids, determined by the chemical structure of the weak acid, in particular, by its lipophilicity. Several genes have been implicated in the weak acid stress response and adaptation such as: the ATP-binding cassette (ABC) efflux pump Pdr12p, is a major factor counteracting intracellular anion accumulation; the plasma membrane H^+-ATPase Pma1p, the gene *TPO2* and *TPO3*, encoding a multidrug resistance transporter. [1]

Nowadays, the use of bioinformatics tools, in particular, the YEASTRACT database, has been crucial to obtain a transcriptomic analysis of weak acid-stressed cells, allowing the clustering of genes with their documented regulators, which facilitates the identification of novel transcription factors that may be correlated with *S. cerevisiae* transcriptional response to weak acid stress. Based on that, four regulatory pathways dependent on the following transcription factors have been identified: Haa1 protein , Rim101 protein, Msn2 protein/Msn4 protein and War1 protein. [1], [2], [25], [26].

In the following section the role in *S. cerevisiae* response to acetic acid of Haa1 transcription factor and the role of Tpo3 and Hrk1 proteins will be discussed in detail, due to its importance in the purpose of this thesis.

2.3.2. The role of Haa1 transcription factor and TPO3 protein

The Haa1 is a transcription factor and its first biological function was attributed based on its homology with cooper-activated transcription factors in tolerance to acetic and propionic acids in yeast. [1] However, unlike its homologous proteins, the function of Haa1 protein is independent of the cooper. [27] The *HAA1* gene has a protective effect in yeast acid stressed cells and was found that effect decrease significantly as the lipophilicity of the weak acid increases, which means that the level of activation mediated by Haa1 protein in response to weak acid changes. Moreover, the expression of the *HAA1* gene was shown to lead to the reduction of the duration of the adaptation period of a yeast cell population suddenly exposed to toxic concentrations of weak acids, through decreasing the loss cell viability occurring during the lag phase. It was also shown that in the absence of acetic acid, the elimination of *HAA1* gene only had a slight effect on the *S. cerevisiae* transcriptome, 11 genes exhibited an increased expression level in *Δhaa1* cells. In the presence of acetic acid, the elimination of the *HAA1* gene reduced the transcription of 85 out of the 112 acetic activated genes in the parental strain, corresponding to approximately 80% of the upregulated genes that are dependent upon *HAA1* gene expression. The genes regulated by Haa1 protein could be separated in two major classes, they are: the first one includes 64 genes whose acetic acid-induced transcriptional activation is totally dependent

on Haa1 protein and the second one includes 21 genes whose acetic acid-induced transcriptional activation was only partially dependent on Haa1 protein.

The genes *PHM8*, *TPO2*, *YRO2*, *TPO3*, *YGP1*, *YER130*, *YIR035c*, *YLR297w*, *YPR157w*, *YPR127w* and *SPI1* were confirmed to be dependent on the presence of Haa1 protein , because its expression is significantly decreased in *Δhaa1* acetic acid stressed cells. However only *TPO2*, *YPR157* and *YGP1* provided protection against acetic acid, being direct Haa1 protein targets. [2] The genes whose activation was known to be dependent on Haa1 protein encodes proteins belonging to the well following biological functions: “Transcription factors”, “Multidrug resistance transporters”, “Cell wall”, “Lipid metabolism”, “Regulation of carbohydrate metabolism”, “Protein folding”, “Carbohydrate metabolism”, “Amino acid metabolism” and “Nucleic acid processing”. It has also been demonstrated that Haa1 protein specially regulates almost one-half of the acetic acid-induced genes, about 51 of 112 genes. In the large number of genes regulated by Haa1-regulon the following have a more prominent effect against acetic acid; *TPO2* and *TPO3*, encoding two membrane transporters of the Major Facilitator Superfamily proposed to mediate the efflux of acetate from the cell interior during cultivation in the presence of acetic acid; the *SAP30* gene, which encodes a subunit of the histone deacetylase RP3 complex, has recently been demonstrated to be involved in the regulation of yeast transcriptional response to environmental stress; *HRK1,* which encodes a kinase belonging to family of kinases involved in the post-translational regulation of plasma membrane transporters. All the genes dependent on Haa1 protein are involved in the reduction of the internal concentration of acetate. [2], [28]. In **Figure 2.3.1** the role of Haa1 protein in Tpo3 transmembrane protein in response to acetic acid is represented.

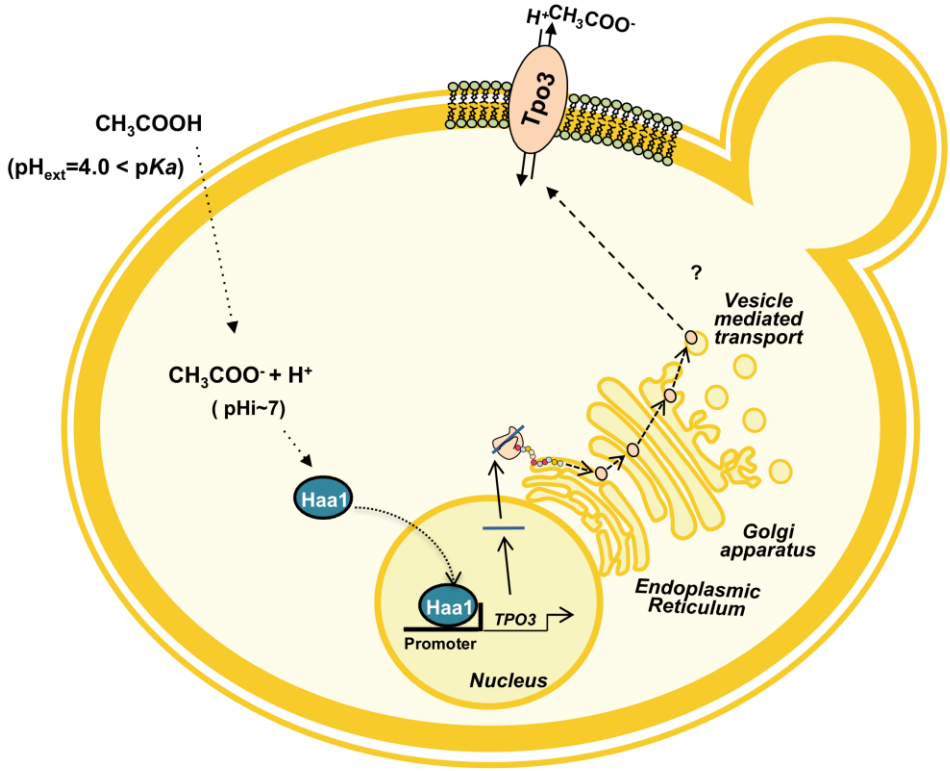

Figure 2.3.1 – Mechanism model for the adaptive yeast response to acetic acid-induced stress. The entrance of acetate in the cell interior stimulates the activity of Haa1 protein, which regulates the transcription of *TPO3* gene leading to the reduction of acetate in cell interior, by extrusion.

2.3.3. The role of HRK1 protein

The *HRK1* gene is transcriptionally controlled by Haa1 protein. *HRK1* encodes a protein kinase belonging to a family of kinases dedicated to the post-translational regulation of plasma membrane transporters. It was revealed that the deletion of the *HRK1* gene led to an increased accumulation of acetic acid into *Saccharomyces cerevisiae* cells cultivated in the presence of this weak acid, a similar phenotype to the one observed upon *HAA1* deletion, which seems to indicate the involvement of Haa1 protein and Hrk1 protein in the reduction of intracellular acetate concentration. [1] Hrk1 protein was proposed to be a positive regulator of plasma membrane (PM) H^+-ATPase (Pma1p) activity in response to glucose metabolism. Because Hrk1 protein belongs to a family of protein kinases dedicated to the regulation of plasma membrane transporters, it is believed that Hrk1 protein may be involved in the reduction of the intracellular acetate concentration through the activation, by phosphorylation, of putative plasma membrane acetate exporter, like Tpo3 protein. This mechanism was considered because the concentration of acetate is higher in Δ*haa1* cells and this effect could not be fully attributed to other candidate targets of Haa1 protein , specifically to the plasma membrane drug-H+ antiporters Tpo2p and Tpo3 protein. A recent analysis on phosphoproteome of yeast cells (*Saccharomyces cerevisiae*) under acetic acid stress, showed that there is no positive effect of *HRK1* expression in the in vivo activity of PM-H^+-ATPase. However, the increased susceptibility of Δ*haa1* cells to hygromycine B – a compound known to disrupt plasma membrane electrochemical potential, support the idea that Hrk1 protein counteract the acetic acid-induced decrease of plasma membrane electrochemical potential. [2]

3

Methods and Materials for Image Processing

In this chapter is described the materials and methods.

3.1. Biological Material and Data

In this section the strains and the growth media used are presented as well as the susceptibility assays with acetic acid.

3.1.1. Strains and growth media

The *S. cerevisiae* BY4741 *TPO3*-GFP strain (MATa; *his3*Δ1; *leu2*Δ0; *met15Δ0*; *ura3*Δ0 *TPO3*::GFP), the deletion mutants BY4742 *TPO3*-GFP *haa1*△ (MATa; *his3*Δ1; *leu2*Δ0; *lys2Δ0*; *ura3*Δ0; *YPR008W*::KanMX *TPO3*::GFP) and BY4742 *TPO3*-GFP *hrk1*△ (MATa; *his3*Δ1; *leu2*Δ0; *lys2Δ0*; *ura3*Δ0; *YOR267c*::KanMX *TPO3*::GFP) used in this work were batch cultured at 30ºC with orbital agitation (250 rpm) in minimal medium MM4 which contains, per liter, 1.7 g yeast nitrogen base without amino acids or NH_4^+ (Difco), 2.65 g $(NH_4)_2SO_4$ (Merck), 20 g glucose (Merck), 20 mg methionine, 20 mg histidine, 20 mg uracil, 30 mg lysine and 60 mg leucine (all from Sigma). The pH of the MM4 growth medium was adjusted to 4 using HCl.

3.1.2. Acetic Acid Susceptibility Assays

Strain *S. cerevisiae* BY4741 *TPO3*-GFP (*WT* strain) and the mutant strains *haa1*Δ and *hrk1*Δ susceptibility to acetic acid was assessed by comparing the growth curve in the MM4 medium either supplemented or not with 50 mM of acetic acid (at pH 4.0). Cells cultivated until mid-exponential phase (OD_{600nm}= 0.8 ± 0.08) in MM4 growth medium (at pH 4.0) were used to re-inoculate this same basal growth medium as above supplemented with 50 mM acetic acid. The volume of inocula used was calculated to obtain a cell suspension with an initial OD_{600nm} of 0.4 ± 0.04. During batch cultivation, the growth curve in the presence or absence of acetic acid was accompanied by measuring the increase of culture OD_{600nm} (see **Figure 3.1.1**). In **Table 3.1.1** is described the number of biological replicas of each studied condition developed for the biological set material.

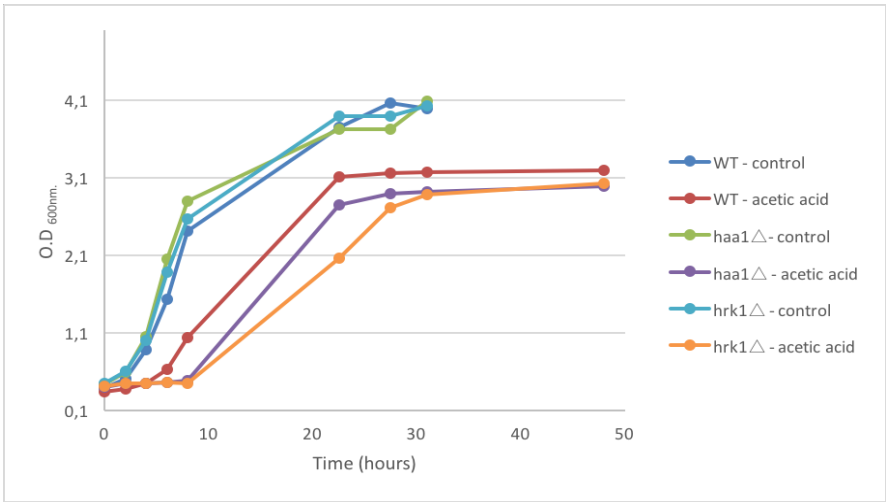

Figure 3.1.1 – Growth curves in the presence and absence of acetic acid of the wild type and mutant strains during batch cultivation.

Table 3.1.1 – Biological replies of each condition used for the set of biological material.

Time Course (h)	**Number of Biological Replies**					
	Control Conditions (in the absence of acetic acid)			Stress Conditions (in the presence of acetic acid)		
	WT	***haa1*Δ**	***hrk1*Δ**	**WT**	***haa1*Δ**	***hrk1*Δ**
0	9	10	10	-	-	-
1	8	8	8	8	8	8
2	8	8	8	7	7	7
4	8	6	6	8	4	7

3.1.3. Microscope Analysis

Cell samples were harvested by centrifugation after 5 minutes, 1h, 2h and 4h of cultivation, in the presence and absence of the acid as described above, and resuspended in sterile water. Distribution of Tpo3-GFP fusion protein in living cells was detected by fluorescence microscopy using a Zeiss Axioplan microscope (Carl Zeiss MicroImaging), using excitation and emission wavelengths of 395 and 509 nm, respectively. Fluorescence images were captured using a cooled, charge-coupled device camera (Cool SNAPFX, Roper Scientific Photometrics).

3.2. Fluorescence Microscopy

The fluorescence microscopy is a powerful tool. It provides a way to study the physiology of living cells at sub-cellular levels of resolution, and allows the study of fixed and living cells because of its versatility, specificity, and high sensitivity. This efficient approach has an inherently greater sensitivity and range than methods based upon changes in optical density or chemiluminescent emission. this particular case, fluorescence microscopy enables the study of protein location - Tpo3. [29]

3.2.1. Fluorescence Characteristics

Fluorescence as a phenomenon is part of a larger family of related luminescent processes in which a susceptible substance absorbs light, only to reemit light (photons) from electronically excited states after a given time. Fluorescence follows a series of discrete steps of which the outcome is the emittance of a photon with a longer wavelength.

When light of a particular wavelength hits a fluorescent sample, the atoms, ions or molecules therein absorb a specific quantum of light, which pushes a valence electron from the ground state GS_0 – this initial state is an electronic singlet in which all electrons have opposite spin and the net spin is 0 into a higher level, creating an excited state ES_n. After excitation to the higher energy level ES_n, the electron quickly relaxes to the lowest possible excited sublevel, which is in the picosecond range. The energy decay from dropping to a lower vibrational sublevel occurs through intramolecular non-radiative conversions and the converted heat is absorbed via collision of the excited state fluorescent molecule with the solvent molecules.

The energy of photons involved in fluorescence and generally a quantum of light can be expressed by Planck's law:

$$\boldsymbol{E = h.v = h.\frac{c}{\lambda}}$$

where E is the quantum's energy (J), h is Planck's constant (J.s), v is the frequency (s^{-1}), λ is the wavelength of the proton (m), and c is the speed of light ($m.s^{-1}$). [30]

Fluorescence has some essential characteristics and parameters that are used in fluorescence microscopy, such as the fluorescence life time, quantum yield, anisotropy, fluorescence quenching, auto fluorescence, photo bleaching, resonance energy transfer, and so on.

- **Fluorescence lifetime (the fluorochrome's fluorescence lifetime – τ)** – Refers to the average time the electron spends in the excited state before returning to the ground state. The fluorescence intensity (I_t) decays exponentially over time (t), that can be expressed by the following expression: $I_t = I_0 exp\left(\frac{-t}{\tau}\right)$.

This decay through radiative (Γ) and non-radiative processes (k_{nr}) follows an exponential decay and the time of this process is the fluorescence lifetime: $\tau = \frac{1}{\Gamma + k_{nr}}$. [30]

- **Quantum yield (Φ) –** Determines how bright a fluorochrome's emission is. It is given by the ratio of the number of emitted to absorbed photons, which is determined by the rate constants of emission (Γ) and the sum of all non-radiative decay processes (k_{nr}) that depopulate the excited state. [30]

- **Anisotropy –** Refers to the quality of having different properties along different axes: in a pool of randomly oriented fluorochromes, only those fluorochromes with transition dipole moments that are aligned parallel to the polarization direction of the excitation beam will be excited (photo selection). [30]

- **Fluorescence quenching –** Refers to the phenomenon by which interaction of a molecule (the quencher), with the fluorochrome reduces the quantum yield or the lifetime. [30]

- **Auto fluorescence –** Fluorescence that does not originate from the fluorochrome of interest, but rather from cellular components that have fluorescent properties (background fluorescence). [30]

- **Photo bleaching *(fading)* –** Refers to the photochemical process in which the fluorochromes ability to enter repetitive excitation/emission cycles is permanently interrupted by destruction or irreversible covalent modification of the fluorochrome by reaction with surrounding (bio)molecules. [30]

- **Resonance energy transfer –** Refers to the photo physical process in which the excited state energy from a donor fluorochrome is transferred via a non-radiative mechanism to a ground state acceptor chromophore via weak long-rage dipole-dipole coupling. [30]

3.3. Images Pre-processing Pipeline

In this work, a bioinformatic tool was designed and implemented in *Matlab* ®, to manage the images sets and process them with algorithms described throughout this chapter. All images will be analysed according to the following previously established and developed pipeline.

- **Cell selection –** using a Graphical User Interface to facilitate the manual selection of the cells, this step is crucial for the success of the method because cells should be correctly chosen in

the image from fluorescence microscopy. Afterwards, the selected cells are manually segmented. (see section 3.3.1)

- **Segmentation and centroid detection –** cell region identification at the image and determination of the its geometrical. (see section 3.3.2)

- **Radial Maps building –** determination of the radial profile map of each cell, where each cell is characterized by 72 radial profiles with 100 points length each. The radial profile starts in the centroid and ends at the boundary of the cell. (see section 3.3.3)

- **Single-cell quantification –** the set of radial profiles of each cell allows the performance of a single-cell characterization based on the abundance of the Tpo3 protein. Thereby, a mean profile of each cell is obtained as well as a standard deviation profile. These profiles enable us to determine the intensity value of the protein along the cellular space (intracellular and membrane). (see section 3.3.4)

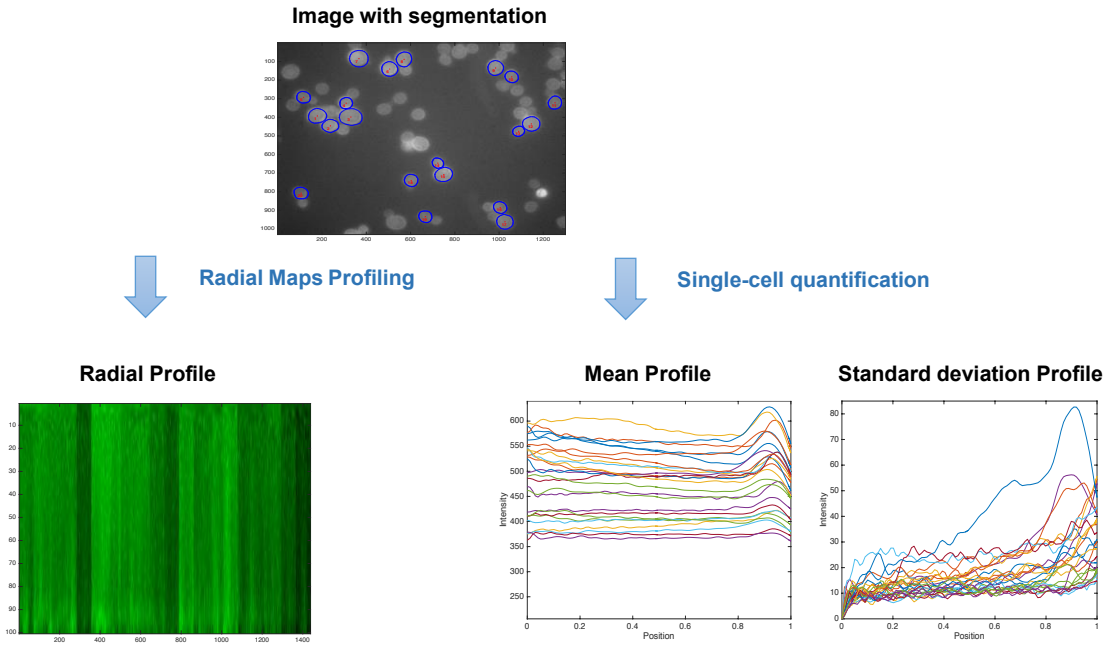

Figure 3.3.1 – Pipeline for image treatment from the segmented image to the RD profile and single-cell quantification.

3.3.1. Cell Selection

In this work a Graphical User Interface (GUI) was developed to allow an expert to manually select in each FM image the cell to evaluate. The biologist selects the cells in each image that are representative of the natural behaviour of the cell in stress or non-stress condition, which means they can give relevant biological information. This semi-automated approach allows the expert to exclude all negative cells from the analysis, that may represent technical pitfalls of fluorescence or protein degradation. This interface comprises the selection of single cells with the *Matlab* ® function *ginput* and the creation of a .txt file with the centroids position (x_i, y_i), where i is the cell number. This graphical user interface received the name of Programa Leveduras and was designed using *Matlab* ®.

The initial menu is shown in **Figure 3.3.2 a)**. Initially the set of images is loaded by defining the default folder of images (selecting the *Directoria Imagens* button) If corrected loaded the photo from the images directory will appear in the initial menu and the user can inspect if it is the correct one (see **Figure 3.3.2 b)**)

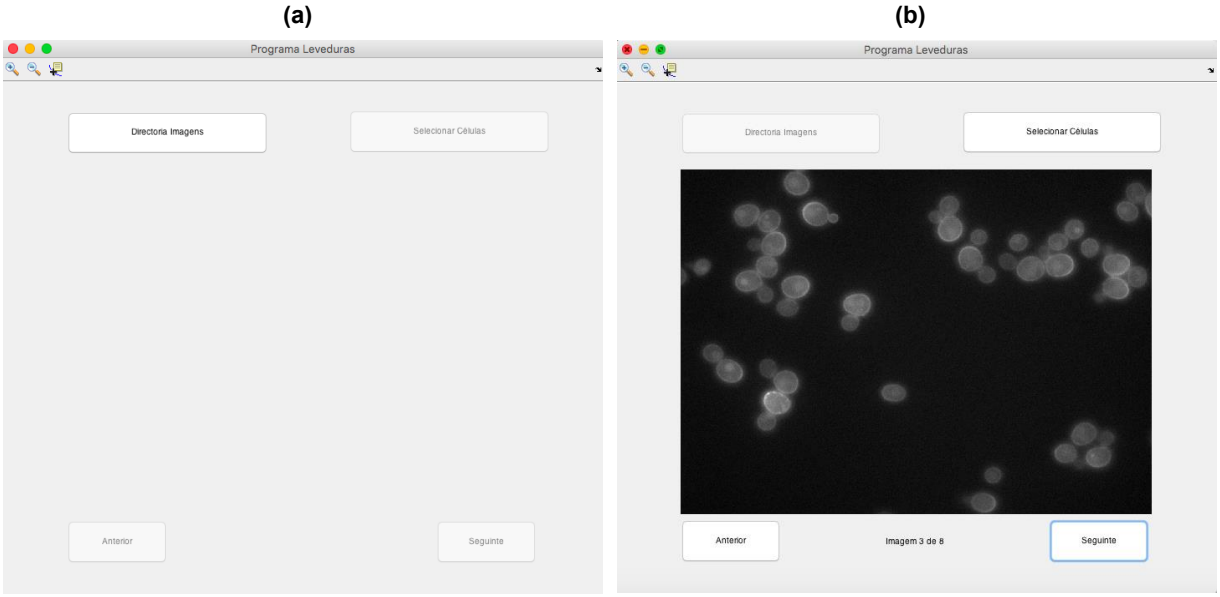

Figure 3.3.2 – Programa Leveduras – (a) Initial Menu, (b) Menu After loading Image

After loading the image, the user can decide to proceed to the cell selection proceeding (pressing *Selecionar Células*) or in case it was not the correct image repeat the previous steps (pressing *Directoria Imagens*). The *Selecionar Células* option allows the expert to proceed to the selection of the individual

cells desired and, after the 1st image is complete the expert can proceed to the 2nd until he has finished the images of the set chosen (pressing *Seguinte*). (see **Figure 3.3.3**)

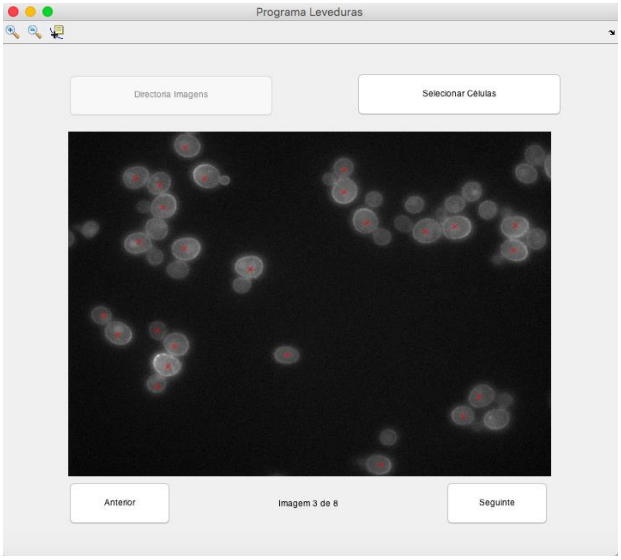

Figure 3.3.3 – Programa Leveduras – Cell selection from the set of images to analyse.

After finishing the selection procedure, the data will be saved in a folder with the name of the image analysed in the directory of the program. The folder contains the initial image and a .txt document with all the coordinates (x, y) of the cell centroids selected. After saving the data, the user can close the program or proceed to another selection repeating all the steps from the beginning.

3.3.2. Segmentation and Centroid Detection

Segmentation is a process that allows the division of images into regions that distinguish objects of interest. This process is characterized for having a typically low accuracy and consistency output when applied to most images. It is often referred to as the first, most important and most difficult step in image processing, determining the success of the final analysis. Several segmentation techniques can be used however in this work, the segmentation was manual in *Matlab* ®. After obtaining the .txt file with the centroids of cells of each image analysed, the file is imported to *Matlab* ®. Then, all the cells previously chosen are manually selected with the *Matlab* ® function – *roipoly*, this function allows us to create a mask of each cell. (see **Figure 3.3.4**)

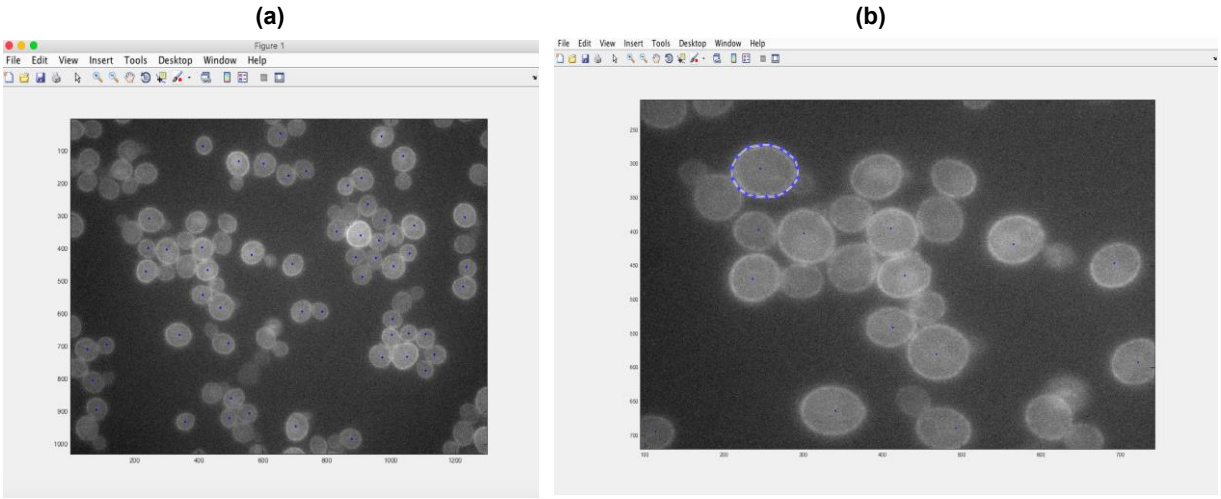

Figure 3.3.4 – (a) Viable cells previously chosen to be analysed, (**b)** Cell mask obtain with the roipoly function.

After all the masks of cells are selected with roipoly function, the next step is calculating the boundaries of the cells, with the *Matlab* ® function *bwboundaries* – which gives a set of points that describes the membrane bound, and finally is made an interpolation with each set of points with *Matlab* ® functions *cscvn* and *fnplt*. (see **Figure 3.3.5**)

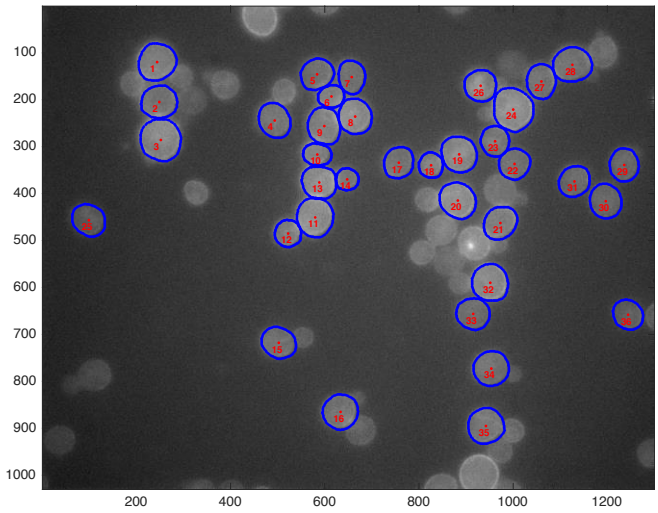

Figure 3.3.5 – Set of cells with the boundaries selected in Matlab ®.

3.3.3. Radial Profile Collection

The Radial Profiles (RDPs) store the nucleus-to-membrane radial environment surrounding each nucleus, to study Tpo3 protein distribution within the cell. In the *wild-type* context and in normal cell conditions, Tpo3 protein are mainly concentrated at the membrane since it is a transmembrane protein, being the abundance at the cytoplasm low and uniformly distributed. However, in acetic acid-stress conditions, the levels of Tpo3 protein expressed increase, in order to decrease the level of acetate in the cell interior. These profiles contain a set of intensity lines extracted from the radial surroundings relative to the centre coordinates of each of the selected cells. All the profiles were made in *Matlab* ®.

3.3.3.1. Methodology

The *Matlab* ® function *Improfile* was used– which gives the intensity values of pixels along a line and displays a plot of the intensity values, creating a two-dimensional plot of intensity values versus the distance along the line segment. The information is rearranged in different radial coordinates, ρ ($\rho = \mathrm{N}$) being $\mathrm{N} = \mu_{\mathrm{dist}}$, where μ_{dist} is the mean of the distance vector (from the centre to the membrane) and θ, with the referential in the centre (see **Figure 3.3.6**). The final RDP dimension is $\mathrm{N} \times \theta_n$ being θ_n equal to $\theta_n = \frac{2\times\pi}{\theta_{step}}$. This way the number of lines gathered depends on θ_{step}, which is the incremental step of θ. In this case θ_{step} was considered $\frac{\pi}{180}$ (1°). Each cell is characterized by 72 radial profiles with 100 points each. The final map, containing the set of all profiles of all selected cells, is a 72*N*×100 image matrix when *N* is the number of selected cells.

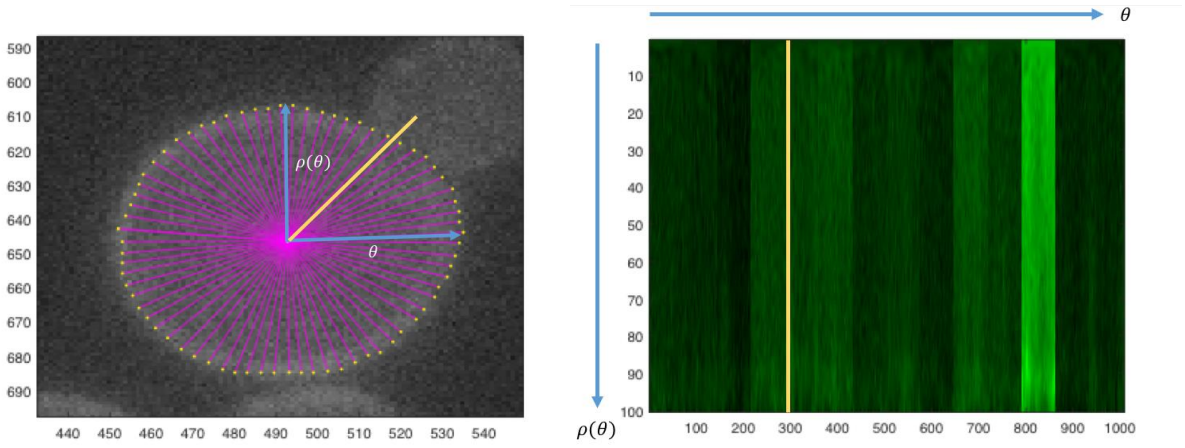

Figure 3.3.6 – Illustration of the radial profile procedure.

3.3.4. Single-cell Quantification

The radial maps (RDMs) allow the extraction of the mean and Standard Deviation profiles (STD). Mean and STD profiles reflect not only the protein Tpo3 concentration distribution but also the relative distribution of the protein with respect to the centre of the cell. Both profiles are obtained from the radial mapping, then a quantification of the quantity of Tpo3 protein along the cell is made, since the nucleus to the membrane, in the study conditions. In **Figure 3.3.7** is illustrated the method applied to extract the mean profile from the radial profile is illustrated, where the cell centre- corresponds to value 0 and the cell membrane corresponds to value 1 in the horizontal axis. Basically, the mean profile is about the sum of each mean in each spatial point in the cells, as illustrated by the yellow line in the mentioned figure. The method for STD profile is the same.

In the Chapter 4 a complete description of the profiles is made and the results are also shown and analysed.

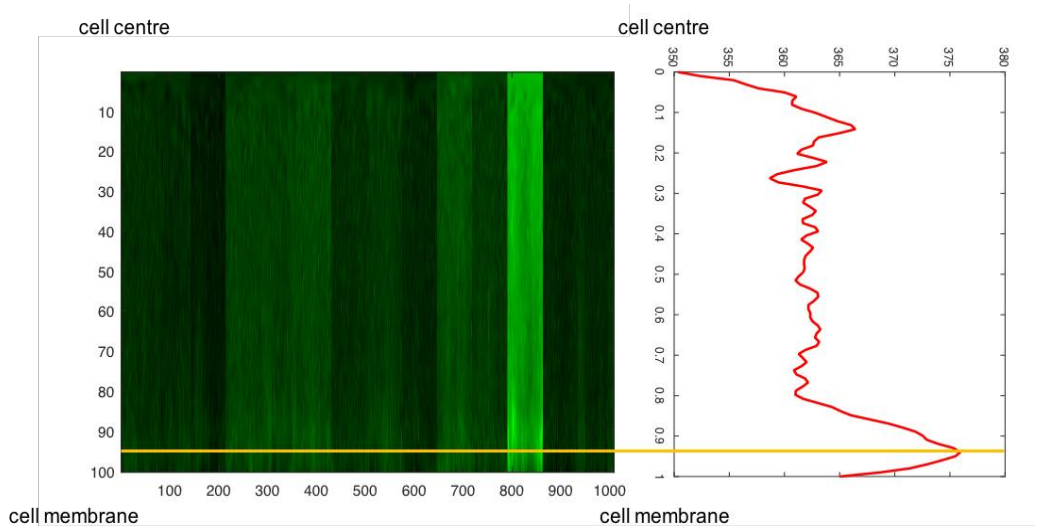

Figure 3.3.7 – Illustration of the mean profile procedure.

3.4. Features Collection and Statistical Analysis

In this section, the features extracted from the mean profiles are considered, is made a brief description of their biological meaning as well as the statistical analysis to study the discriminative potential of the features collected.

3.4.1. Features

From the profiling pipeline employed, RD and mean profiles were obtained, as well as STD profiles. The abundance pattern of Tpo3 protein at cellular level, namely the cell membrane, give information that reflects the functional activity of Tpo3 protein, leading to a better understanding of the function of this protein in the studied conditions. To characterize the distribution both at membrane and cytoplasmic level, several quantitative objective features that reflect Tpo3 protein abundance level are extracted.

The features were collected from the mean profiles and are described in **Table 3.4.1**. These features reflect the distribution of Tpo3 protein within the cell, through the quantification of: high concentrations of Tpo3 protein intensity and relative position; Tpo3 protein concentration in the membrane and cytoplasm.

Table 3.4.1 – Features Description

Membrane Maximum Intensity (MMI)	Maximum value observed in cell membrane. $\boldsymbol{f(x)}$
Position of the MMI	Membrane Maximum Intensity (MI) position, x.
Cytoplasm Mean Intensity (CMI)	Mean intensity value observed in cell cytoplasm. $\boldsymbol{f(x_1)}$
Intensity Differential (δ)	Intensity value obtained from the differential between the cell cytoplasm intensity and the cell membrane intensity.

The MMI match with the maximum intensity observed in mean profile (see **Figure 3.4.1**).

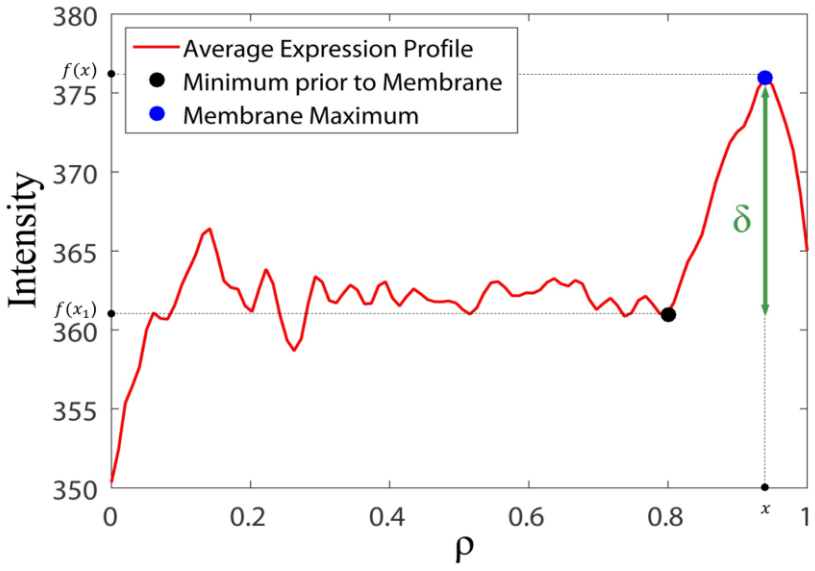

Figure 3.4.1 – Features collection.

3.4.2. Statistical Analysis

In this section, the statistical methods used to evaluate the statistical significance of features between *wild-type* strain and mutated strains are described.

Aiming to make a comparison between two unpaired groups of data (mutated and non-mutated) the T-test and the Mann-Whitney U test (MW) can be used independently, depending on the shape of the curve of the probability density function and on the size of the data of each feature. In this analysis the MW test was used.

The T-test is a parametric statistical test that determines if a statistically significant difference between the means of two unrelated Gaussian groups exists. The null and alternative hypotheses are defined as

$$H_0 : \mu_1 = \mu_2 \qquad H_1 : \mu_1 \neq \mu_2$$

in which μ_1 and μ_2 correspond to the mean of groups 1 and 2, respectively. The result H is 1 if the test rejects the null hypothesis at the 5% significance level, and 0 otherwise. [31], [32]

The Mann-Whitney U test (also called the Mann-Whitney-Wilcoxon (MWW)) is a non-parametric counterpart of the T-test used to compare differences between two independent non-Gaussian groups. In cases where the data have the same shape distribution, the statement is that two populations differ through differences in the medians between the groups. The null and alternative hypotheses are defined as

$$H_0 : \tilde{\mu}_1 = \tilde{\mu}_2 \qquad H_1 : \tilde{\mu}_1 \neq \tilde{\mu}_2$$

in which $\tilde{\mu}_1$ and $\tilde{\mu}_2$ correspond to the median of groups 1 and 2, respectively. The result H is 1 if the test rejects the null hypothesis at the 5% significance level, and 0 otherwise. [31], [32], [33]

The Mann-Whitney U test assumes the existence of a population $x, x_1, x_2, \dots, x_n$ and another population $y, y_1, y_2, \dots, y_n$. Afterwards, the method compares each observation x_i with y_i, obtaining a total number of pairwise comparisons of $n \times m$. The test equivalent to a Mann-Whitney U-test in *Matlab* ® is *ranksum*. *Ranksum* tests the null hypothesis that data in x and y are samples from continuous distributions with equal medians, against the alternative they are not. The function $[p, h] = ranksum(x, y)$ returns the $p - value$ of a two-sided Wilcoxon rank sum test and a logical value indicating the test decision, h. If $h = 1$ indicates a rejection of the null hypothesis, and $h = 0$ indicates a failure to reject the null hypothesis at the 5% significance level. [34]

The F-test in *Microsoft Excel* to determinates the variance in the features extracted was also made. This test able us to compare the variance between the means in the features in the *wild-type* strain and in the mutant strains, and understand if the variance is significantly different.
The principle used was the same that the T-test.

4

Characterization of Tpo3 protein distribution – Experimental Results and Discussion

In this chapter, the obtained results are unravelled and some observations and discussions are made. The characterization of Tpo3 protein distribution is made based on RDPs analysis, described in section 4.1. Then, in several quantitative objective features, which reflect Tpo3 protein abundance level are extracted to characterize the distribution both at membrane and cytoplasmic level as well as the results of the statistical analysis, as detailed in section 4.1.2 and in section 4.1.3. A final discussion about the results is made in section 4.2.

4.1. Experimental Results

4.1.1. Radial Profiles Characterization

The intensity behaviour of the RDM is described through mean intensity and STD profiles. Both of these profiles were collected in linear direction, to study Tpo3 protein distribution along the cell. To study the Tpo3 protein abundance intensity and location, the mentioned profiles are displayed together, to give a complete analyse of the protein behaviour. A particular discussion of the mean profiles will be made in order to quantify the level of intensity of the protein, different replicas for each strain and condition were chosen to give a wide interpretation of the results. The remaining results can be found in Appendix A.

In this section the error bar profiles, which represent the error associated to the mean profile extraction are left unshown, given their lower contribution towards interpretation but are available in Appendix A.

4.1.1.1. *Wild-type* strain

The *wild-type* strain is considered the model in this analysis since it has not undergone any type of deletion in its genetic code. Based on this, the behaviour of these cells should be as the expected when the yeast cells are in stress conditions. As mentioned before, when *Saccharomyces cerevisiae* cells are exposed to an inhibitory sub-lethal concentration of acetic acid (stress condition), the cell machinery is activated to counteract the effects of the intracellular acidification, in this process the Tpo3 gene is activated and the multidrug resistance transporter Tpo3 is expressed. The role of this protein is crucial for the cells resistance to acetic acid and its abundance is strongly increased during this process. **Figure 4.1.1** evidences the profiles for the Tpo3 protein abundance along the cell after 0h hours in incubation. In the mean profile **(b)** a peak in the protein intensity approximately at positions 0,89 – 0,92 is evident, which indicates that the abundance was mostly at the cell transmembrane level. That makes sense since Tpo3 is a transmembrane protein, at cytoplasmic level the abundance is considered uniform. Almost the same behaviour occurs after 1, 2 and 4 hours in absence of acetic acid as shown in **Figure 4.1.2** to **Figure 4.1.4**. A difference is evident after 4 hours, the level of intensity is higher when compared

with the other time points. During the analysed period the cells are in the latency period which means they are in constant adaptation to the exposed conditions, but after 4 hours in incubation they are better adapted which explains the higher levels of abundance when compared with the first hours.

The RDPs for the 0, 1, 2 and 4 hours in absence of acetic acid shows that the Tpo3 protein is more expressed in the transmembrane domain of the cell and has also uniform level of abundance at cytoplasmic domain.

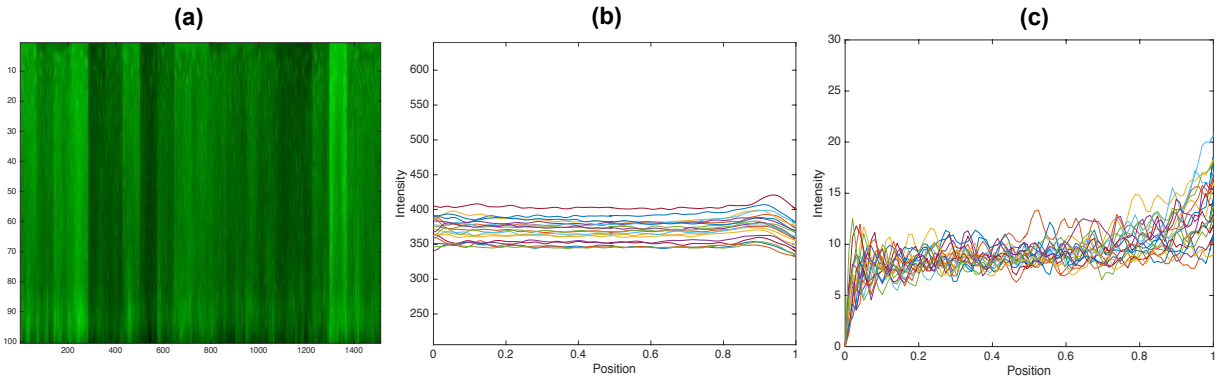

Figure 4.1.1 – Representative profiles for replica **WT_2** after **0 hour** in incubation. (a) Radial Profile (RDP) (b) Mean Profile (c) Standard Deviation (STD) Profile.

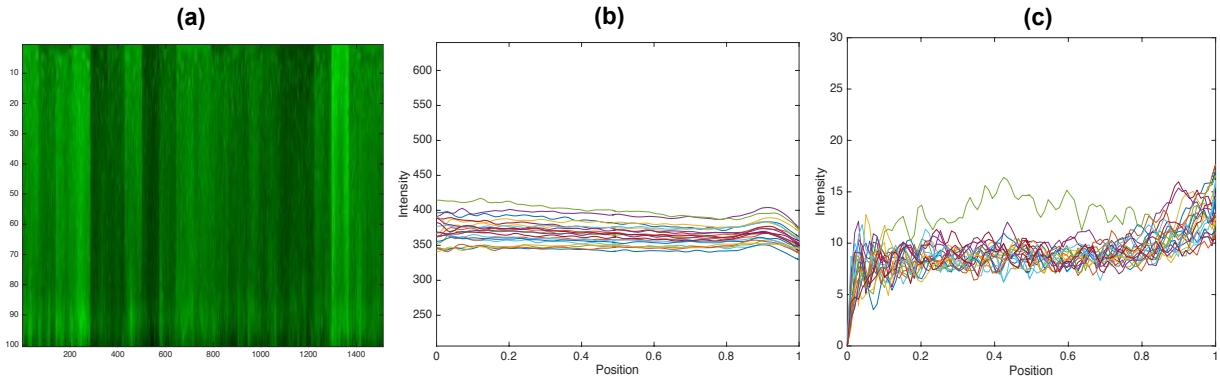

Figure 4.1.2 – Representative profiles for replica **WT_7** after **1 hour** in incubation in the absence of acetic acid. (a) Radial Profile (RDP) (b) Mean Profile (c) Standard Deviation (STD) Profile.

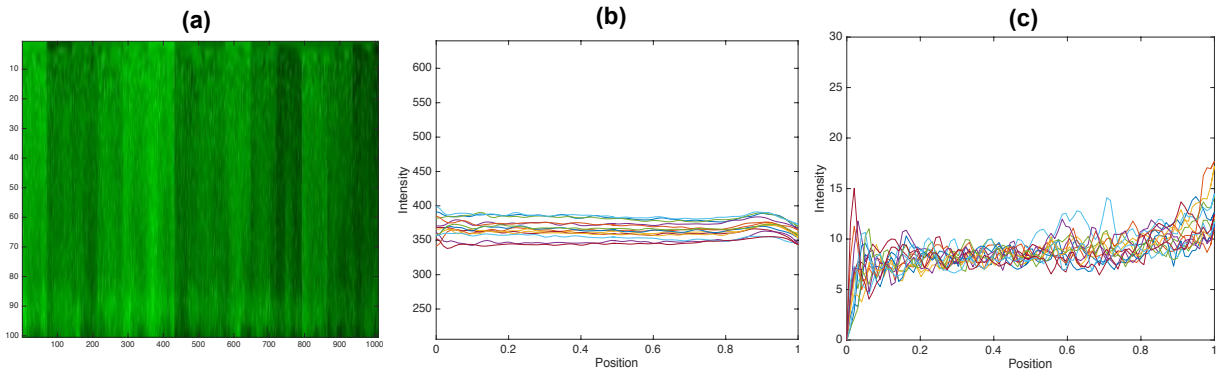

Figure 4.1.3 – Representative profiles for replica **WT_6** after **2 hour** in incubation in the absence of acetic acid. (a) Radial Profile (RDP) (b) Mean Profile (c) Standard Deviation (STD) Profile.

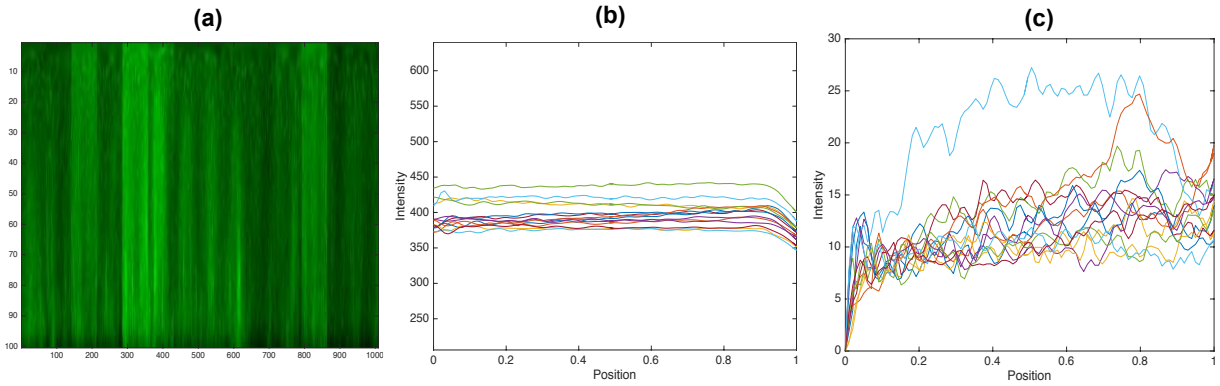

Figure 4.1.4 – Representative profiles for replica **WT_7** after **4 hour** in incubation in the absence of acetic acid. (a) Radial Profile (RDP) (b) Mean Profile (c) Standard Deviation (STD) Profile.

After 2 hours and 4 hours in incubation under acetic acid stress conditions, the cells reveal an increase in the abundance of Tpo3 protein as displayed in **Figure 4.1.5** and in **Figure 4.1.6** when compared with 0 and 1 hour, the increase of the intensity level on the protein abundance in the cell population is noticeable, particularly after 4 hours in incubation. The mean and RDPs shows that the protein is expressed throughout the cell and its abundance is higher in the transmembrane domain.

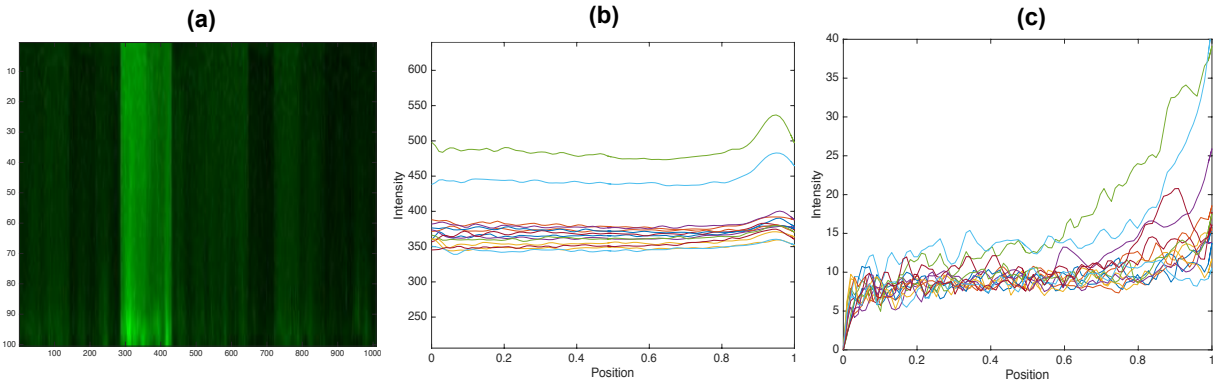

Figure 4.1.5 – Representative profiles for replica **WT_3** after **2 hour** in incubation in the presence of acetic acid. (a) Radial Profile (RDP) (b) Mean Profile (c) Standard Deviation (STD) Profile.

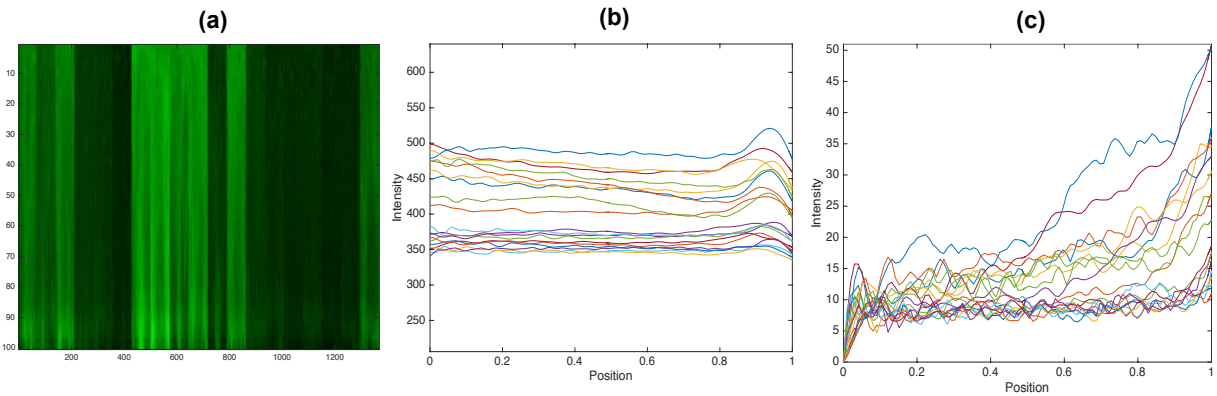

Figure 4.1.6 – Representative profiles for replica **WT_2** after **4 hour** in incubation in the presence of acetic acid. (a) Radial Profile (RDP) (b) Mean Profile (c) Standard Deviation (STD) Profile.

4.1.1.2. Mutant strain *haa1Δ*

The mutant strain *haa1Δ* it was also exposed to an inhibitory sub-lethal concentration of acetic acid. This strain has a deletion in the *HAA1* gene, it is thus expected that the behaviour of this strain will be different when compared with the *wild-type* strain under the studied conditions.

The haa1 protein was found to transcriptionally regulate the *TPO3* gene, which means that *TPO3* is a target-gene of Haa1 protein [2]. It is expected that the concentration of Tpo3 protein decreases, and an increase in the cells susceptibility when exposed to acetic acid. The results displayed in **Figure 4.1.7 (b)** to **Figure 4.1.10 (b)**, show that, during the first 4 hours, the abundance of Tpo3 protein in the absence of acetic acid remained constant (intensity level between the 350 and 450), due to the fact that the cells are in the latency period. However, in **Figure 4.1.9** it is shown that after 2 hours in incubation for the population of cells under analysis the intensity level of protein abundance is lower. The concentration of the protein is likely the wild type strain higher in transmembrane domain approximately at position 0,90 and middling uniform at cytoplasmic level. The difference in the intensity levels in the conditions is due to the heterogeneity of the population of cells. In **Figure 4.1.9** for example the blue line in the mean profile **(b)** as well as in the RDP a significant difference when compared with the other cells can be seen. It can be considered that, in this particular cell, the stage of development and adaptation would be higher and for that reason the abundance of Tpo3 protein is higher than the average abundance of cell population in these conditions.

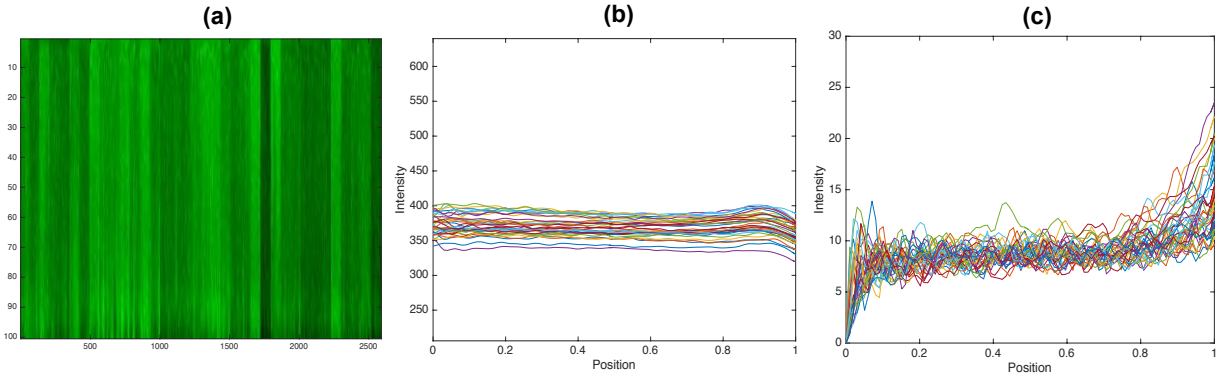

Figure 4.1.7 – Representative profiles for replica **HAA1_2** after **0 hour** in incubation. (a) Radial Profile (RDP) (b) Mean Profile (c) Standard Deviation (STD) Profile.

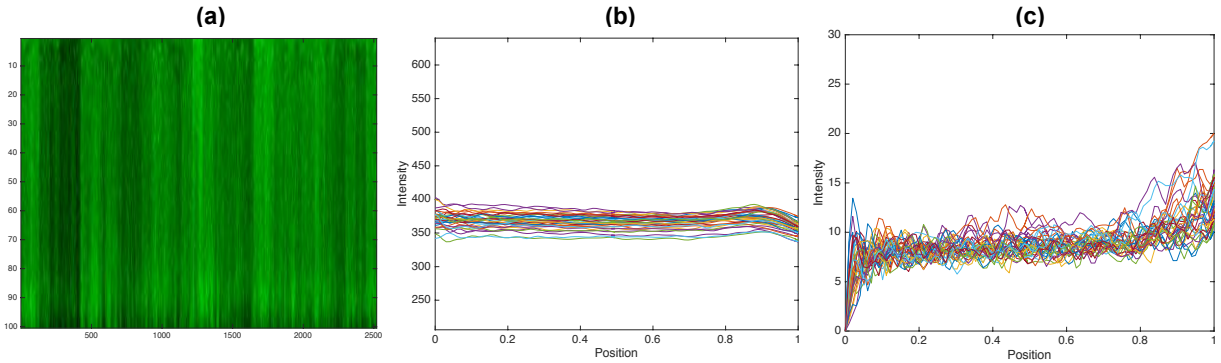

Figure 4.1.8 – Representative profiles for replica **HAA1_7** after **1 hour** in incubation in the absence of acetic acid. (a) Radial Profile (RDP) (b) Mean Profile (c) Standard Deviation (STD) Profile.

This hypothesis is supported by the STD profile **(c)**, where it is clear to see the enormous deviation of the blue line in comparison with the cell population profile.

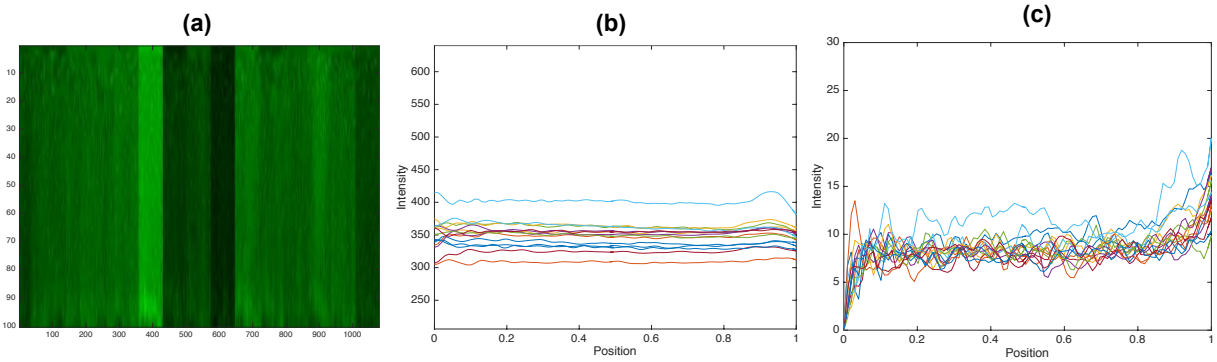

Figure 4.1.9 – Representative profiles for replica **HAA1_4** after **2 hour** in incubation in the absence of acetic acid. (a) Radial Profile (RDP) (b) Mean Profile (c) Standard Deviation (STD) Profile.

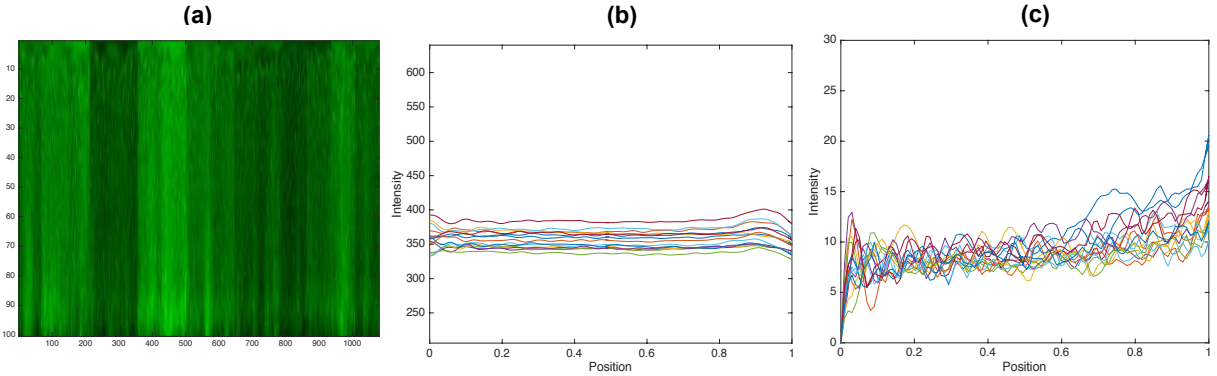

Figure 4.1.10 – Representative profiles for replica **HAA1_1** after **4 hour** in incubation in the absence of acetic acid. (a) Radial Profile (RDP) (b) Mean Profile (c) Standard Deviation (STD) Profile.

In **Figure 4.1.11** it can be seen that the level of protein abundance intensity in the mean profile and RDP is lower (between 300 and 350 in mean profile) when compared with the **Figure 4.1.8**. After 4 hours in incubation in the presence of acetic acid, the level of abundance of the Tpo3 protein is slightly higher when compared to 2 hours in incubation as shown in mean profiles and RDPs in **Figure 4.1.12** and in **Figure 4.1.13**.

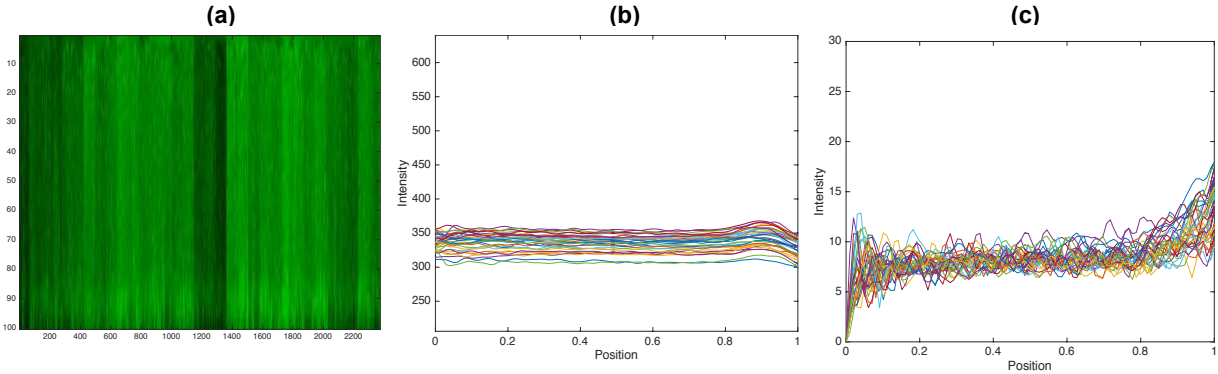

Figure 4.1.11 – Representative profiles for replica **HAA1_7** after **1 hour** in incubation in the presence of acetic acid. (a) Radial Profile (RDP) (b) Mean Profile (c) Standard Deviation (STD) Profile.

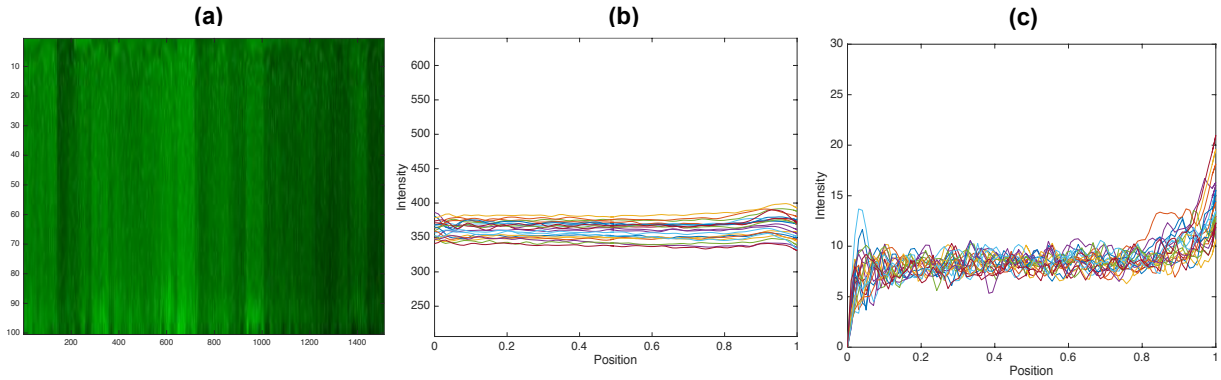

Figure 4.1.12 – Representative profiles for replica **HAA1_6** after **2 hour** in incubation in the presence of acetic acid. (a) Radial Profile (RDP) (b) Mean Profile (c) Standard Deviation (STD) Profile.

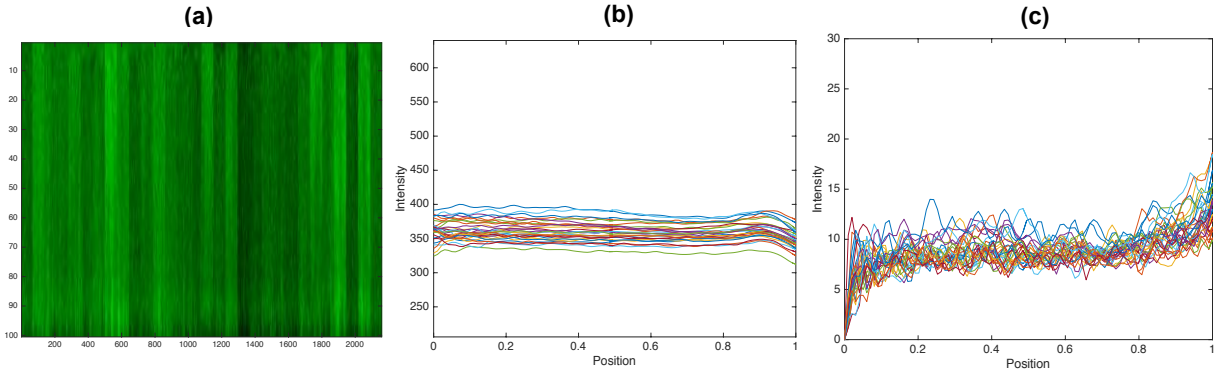

Figure 4.1.13 – Representative profiles for replica **HAA1_3** after **4 hour** in incubation in the presence of acetic acid. (a) Radial Profile (RDP) (b) Mean Profile (c) Standard Deviation (STD) Profile.

4.1.1.3. Mutant strain *hrk1Δ*

The mutant strain *hrk1Δ* it was exposed to an inhibitory sub-lethal concentration of acetic acid as well as the wild-type strain and mutant strain haa1Δ. Since this strain has a deletion in HRK1 gene, it is thus expected that the behaviour will be different when compared with the wild-type strain, considered as control. The HRK1 gene encodes a kinase belonging to family of kinases involved in the post-translational regulation of plasma membrane transporters. [2] In a first approach the deletion of this gene should interfere with cell resistance to acetic acid, but not directly in *TPO3* gene activation. The following results show that after 0 hours in incubation in the absence of acetic acid the cells expressed more Tpo3 protein than after 1 hour and 2 hours, as we can see in mean profiles and RDPs in **Figure 4.1.14** to **Figure 4.1.16**. The intensity level of Tpo3 protein abundance after 0 hours in control conditions is about 349 to 400 as illustrated in the mean profile in **Figure 4.1.14** and the level of intensity is 315 to 380 in mean profiles after 1 hour and 2 hours in incubation. As mentioned before, the location of the Tpo3 protein is in the transmembrane level, as shown in RDPs and in the peak in the mean profiles approximately at positions 0,89 and 0,91.

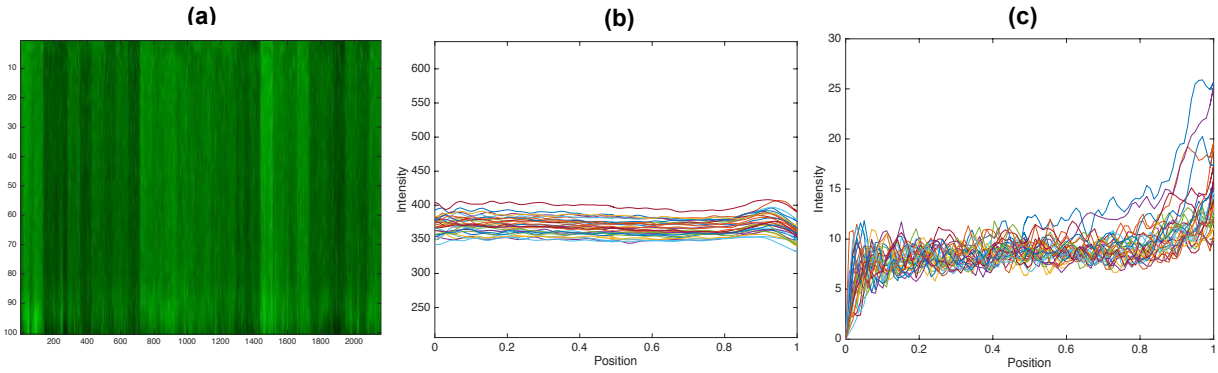

Figure 4.1.14 – Representative profiles for replica **HRK1_3** after **0 hour** in incubation. (a) Radial Profile (RDP) (b) Mean Profile (c) Standard Deviation (STD) Profile.

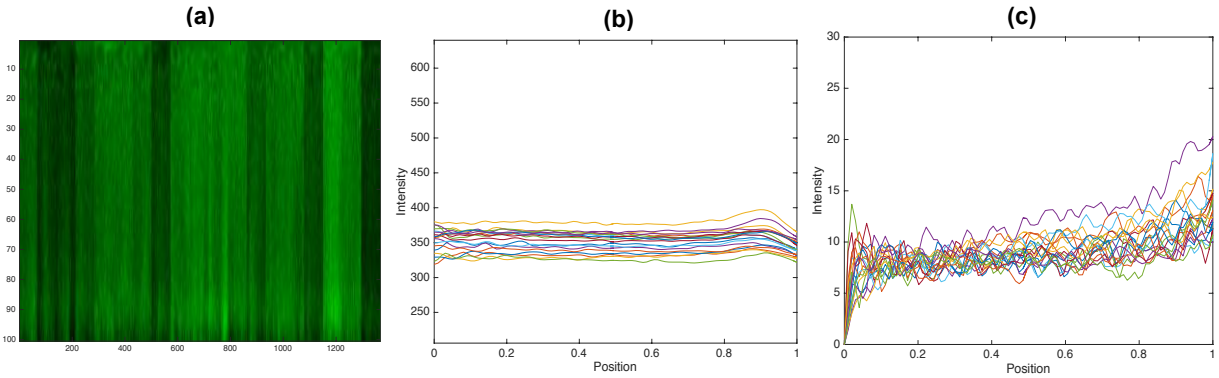

Figure 4.1.15 – Representative profiles for replica **HRK1_7** after **1 hour** in incubation in the absence of acetic acid. (a) Radial Profile (RDP) (b) Mean Profile (c) Standard Deviation (STD) Profile.

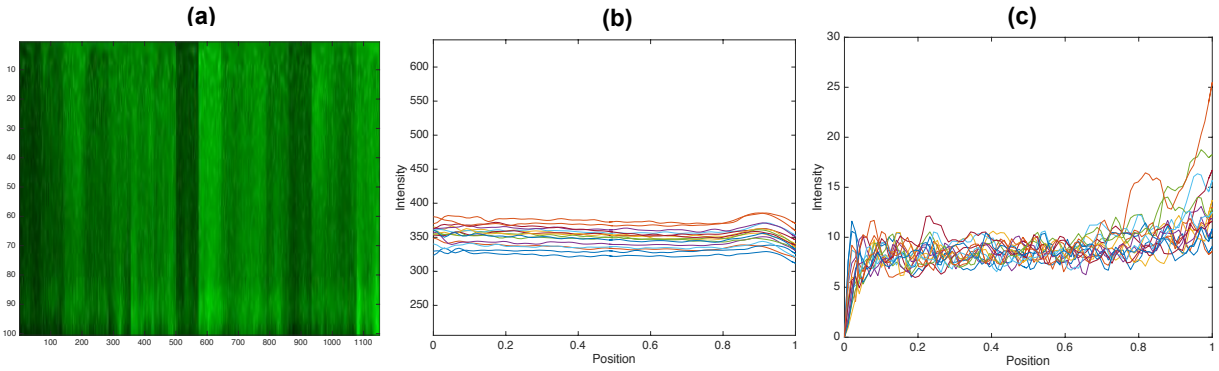

Figure 4.1.16 – Representative profiles for replica **HRK1_6** after **2 hour** in incubation in the absence of acetic acid. (a) Radial Profile (RDP) (b) Mean Profile (c) Standard Deviation (STD) Profile.

In the following results it is possible to see a different behaviour of cell population in the same conditions. After 4 hours in incubation the intensity level of Tpo3 protein abundance is higher when compared with the first hours reaching a maximum value of 449 (**Figure 4.1.18 b)**). However, in **Figure 4.1.17** the intensity level of protein abundance in the mean profile is lower in comparison with the intensity level in the mean profile in **Figure 4.1.18**. The cell population where the level of protein abundance is higher having a STD profile more heterogeneous than the other where the level of protein abundance is lower.

This one is a value example of the heterogeneity of the cell population, despite experiencing the same conditions some cells developed a different level of intensity for the Tpo3 protein.

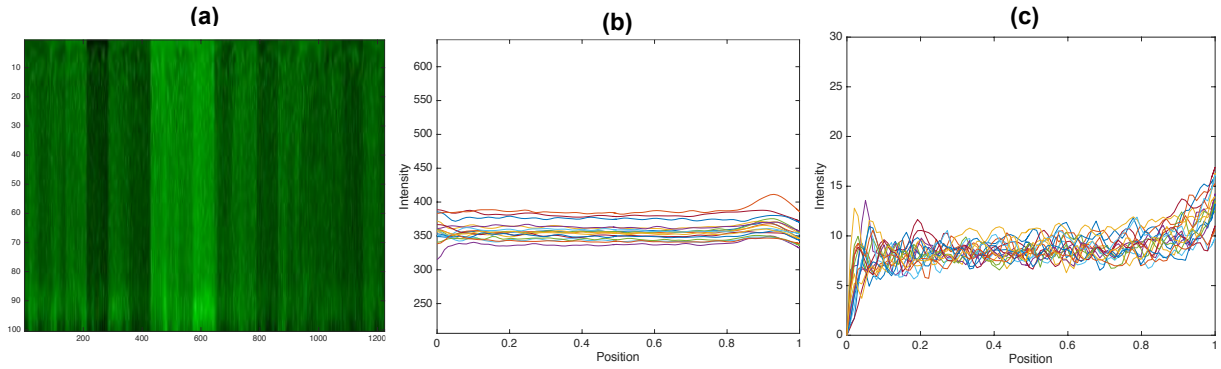

Figure 4.1.17 – Representative profiles for replica **HRK1_1** after **4 hour** in incubation in the absence of acetic acid. (a) Radial Profile (RDP) (b) Mean Profile (c) Standard Deviation (STD) Profile.

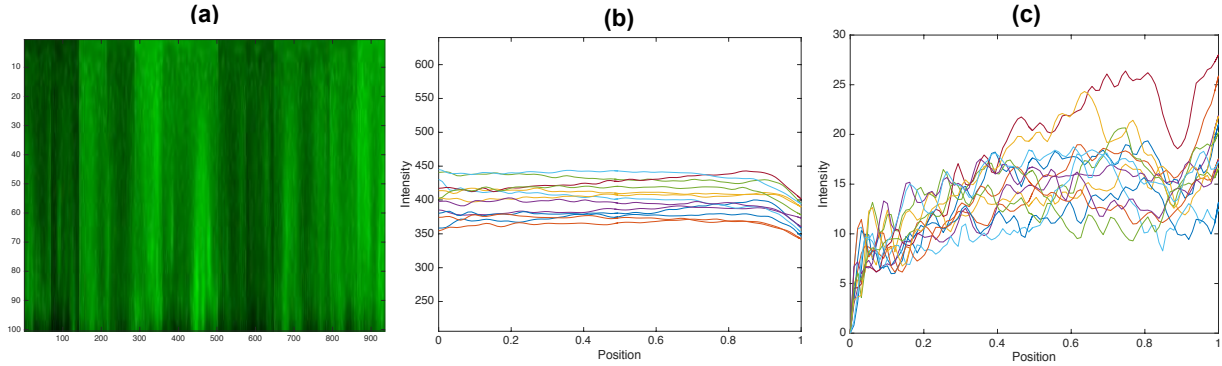

Figure 4.1.18 – Representative profiles for replica **HRK1_5** after **4 hour** in incubation in the absence of acetic acid. (a) Radial Profile (RDP) (b) Mean Profile (c) Standard Deviation (STD) Profile.

As can be seen in the following results the profiles after 1 hour and 2 hours in incubation in the presence of acetic acid are quite similar, however with further attention it is possible to see that the maximum of intensity level of protein abundance in **Figure 4.1.20** is higher than in **Figure 4.1.19**, meaning that some cells expressed more protein after 2 hours in incubation in stress conditions. On the other hand, after 4 hours in incubation the cells reveal high a level of abundance, as shown in the mean and RDP in **Figure 4.1.21** and also a high STD. As expected, the peak of intensity in protein abundance occurs at membrane.

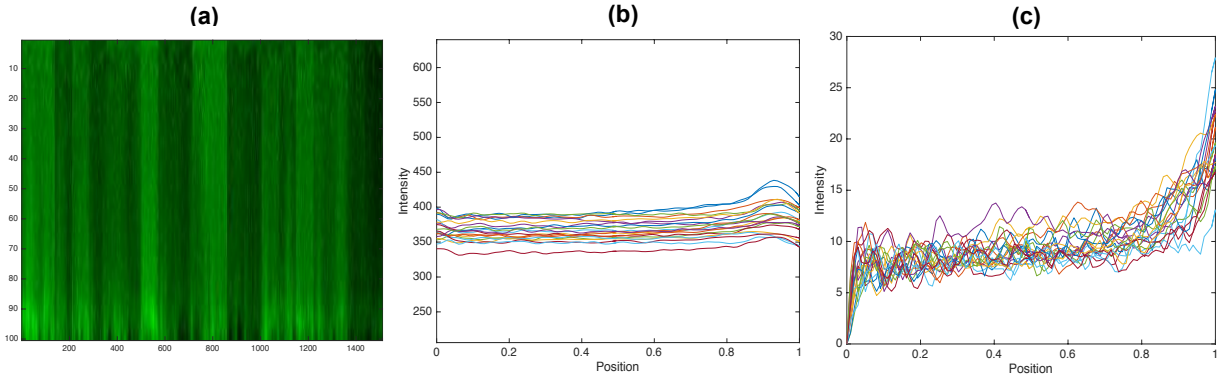

Figure 4.1.19 – Representative profiles for replica **HRK1_5** after **1 hour** in incubation in the presence of acetic acid. (a) Radial Profile (RDP) (b) Mean Profile (c) Standard Deviation Profile (STD).

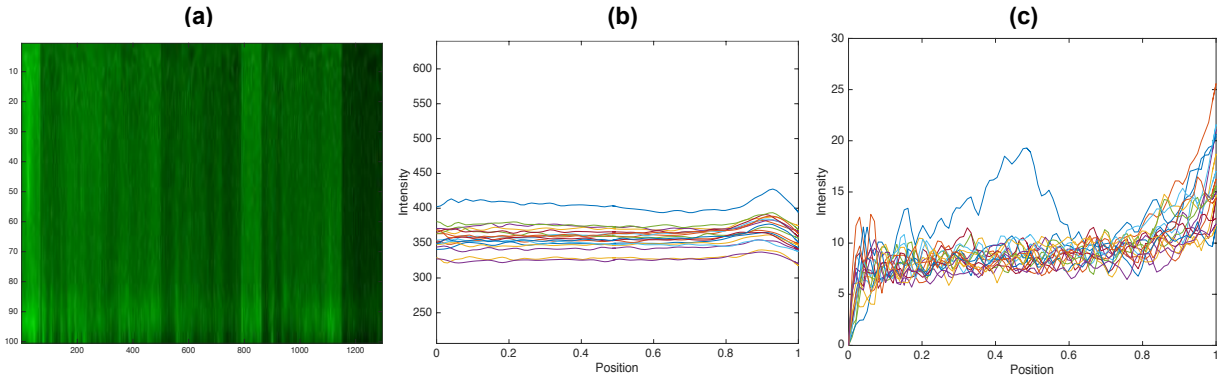

Figure 4.1.20 – Representative profiles for replica **HRK1_3** after **2 hour** in incubation in the presence of acetic acid. (a) Radial Profile (RDP) (b) Mean Profile (c) Standard Deviation Profile (STD).

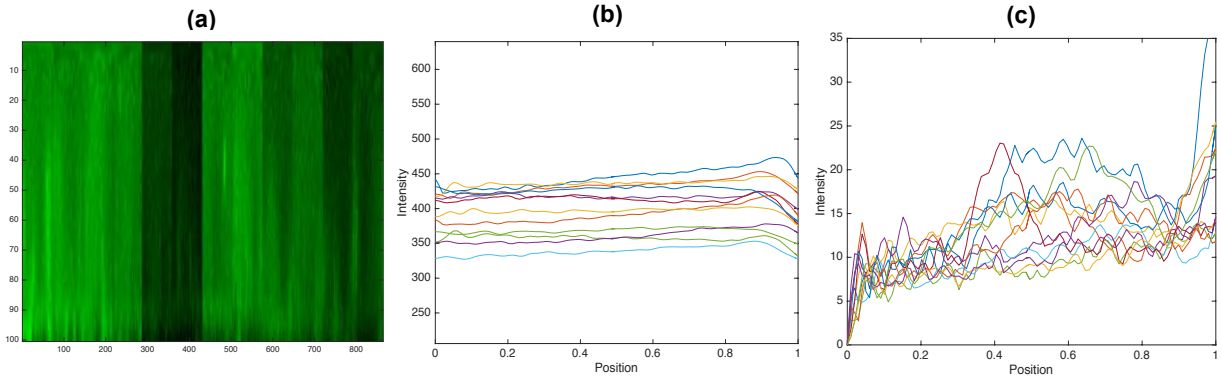

Figure 4.1.21 – Representative profiles for replica **HRK1_6** after **4 hour** in incubation in the presence of acetic acid. (a) Radial Profile (RDP) (b) Mean Profile (c) Standard Deviation Profile (STD).

4.1.2. Feature Collection

To characterize and distinguish Tpo3 protein abundance levels in RDPs, objective features were extracted from mean profiles. The features collected from the mean profile were: Membrane Maximum Intensity (MMI), position of the MMI, Cytoplasm Mean Intensity (CMI) and Intensity Differential (δ). The quantitative results of feature collection are displayed in **Table 4.1.1** and in **Figure 4.1.22**, all the results for the features were obtained through the average for each set of cells in each condition.

Table 4.1.1 – Features collected from mean profiles in the studied conditions.

Strains	Membrane Maximum Intensity (MMI)	Position of MMI	Cytoplasm Mean Intensity (CMI)	Intensity Differential (δ)
0 hours				
WT	$3{,}83\times10^{2}$	$9{,}15\times10^{-1}$	$3{,}76\times10^{2}$	$6{,}54\times10^{0}$
***haa1*Δ**	$3{,}76\times10^{2}$	$8{,}88\times10^{-1}$	$3{,}70\times10^{2}$	$4{,}66\times10^{0}$
***hrk1*Δ**	$3{,}74\times10^{2}$	$8{,}96\times10^{-1}$	$3{,}67\times10^{2}$	$6{,}98\times10^{0}$
1 hour in control condition (in the absence of acetic acid)				
WT	$3{,}72\times10^{2}$	$9{,}00\times10^{-1}$	$3{,}66\times10^{2}$	$6{,}10\times10^{0}$
***haa1*Δ**	$3{,}68\times10^{2}$	$8{,}92\times10^{-1}$	$3{,}61\times10^{2}$	$7{,}08\times10^{0}$
***hrk1*Δ**	$3{,}60\times10^{2}$	$8{,}88\times10^{-1}$	$3{,}53\times10^{2}$	$6{,}99\times10^{0}$
1 hour in stress condition (in the presence of acetic acid)				
WT	$3{,}67\times10^{2}$	$8{,}99\times10^{-1}$	$3{,}58\times10^{2}$	$8{,}28\times10^{0}$
***haa1*Δ**	$3{,}50\times10^{2}$	$9{,}06\times10^{-1}$	$3{,}43\times10^{2}$	$7{,}54\times10^{0}$
***hrk1*Δ**	$3{,}96\times10^{2}$	$9{,}13\times10^{-1}$	$3{,}76\times10^{2}$	$1{,}97\times10^{1}$
2 hours in control condition (in the absence of acetic acid)				
WT	$3{,}67\times10^{2}$	$9{,}02\times10^{-1}$	$3{,}61\times10^{2}$	$6{,}32\times10^{0}$
***haa1*Δ**	$3{,}63\times10^{2}$	$9{,}24\times10^{-1}$	$3{,}58\times10^{2}$	$5{,}15\times10^{0}$
***hrk1*Δ**	$3{,}59\times10^{2}$	$9{,}17\times10^{-1}$	$3{,}54\times10^{2}$	$5{,}69\times10^{0}$
2 hours in stress condition (in the presence of acetic acid)				
WT	$3{,}77\times10^{2}$	$9{,}26\times10^{-1}$	$3{,}63\times10^{2}$	$1{,}34\times10^{1}$
***haa1*Δ**	$3{,}65\times10^{2}$	$9{,}15\times10^{-1}$	$3{,}57\times10^{2}$	$7{,}94\times10^{0}$
***hrk1*Δ**	$3{,}77\times10^{2}$	$9{,}07\times10^{-1}$	$3{,}61\times10^{2}$	$1{,}56\times10^{1}$
4 hours in control condition (in the absence of acetic acid)				
WT	$3{,}90\times10^{2}$	$9{,}01\times10^{-1}$	$3{,}82\times10^{2}$	$8{,}10\times10^{0}$
***haa1*Δ**	$3{,}76\times10^{2}$	$8{,}97\times10^{-1}$	$3{,}68\times10^{2}$	$7{,}69\times10^{0}$
***hrk1*Δ**	$4{,}09\times10^{2}$	$8{,}75\times10^{-1}$	$4{,}02\times10^{2}$	$7{,}00\times10^{0}$
4 hours in stress condition (in the presence of acetic acid)				
WT	$4{,}43\times10^{2}$	$9{,}17\times10^{-1}$	$4{,}29\times10^{2}$	$1{,}36\times10^{1}$
***haa1*Δ**	$3{,}73\times10^{2}$	$9{,}05\times10^{-1}$	$3{,}66\times10^{2}$	$6{,}82\times10^{0}$
***hrk1*Δ**	$3{,}98\times10^{2}$	$9{,}10\times10^{-1}$	$3{,}81\times10^{2}$	$1{,}62\times10^{1}$

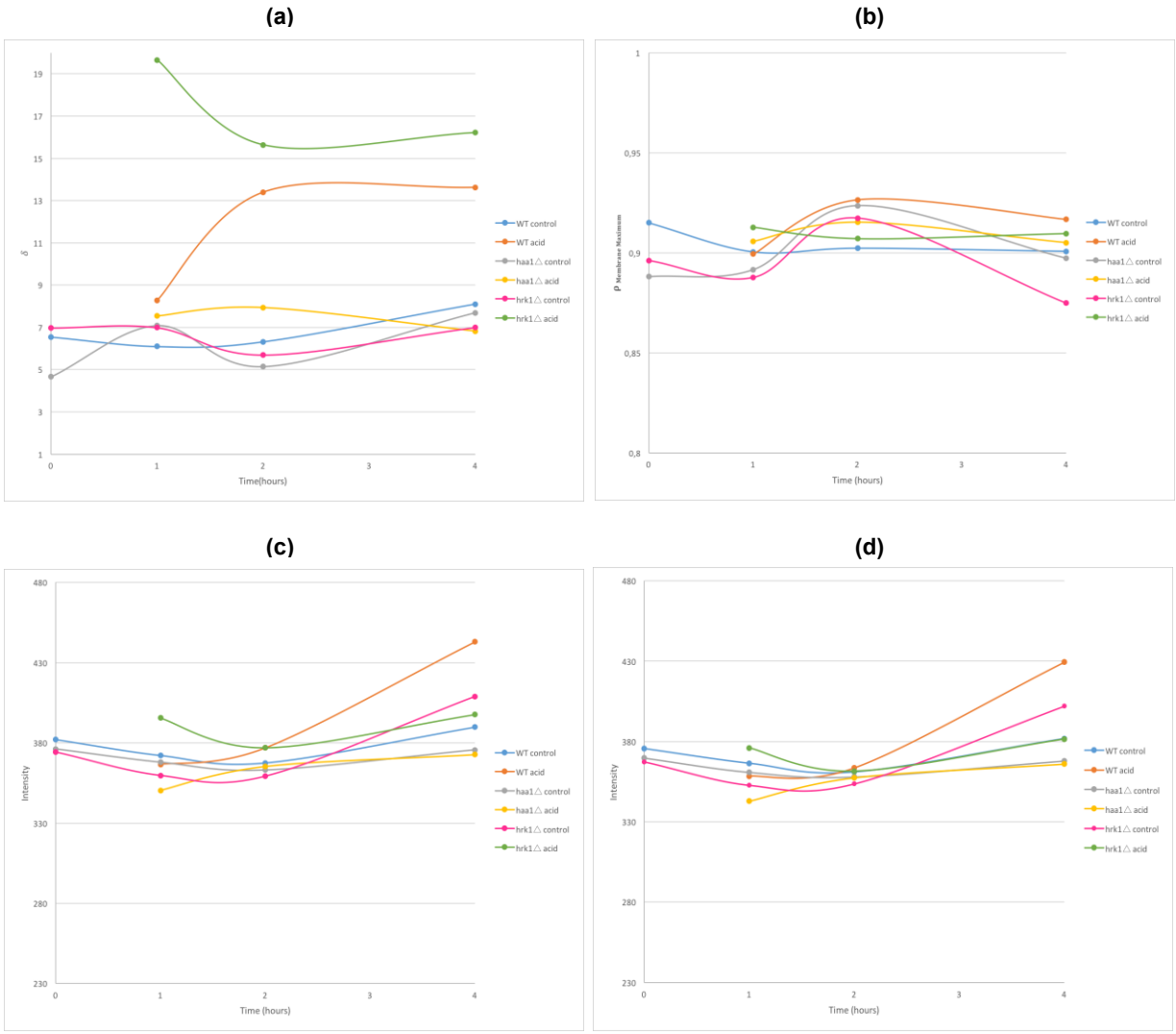

Figure 4.1.22 – Graphics with the features collected from the mean profiles. (a) The graphic represents the Intensity Differential (δ), which corresponds to the abundance of the Tpo3 transporter along the cell over the incubation time 0, 1, 2 and 4 hours under the studied conditions. **(b)** The graphic represents the Position of the Membrane Maximum Intensity, which corresponds to the position of Tpo3 transporter ($\rho_{\text{Membrane Maximum}}$) along the cell during incubation time 0, 1, 2 and 4 hours under the studied conditions. In the vertical axis the 0 means the cell centroid and 1 means the plasma membrane. **(c)** The graphic represents the Membrane Maximum Intensity, which corresponds to the Tpo3 protein maximum intensity value or expression observed in the cell membrane during the incubation time 0, 1, 2 and 4 hours under the studied conditions. **(d)** The graphic represents the Cytoplasm Mean Intensity, which corresponds to the Tpo3 protein mean intensity value or expression observed in cell cytoplasm on the incubation time 0, 1, 2 and 4 hours under the studied conditions.

4.1.3. Statistical Analysis

In this section, Mann-Whitney U (MW) tests are performed to the features selected to characterize Tpo3 protein mean profiles. The purpose of this statistical analysis is to understand the capacity of these features to discriminate between *WT* strain and the *haa1Δ* and *hrk1Δ* mutant strains. Therefore, Mann-Whitney U tests were performed comparing the *WT* strain with both mutant strains in the time course in analyse in absence or presence of acetic acid. The results of the tests performed are displayed in **Table 4.1.2**.

Besides the MW analysis, analyses of the variance of the means in the extracted features were also made, these analysis were made comparing the means of the features to WT strain with the *haa1Δ* and *hrk1Δ* mutant strains as described in **Table 4.1.3**.

Table 4.1.2 – Outcome of the MW statistical analysis of the features extracted in **Table 4.1.1**, in which H=1 indicates statistical significance and H=0 absence of it.

***WT* strain versus**	**Membrane Maximum Intensity (MMI)**	**Position of MMI**	**Cytoplasm Mean Intensity (CMI)**	**Intensity Differential (δ)**
0 hours				
***haa1*Δ strain**	H=0 $8,84\times10^{-1}$	H=0 $4,63\times10^{-1}$	H=0 $8,38\times10^{-1}$	H=0 $6,71\times10^{-1}$
***hrk1*Δ strain**	H=0 $1,00\times10^{0}$	H=0 $4,63\times10^{-1}$	H=0 $3,88\times10^{-1}$	H=0 $6,82\times10^{-1}$
1 hour in control condition (in the absence of acetic acid)				
***haa1*Δ strain**	H=0 $6,51\times10^{-1}$	H=0 $5,06\times10^{-1}$	H=0 $7,92\times10^{-1}$	H=0 $6,92\times10^{-1}$
***hrk1*Δ strain**	H=0 $3,86\times10^{-1}$	H=0 $2,86\times10^{-1}$	H=0 $6,24\times10^{-1}$	H=0 $7,34\times10^{-1}$
1 hour in stress condition (in the presence of acetic acid)				
***haa1*Δ strain**	H=0 $2,83\times10^{-1}$	H=0 $8,88\times10^{-1}$	H=0 $2,66\times10^{-1}$	H=0 $8,95\times10^{-1}$
***hrk1*Δ strain**	H=0 $2,50\times10^{-1}$	H=0 $9,52\times10^{-1}$	H=0 $4,51\times10^{-1}$	H=0 $4,17\times10^{-1}$
2 hours in control condition (in the absence of acetic acid)				
***haa1*Δ strain**	H=0 $3,94\times10^{-1}$	H=0 $3,86\times10^{-1}$	H=0 $3,49\times10^{-1}$	H=0 $9,34\times10^{-1}$
***hrk1*Δ strain**	H=0 $7,24\times10^{-1}$	H=0 $3,62\times10^{-1}$	H=0 $3,71\times10^{-1}$	H=0 $9,01\times10^{-1}$
2 hours in stress condition (in the presence of acetic acid)				
***haa1*Δ strain**	H=0 $3,70\times10^{-1}$	H=0 $6,23\times10^{-1}$	H=0 $6,46\times10^{-1}$	H=0 $6,62\times10^{-1}$
***hrk1*Δ strain**	H=0 $4,48\times10^{-1}$	H=0 $4,92\times10^{-1}$	H=0 $7,83\times10^{-1}$	H=0 $8,90\times10^{-1}$
4 hours in control condition (in the absence of acetic acid)				
***haa1*Δ strain**	H=0 $5,16\times10^{-1}$	H=0 $6,73\times10^{-1}$	H=0 $8,89\times10^{-1}$	H=0 $1,00\times10^{0}$
***hrk1*Δ strain**	H=0 $6,59\times10^{-1}$	H=0 $5,35\times10^{-1}$	H=0 $3,18\times10^{-1}$	H=0 $1,00\times10^{0}$
4 hours in stress condition (in the presence of acetic acid)				
***haa1*Δ strain**	H=0 $6,03\times10^{-1}$	H=0 $1,00\times10^{0}$	H=0 $7,36\times10^{-1}$	H=0 $8,30\times10^{-1}$
***hrk1*Δ strain**	H=0 $4,18\times10^{-1}$	H=0 $1,00\times10^{0}$	H=0 $2,71\times10^{-1}$	H=0 $9,50\times10^{-1}$

Table 4.1.3 – Outcome of the F-test statistical analysis of the features extracted in **Table 4.1.1**, in which H=1 indicates statistical significance and H=0 absence of it

***WT* strain versus**	**Membrane Maximum Intensity (MMI)**	**Position of MMI**	**Cytoplasm Mean Intensity (CMI)**	**Intensity Differential (δ)**
0 hours				
***haa1*Δ strain**	H=0 $1{,}64\times10^{-1}$	H=0 $1{,}24\times10^{-1}$	H=0 $2{,}04\times10^{-1}$	H=0 $3{,}31\times10^{-1}$
***hrk1*Δ strain**	**H=1** $\mathbf{4{,}69\times10^{-2}}$	**H=1** $\mathbf{2{,}21\times10^{-2}}$	H=0 $7{,}42\times10^{-2}$	H=0 $2{,}22\times10^{-1}$
1 hour in control condition (in the absence of acetic acid)				
***haa1*Δ strain**	H=0 $1{,}37\times10^{-1}$	**H=1** $\mathbf{2{,}69\times10^{-2}}$	H=0 $2{,}93\times10^{-1}$	H=0 $7{,}17\times10^{-1}$
***hrk1*Δ strain**	**H=1** $\mathbf{1{,}01\times10^{-2}}$	H=0 $6{,}94\times10^{-1}$	**H=1** $\mathbf{1{,}40\times10^{-2}}$	H=0 $9{,}20\times10^{-1}$
1 hour in stress condition (in the presence of acetic acid)				
***haa1*Δ strain**	**H=1** $\mathbf{7{,}78\times10^{-3}}$	**H=1** $\mathbf{4{,}50\times10^{-2}}$	**H=1** $\mathbf{1{,}80\times10^{-2}}$	**H=1** $\mathbf{1{,}27\times10^{-2}}$
***hrk1*Δ strain**	H=0 $9{,}70\times10^{-1}$	H=0 $1{,}37\times10^{-1}$	H=0 $7{,}88\times10^{-1}$	H=0 $6{,}33\times10^{-1}$
2 hours in control condition (in the absence of acetic acid)				
***haa1*Δ strain**	H=0 $1{,}46\times10^{-1}$	H=0 $1{,}19\times10^{-1}$	H=0 $1{,}21\times10^{-1}$	**H=1** $\mathbf{3{,}49\times10^{-2}}$
***hrk1*Δ strain**	H=0 $3{,}87\times10^{-1}$	H=0 $2{,}28\times10^{-1}$	H=0 $2{,}55\times10^{-1}$	H=0 $4{,}70\times10^{-1}$
2 hours in stress condition (in the presence of acetic acid)				
***haa1*Δ strain**	H=0 $9{,}07\times10^{-1}$	H=0 $9{,}08\times10^{-1}$	H=0 $7{,}64\times10^{-1}$	H=0 $3{,}02\times10^{-1}$
***hrk1*Δ strain**	H=0 $9{,}44\times10^{-1}$	H=0 $2{,}29\times10^{-1}$	H=0 $6{,}70\times10^{-1}$	H=0 $8{,}04\times10^{-1}$
4 hours in control condition (in the absence of acetic acid)				
***haa1*Δ strain**	H=0 $5{,}79\times10^{-1}$	**H=1** $\mathbf{9{,}10\times10^{-2}}$	H=0 $7{,}16\times10^{-1}$	H=0 $8{,}74\times10^{-1}$
***hrk1*Δ strain**	H=0 $4{,}95\times10^{-1}$	H=0 $8{,}50\times10^{-1}$	H=0 $4{,}33\times10^{-1}$	H=0 $4{,}78\times10^{-1}$
4 hours in stress condition (in the presence of acetic acid)				
***haa1*Δ strain**	H=0 $2{,}38\times10^{-1}$	H=0 $7{,}80\times10^{-1}$	H=0 $2{,}03\times10^{-1}$	H=0 $1{,}41\times10^{-1}$
***hrk1*Δ strain**	H=0 $3{,}02\times10^{-1}$	H=0 $3{,}95\times10^{-1}$	H=0 $2{,}96\times10^{-1}$	H=0 $8{,}94\times10^{-2}$

4.2. Discussion

In this section, all the results related to the abundance of Tpo3 protein are discussed in an integrated manner in order to clarify their ability to understand the behaviour of the *wild-type* strain in comparison with the mutant strains under the studied conditions.

Acetic acid is one of the most commonly used food preservatives and an important inhibitor in many industrial fermentation processes, so it became important understand and examine the response of the *Saccharomyces cerevisiae* to this acid. The understanding of the molecular mechanisms underlying *S. cerevisiae* tolerance to these weak acid is essential for the rational selection of optimal fermentation conditions and for the development of more robust industrial strains to be used in industrial processes such as wine and bioethanol production.

In a medium with pH below the acetic acid pk_a, this weak acid is mainly in its undissociated lipophilic form, which is able to diffuse across the cell membrane of yeast, in these conditions the yeast cell is under stress so develops strategies to overcome the low intracellular pH (pH_i). One of the strategies is the activation of the transcription of the Major Facilitator Superfamily (MFS) transporter Tpo3, this process is highly dependent on the presence of acetic acid as well as the presence of the transcription factor Haa1 protein as illustrated *in* **Figure 2.3.1**. The Tpo3 transporter has a key role in the expulsion of acetate from the cytosol, protecting the cell immediately following acid aggression, thus contributing to the reduction of the lag phase. Based on this approach it is expected that the concentration of Tpo3 protein in the cell membrane increases during cell growth and adaptation in order to counteract the negative effects from acetic acid stress. In this work the growth of the yeast cells in the first four hours in batch cultivation was analysed. During this period, while the cells are in the latency phase or lag phase, this is the period of time following the inoculation of the cell culture and is usually when the cells have to adapt to the new conditions. During this initial stage, the cell multiplication cannot occur, at least in equilibrium conditions.

The analysis of the genomic expression in yeast in response to acetic acid was made and it is possible have an idea about the behaviour of the *wild-type* strain and the mutant strains in the presence and absence of acetic acid. The *TPO3* gene, encoding a multidrug resistance transporter, was found to be induced in response to a range of weak acids, indicating that the existence of a general weak acid response is rather limited in yeast cells. So far, a few studies have tried to clarify the role of the *HRK1* gene in yeast cell resistance to acetic acid and it is well known that this gene encodes a kinase involved in the regulation of the Tpo3 transporter but this process is not yet fully understood. Hrk1 protein was proposed to be a positive regulator of plasma membrane H^+-ATPase activity in response to glucose metabolism, and may be involved in the reduction of the intracellular acetate concentration through the activation of the Tpo3 transporter. The elimination of this gene led to a strong susceptibility phenotype to acetic acid. [2]

In contrast, several studies have demonstrated the key role played by the Haa1 protein in yeast's response to acetic acid. The Haa1 protein was found to regulate, directly or indirectly, the transcription

of approximately 80% of the acetic acid-activated genes, suggesting that Haa1 protein is the main player in the control of yeast response to acetic acid being the *TPO3* gene a target of the Haa1 protein. [2] Moreover, studies suggest that *TPO3* transcription activation occurs during an acid-induced lag phase, this activation being dependent, although not exclusively, on the presence of the Haa1 protein. Beside this, the Haa1 protein -regulated gene, *TPO3* was found to play some role in yeast resistance to acetic acid, by protecting the cell immediately following acid aggression, thus contributing to the reduction of the duration of the lag phase. [15] Moreover, it was demonstrated that in the absence of acetic acid stress, the elimination of the *HAA1* gene only had a slight effect on the yeast transcriptome: 11genes exhibited an increased expression level in *haa1Δ* cells and the level of 15 transcripts was decreased in this mutant strain, suggesting that a major impact in the *haa1Δ* mutant strain occurs in the presence of acetic acid. [2]

Considering the above mentioned point, it was thus expected that the level of abundance of Tpo3 protein decreases in the *haa1Δ* strain, mainly in the presence of acetic acid stress.

It should be noted that the results shown in this chapter only represents part of the results, those remaining are exposed in Appendix A, the considerations were made only to the more significantly results, a widely vision of the results can be obtained through analysis of all the profiles in all replicas and the features extracted as illustrated in **Figure 4.1.22**.

Overall, in the results it can be observed that the cells exhibit different behaviours inside the cell population, as mentioned above during the lag phase the cells are in constant adaptation to the surrounding environment. It was observed in the profiles, particularly in the mean profiles that some cells adapt better than others and that is clearly evident in the intensity level of Tpo3 protein under the different analysed conditions.

The **Figure 3.1.1** shows the growth curves in the presence and absence of acetic acid of the wild type and mutant strains during batch cultivation, and through the observation of the curves it appears that in the absence of acetic acid the *wild- type* strain is the more adapted and the mutant strains also show an acceptable growth rate in comparison, consistent with the fact that cells are not under stress. The supplementation of the medium with 50 mM acetic acid, led to an increase of yeast growth inhibition, and the *hrk1Δ* mutant strain is the most susceptible, with a lower rate of cell growth. The mutant strains harvested in the presence of acetic acid have a higher lag phase when compared with the strains in the control condition. After 2 hours in incubation the *wild-type* strain enters the exponential phase while the mutant strains in acid conditions are still in the lag phase with a duration of approximately 9 hours. The increased susceptibility to acetic acid of the *haa1Δ* and *hrk1Δ* mutants, suggests that the deletion of the *HAA1* and *HRK1* genes may affect yeast's resistance to this weak acid.

The obtained profiles show generally coherent results, however with some dispersion in the behaviour of several cells inside the cell population, which means that some cells were in a different stage of adaptation and maturity that is noticed in the Tpo3 protein level of abundance in the mean profiles and RDPs as well as in the STD profiles. The mean profiles show that the *haa1Δ* mutant strain expressed less protein than wild-type strain both in the control condition and acetic acid stress condition, as expected.

Concerning the features extracted, in **Table 4.1.1** the quantification of the maximum intensity of protein abundance in membrane is described, the location in the cell of the maximum membrane intensity, the mean intensity expressed in cell cytoplasm and the intensity differential, these features are relevant to give an overview of the level of protein abundance in the cell and its location. It is important to highlight that the features were calculated based on the average of each cell analysed, so these results show the average behaviour of the cells under the studied conditions.

A statistical analysis of features based on the MW test was performed and the results exposed in **Table 4.1.2** show that they are not statistically significant, which means that the means of the features do not differ significantly, since the results show high p-values. The features do not discriminate perfectly between the *wild-type* strain and the mutant strains. The null hypothesis was not refuted so the conclusion is there are no statistically significant differences in the means analysed. It is important to highlight that these results cannot be crucial for the importance of the features extracted, the results indeed show high p-values but it could result from a great range of causes.

Usually it is very easy to confuse statistical significance with theoretical or substantive significance, but in fact they are different, it is important to recognize the differences between statistical significance and practical significance. The p-value cannot inform us about the magnitude of the effect of X on Y, the p-value cannot help us to choose which variable explains the most. So, in this particular case it is not totally unreasonable that there are no significant differences in the means since the means are in fact very similar. This result may be due to the low quantity of data used to perform this analysis as well as the short time course used.

A statistical analysis of the variance of the means in features was performed in order to achieve a better understanding of the variance of the population of cells analysed. For a p–value below the significance level – 0,05 the null hypothesis will be rejected, and the opposite if the p–value is higher than 0,05. Different levels of significance can occur, but the results observed are statistically significant if the alternative hypothesis is accepted (h=1), meaning that there are differences in variances of the means tested.

Considering the F-test described in **Table 4.1.3** the results revealed statistical significance differences for the features extracted for the *haa1Δ* mutant strain after 1 hour in incubation in the presence of acetic acid being higher than the *wild-type* strain. Taking into account a biological point of view, the mutation in the *HAA1* gene leads to a decrease of Tpo3 protein abundance, thereby increasing the cell susceptibility to acetic acid, and this appears be related to the variance and heterogeneity between the mutant strain and the parental strain.

Furthermore, the obtained results for the p-value reveal that for membrane maximum intensity (MMI) feature there are evidently statistically significant differences in the variance of the means for the *hrk1Δ* mutant strain after 0 hours and 1 hour in incubation in control condition in comparison with the *wild-type* cell line in the same condition. In addition, position of MMI discriminate perfectly between the *haa1Δ* mutant form and *wild-type* form after 1 hour and 4 hours in absence of acetic acid as well as for *hrk1Δ* mutant form after 1 hour in incubation in absence of acetic acid stress. A lower discrimination between the mutants strains and *wild-type* strain in the remaining conditions were also obtained, where the p-

value is higher than the significance level considered, as noted in **Table 4.1.3**. This result may be due to the low quantity of data used to perform this analysis as well as the short time course used.

The statistical analysis with F-test shows that both membrane maximum intensity (MMI) and the position of MMI are the features with a higher statistical significance.

With regard to the abundance of Tpo3 protein along the cells (see **Figure 4.1.22 a)**), after 4 hours in incubation the tested strains reveal an increase in the expression except the *haa1Δ* and *hrk1Δ* strains in the presence of acetic acid. The strain that appeared to have a significantly high level of expression during the 4 hours is the *hrk1Δ* strain in the presence of acetic acid.

It can be seen that acid-challenged cells expressed more Tpo3 protein during the incubation period analysed, that could possibly be a defence mechanism against the stress they are experiencing. These observations also suggest that the deletion of the *HRK1* gene appears not to be directly related with the Tpo3 protein abundance, as expected in the deletion of *HAA1* gene, since the level of abundance is higher than the *wild-type* strain under the same conditions.

Concerning the location of the membrane maximum protein (see **Table 4.1.1** and **Figure 4.1.22 b)**), all the results show that the Tpo3 protein is expressed and directed to the plasma membrane during the cell growth. There are quantitative differences between the conditions on the position of the protein membrane maximum but in general the protein is located in the plasma membrane, as expected. However, the analysis of the **Figure 4.1.22 b)** reveals that the protein location reaches its maximum (0,91 to 0,93) after 2 hours in incubation for the wild-type strain in the presence of acetic acid, for the the *haa1Δ* strain and for the *hrk1Δ* strain in the absence of acetic acid. For the *wild-type* strain in control conditions the location of the protein is uniform between 2 and 4 hours in incubation and for the *hrk1Δ* mutant strain in stress conditions the location of the protein is uniform throughout the incubation period.

Furthermore, the obtained radial profiles as well as the mean profiles are coherent, showing that after 4 hours in incubation almost all the cells reveal an increase in Tpo3 protein abundance. Taking into account the results show in **Figure 4.1.22 c)** and **d)**, the wild-type strain in the presence of acetic acid after 4 hours in incubation is the strain where the abundance of the protein is higher, followed by the *hrk1Δ* mutant strain under the same conditions.

Finally, regarding the Tpo3 protein abundance, a significant outcome was obtained with the approach based on radial and mean profiles, since the Tpo3 protein abundance is higher in the parental strains when compared with the *haa1Δ* mutant strain. Furthermore, the RD and mean profiles also show that the *hrk1Δ* mutant strain has an increase in Tpo3 protein abundance after 1 hour in the presence of acetic acid and after 4 hours in the absence of acetic acid when compared with the parental strain.

Overall, the mutant strains showed an increase in cell susceptibility in the presence of acetic acid when compared with the *wild-type* strain, suggesting the importance of the Haa1 protein and Hrk1 protein in *Saccharomyces cerevisiae* tolerance to acetic acid.

5

Conclusions and Future Work

Throughout this dissertation several conclusions were drawn, namely about Tpo3 protein molecular distribution within the cell, level of Tpo3 protein abundance in the cell and about the efficiency of the software developed.

The major advantage of developed software regarding several others, is the possibility to do a quantitative analyse of the protein abundance within the cells, while the fluorescence images only enable a qualitative analyse of the protein abundance in the cells. This software could be very useful to biologists to quantify the level of transcripts of interest in a specific organelle in cell and condition. Moreover, this technique has potential to analyse more organelles within the cell besides the cell membrane and should be interesting do a different staining of each organelle of interest in conventional fluorescence images or confocal images to allow the extraction of data in different focal planes.

An overcome in this technique is the manual segmentation, the segmentation process should be improved in order to be automatic, and this way enable the selection of the organelle in interest for the biologist.

In respect to the results obtained, although in this study it was used exclusively FM images, there is no evidence that this software is not functional in other kinds of imaging cell. A further study in order to quantify the level of intercellular acetate during the growth can be done.

The work developed in this dissertation can still be improved, namely in the time course used that should be longer. In RD analysis, due to the insufficient number of images processed, some results were not clear. In this thesis, the number of images processed was limited by the number of *in vitro* assays developed. To improve and validate the biological results obtained, the number of images processed by this method has to be increased.

Finally, considering the results obtained by the RD and mean profiles, the *wild-type* strain showed a higher level of Tpo3 protein abundance after 4 hours in incubation in the presence of acetic acid when compared with the *haa1Δ* and *hrk1Δ* mutants strains. The results also show that the *haa1Δ* mutant line has less protein abundance namely in stress conditions, suggesting that the *HAA1* gene is a direct regulator in the *TPO3* gene activation. However, the *TPO3* gene is not only dependent of the Haa1 protein and the Hrk1 protein.

Through a careful analyse of all the profiles it can be observed that the *hrk1Δ* mutant line show higher levels of protein abundance in membrane when compared with the other mutant line, this result could suggest that the *TPO3* gene has not a direct target of the Hrk1 protein.

However, some studies reveal that the Hrk1 protein is important in Tpo3 protein regulation. Considering this approach, a study where the functionality of Tpo3 protein is tested specially in the *hrk1Δ* mutant strain can be done.

References

[1] N. P. Mira, M. C. Teixeira and I. Sá-Correia, “Adaptative Response and Tolerance to Weak Acids in Saccharomyces cerevisiae: A Genome-Wide View,” *A Journal of Integrative Biology,* vol. 14, 2010.

[2] N. P. Mira, B. J. D. and I. Sá-Correia, “Genomic Expression Program Involving the Haa1 protein -Regulon in Saccharomyces cerevisiae Response to Acetic Acid,” *A Journal of Integrative Biology,* vol. 14, 2010.

[3] N. P. Mira, M. Palma, J. F. Guerreiro and I. Sá-Correia, “Genome-wide identification of Saccharomyces cerevisiae genes required for tolerance to acetic acid,” *Microbial Cell Factories,* 2010.

[4] J. Eglinton and P. Henschke, “Restarting incomplete fermentations: the effect of highconcentrations of acetic acid,” *Australian Journal of Grape and Wine Research 5,* pp. 71-78, 1999.

[5] D. A. Abbott, T. A. Knijnenburg, L. M. d. Poorter, M. J. Reinders, J. T. Pronk and A. J. v. Maris, “Generic and specific transcriptional responses to diferent weak organic acids in anaerobic chemostat cultures of Saccharomyces cerevisiae,” *Federation of European Microbiological Societies,* 30 April 2007.

[6] E. Palmqvist and B. Hahn-Hagerdal, “Fermentation of lignocellulosic hydrolysates. I: inhibition and detoxification,” *Bioresour Technol,* vol. 74, 2000.

[7] A. Querol and G. H. Fleet, Yeasts in Food and Beverage, vol. 2, Springer.

[8] G. H. Fleet, “Yeasts in foods and beverages: impact on product quality and safety,” *Elsevier,* 1 February 2007.

[9] S. C. dos Santos, M. C. Teixeira, P. J. Dias and I. Sá-Correia, “MFS transporters required for multidrug/multixenobiotic (MD/MX) resistance in the model yeast: understanding their physiological function through post-genomic approaches,” *Frontiersin,* vol. 5, 8 May 2014.

[10] S. C. dos Santos and I. Sá-Correia, “Yeast toxicogenomics: lessons from a eukaryotic cell model and cell factory,” *Elsevier,* pp. 183-191, 24 March 2015.

[11] M. Mollapour, A. Shepherd and P. W. Piper, “Novel stress responses facilitate Saccharomyces cerevisiae growth in the presence of the monocarboxylate preservatives,” *Yeast,* pp. 169-177, 2008.

[12] V. Carmelo, H. Santos and I. Sá-Correia, " Effect of extracellular acidification on the activity of plasma membrane ATPase and on the cytosolic and vacuolar pH of Saccharomyces cerevisiae," *Biochimica et Biophysica Acta 1325,* pp. 63-70, 1997.

[13] N. S. Sanchez, D. E. Castro, M. Calahorra, G. A. Martínez and A. Pena, "Yeast Plasma Membrane and Vacuolar H+- ATPases," *Nova Science Publishers, Inc,* 2012.

[14] N. P. Tenreiro S, N. M. Viegas CA, C. M. Teixeira MC and I. Sá-Correia, "AQR1 gene (ORF YNL065w) encodes a plasma membrane transporter of the major facilitator superfamily that confers resistance to short-chain monocarboxylic acids and quinidine in Saccharomyces cerevisiae.," *Biochem Biophys Res Commun,* pp. 741-748, 2002.

[15] A. Fernandes, N. Vargas, R. Canelhas and I. Sá-Correia, "Saccharomyces cerevisiae adaptation to weak acids involves the transcription factor Haa1 protein and Haa1 protein - regulated genes.," *Biochem Biophys Res Comm,* pp. 95-103, 2005.

[16] T. Simões, N. Mira, A. Fernandes and I. Sá-Correia, "The SPI1 gene, encoding a glycosylphosphatidylinositol (GPI)-anchored cell wall protein, plays a prominent role in the developent of yeast resistance to lipophilic weak acids food preservatives," *Appl Environ Microb 72, 7168-7175.*

[17] M. Mollapour and P. W. Piper, "Hog1 Mitogen-Activated Protein Kinase Phosphorylation Targets the Yeast Fps1 Aquaglyceroporin for Endocytosis, Thereby Rendering Cells Resistant to Acetic Acid," *Molecular and Cellular Biology,* vol. 27(18), p. 6446–6456, september 2007.

[18] B. Almeida, S. Ohlmeier, A. J. Almeida, F. Madeo, C. Leão, F. Rodrigues and P. Ludovico, "Yeast protein expression profile during acetic acid-induced apoptosis indicates causal involvement of the TOR pathway," *Proteomics 9, 720-732,* 2009.

[19] P. Ludovico, M. João Sousa, M. T. Silva, C. Leão and M. Côrte-Real, "Saccharomyces cerevisiae commits to a programmed cell death process in response to acetic acid," *Microbiology 147, 2409-2415,* 2001.

[20] D. C. Gutierrez, T. Eisenberg, S. Buttner, C. Meisinger, G. Kroemer and F. Madeo, "Apoptosis in yeast: triggers, pathways, subroutines," *Cell Death and Differentiation 17, 763-773,* 2010 .

[21] M. Sousa, P. Ludovico, F. Rodrigues, C. Leão and M. Côrte-Real, "Stress and Cell Death in Yeast Induced by Acetic Acid," *ResearchGate,* 2012.

[22] P. Ludovico, F. Rodrigues, A. Almeida, M. T. Silva, A. Barrientos and M. Côrte-Real, "Cytochrome c Release and Mitochondria Involvement in Programmed Cell Death Induced by Acetic Acid in Saccharomyces cerevisiae," *Molecular Biology of the Cell 2598-2606,* vol. 13, 2002.

[23] C. Pereira, S. Chaves, S. Alves, B. Salin, N. Camougrand, S. Manon, M. João Sousa and M. Côrte-Real, "Mitochondrial degradation in acetic acid-induced yeast apoptosis: the role of Pep4 and the ADP/ATP carrier," *Molecular Microbiology 76(6), 1398-1410,* 2010.

[24] N. Guaragnella, L. Antonacci, S. Passarella, E. Marra and S. Giannattasio, “Hydrogen Peroxide and Superoxide Anion Production during Acetic Acid-Induced Yeast Programmed Cell Death,” *Folia Microbiol. 52 (3), 237-240,* 2007.

[25] C. Schuller, Y. M. Mamnun, M. Mollapour, G. Krapf, M. Schuster, B. E. Bauer, P. W.Pper and K. Kuchler, “Global Phenotypic Analysis and Transcriptional Profiling Defines the Weak Acid Stress Response Regulon in Saccharomyces cerevisiae,” *Molecular Biology of the Cell 706-720,* vol. 15, February 2004.

[26] P. Piper, C. Ortiz Calderon, K. Hatzixanthis and M. Mollapour, “Weak acid adaptation: the stress response that confers yeasts with resistance to organic acid food preservatives,” *Microbiology 147, 2635-2642,* 2001.

[27] K. G, R. E., B. P.O. and W. D.R., “Haa1, a protein homologous to the copper-regulated transcription factor Ace1, is a novel transcriptional activator.,” *J Biol Chem 276, 38697-38702,* 2001.

[28] N. P. Mira, S. F. Henriques, G. Keller, M. C. Teixeira, R. G. Matos, C. M. Arraiano, D. R. Winge and I. Sá-Correia, “Identification of a DNA-binding site for the transcription factor Haa1, required for Saccharomyces cerevisiae response to acetic acid stress,” *6896 - 6907 Nucleic Acids Research ,* vol. 39 No. 16, 2011.

[29] H. R. Petty, “Fluorescence Microscopy: Established and Emerging Methods, Experimental Strategies, and Applications in Immunology,” *Microscopy Research and Technique 70: 687-709 ,* 2007.

[30] H. C. Ishikawa-Ankerhold, R. Ankerhold and G. P. C. Drummen, “Advanced Fluorescence Microscopy Techniques—FRAP, FLIP, FLAP, FRET and FLIM,” *Molecules 17(4), 4047-4132,* 2012.

[31] G. Software. [Online]. Available: http://www.graphpad.com/support/ faqid/1790/. [Accessed 31 Outubro 2016].

[32] L. Statistics. [Online]. Available: https://statistics.laerd.com/ statistical-guides/independent-T-test-statistical-guide.php. [Accessed 31 October 2016].

[33] H. Motulsky, "Intuitive biostatistics: a nonmathematical guide to statistical thinking", Oxford University Press, 2013.

[34] MathWorks. [Online]. Available: http://www.mathworks.com/help/stats/ ranksum.html. [Accessed 31 October 2016].

Profiles

A.1. Error Bar Profiles

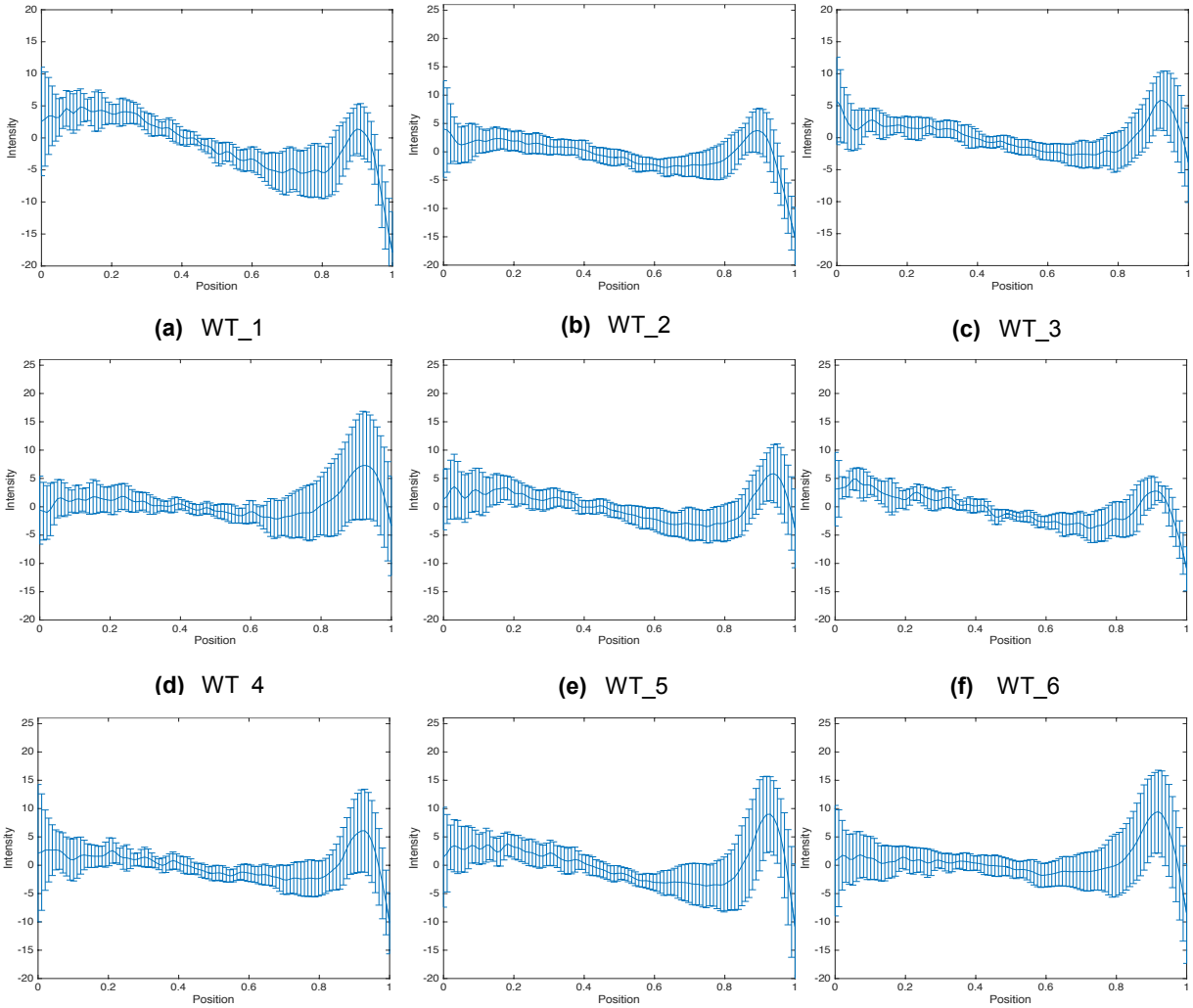

(a) WT_1 **(b)** WT_2 **(c)** WT_3

(d) WT 4 **(e)** WT_5 **(f)** WT_6

(g) WT_7 **(h)** WT_8 **(i)** WT_9

Figure A.1 – Error bar profiles for all replicas of *WT* strain after 0 hours in incubation.

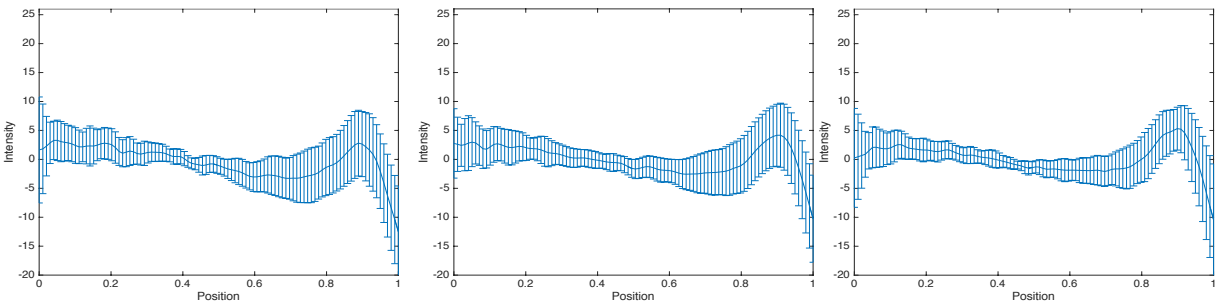

(a) HAA1_1 **(b)** HAA1_2 **(c)** HAA1_3

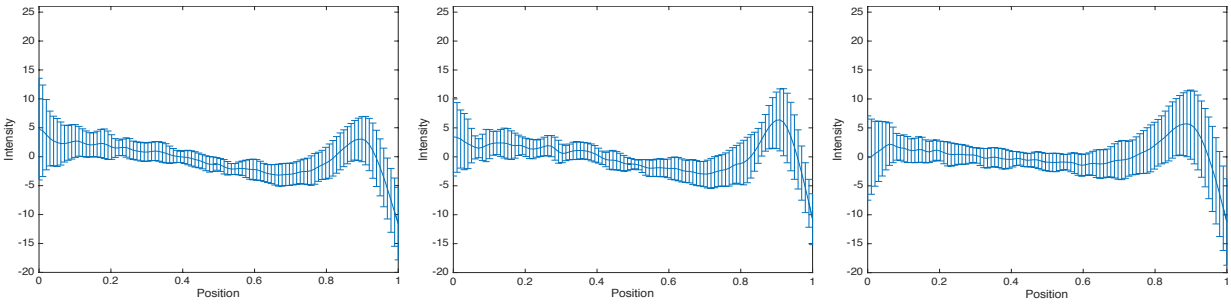

(d) HAA1_4 **(e)** HAA1_5 **(f)** HAA1_6

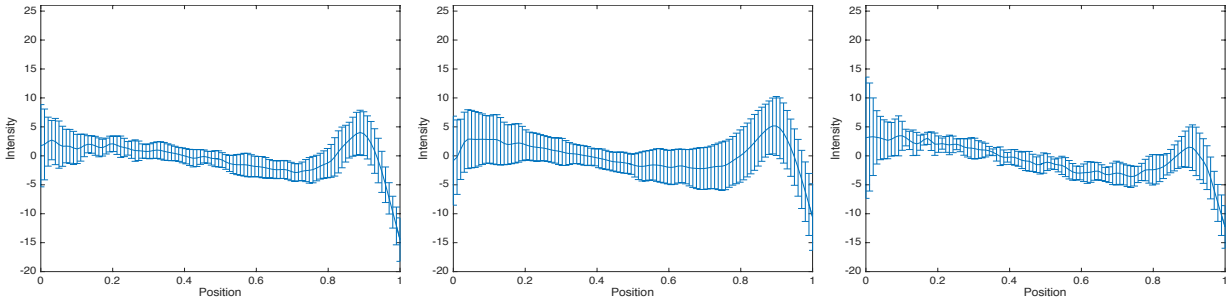

(g) HAA1_7 **(h)** HAA1_8 **(i)** HAA1_9

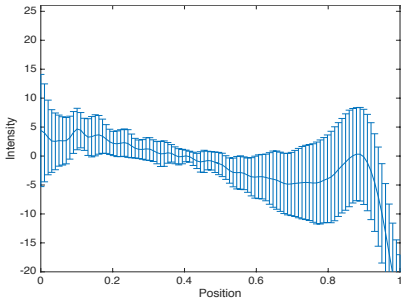

(j) HAA1_10

Figure A.2 – Error bar profiles for all replicas of *HAA1* strain after 0 hours in incubation.

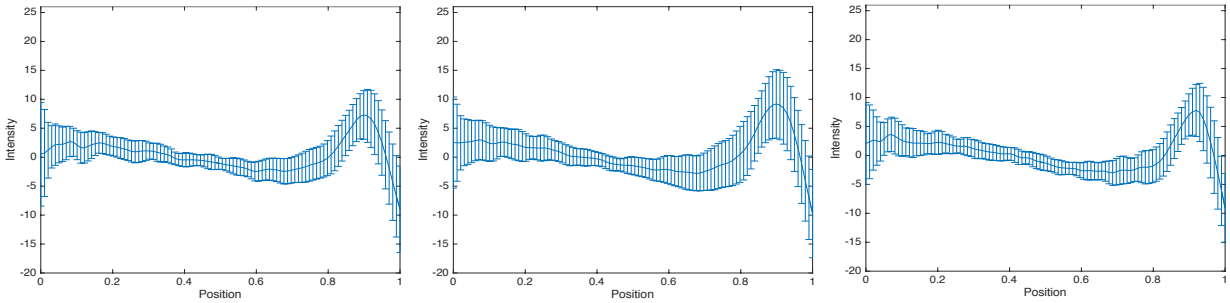

(a) HRK1_1 **(b)** HRK1_2 **(c)** HRK1_3

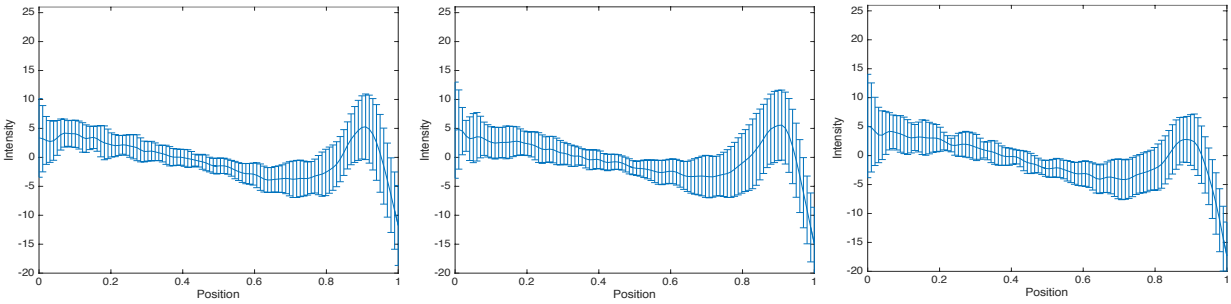

(d) HRK1_4 **(e)** HRK1_5 **(f)** HRK1_6

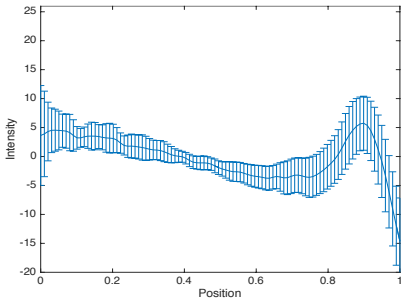

(g) HRK1_7

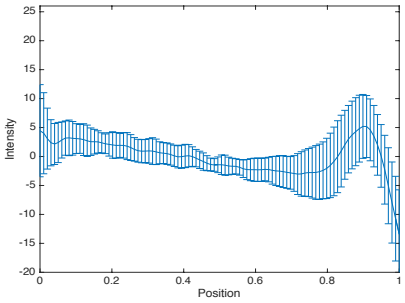

(h) HRK1_8

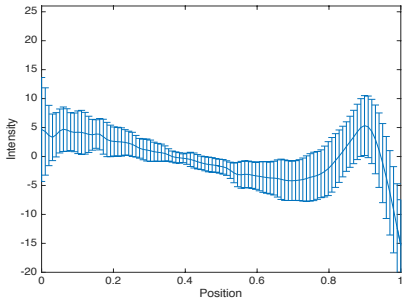

(i) HRK1_9

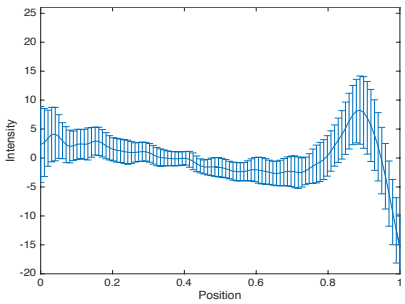

(j) HRK1_10

Figure A.3 – Error bar profiles for all replicas of *HRK1* strain after 0 hours in incubation.

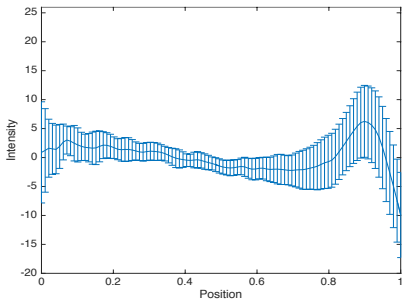

(a) WT_1

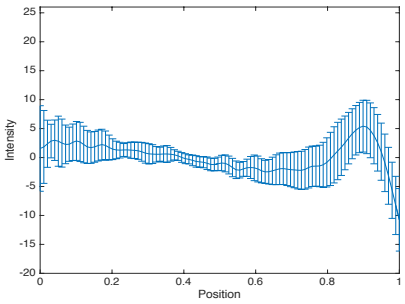

(b) WT_2

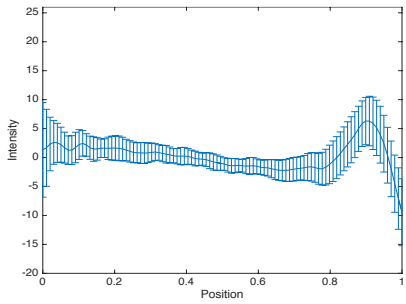

(c) WT_3

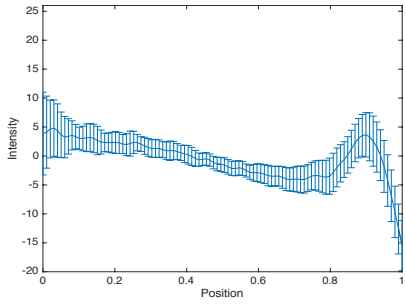

(d) WT_4

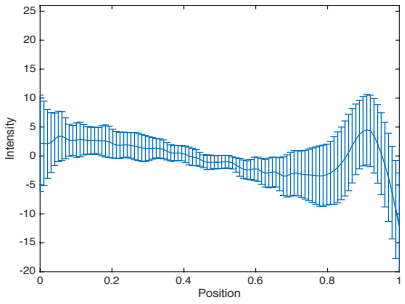

(e) WT_5

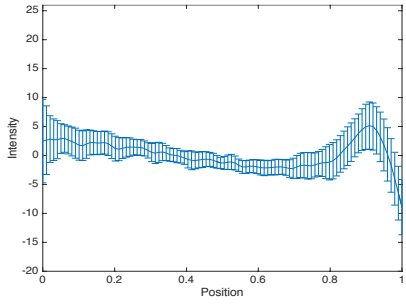

(f) WT_6

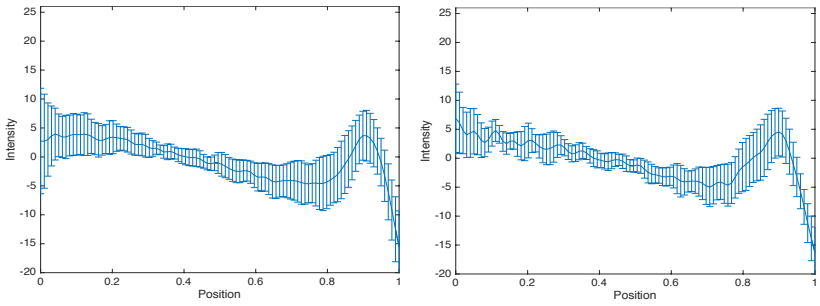

(g) WT_7 **(h)** WT_8

Figure A.5 – Error bar profiles for all replicas of *WT* strain after 1 hour in incubation in the absence of acetic acid.

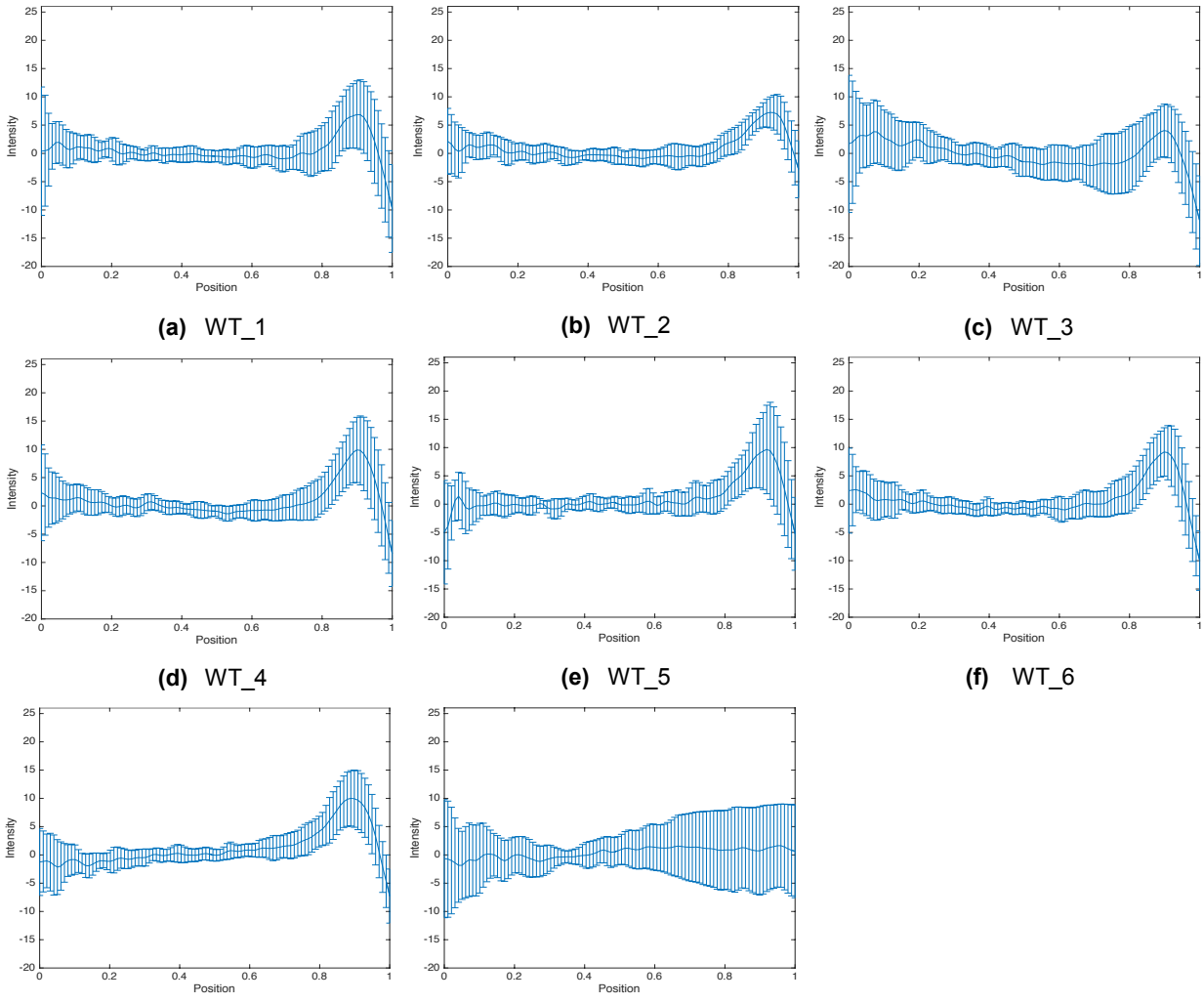

(a) WT_1 **(b)** WT_2 **(c)** WT_3

(d) WT_4 **(e)** WT_5 **(f)** WT_6

(g) WT_7 **(h)** WT_8

Figure A.4 – Error bar profiles for all replicas of *WT* strain after 1 hour in incubation in the presence of acetic acid.

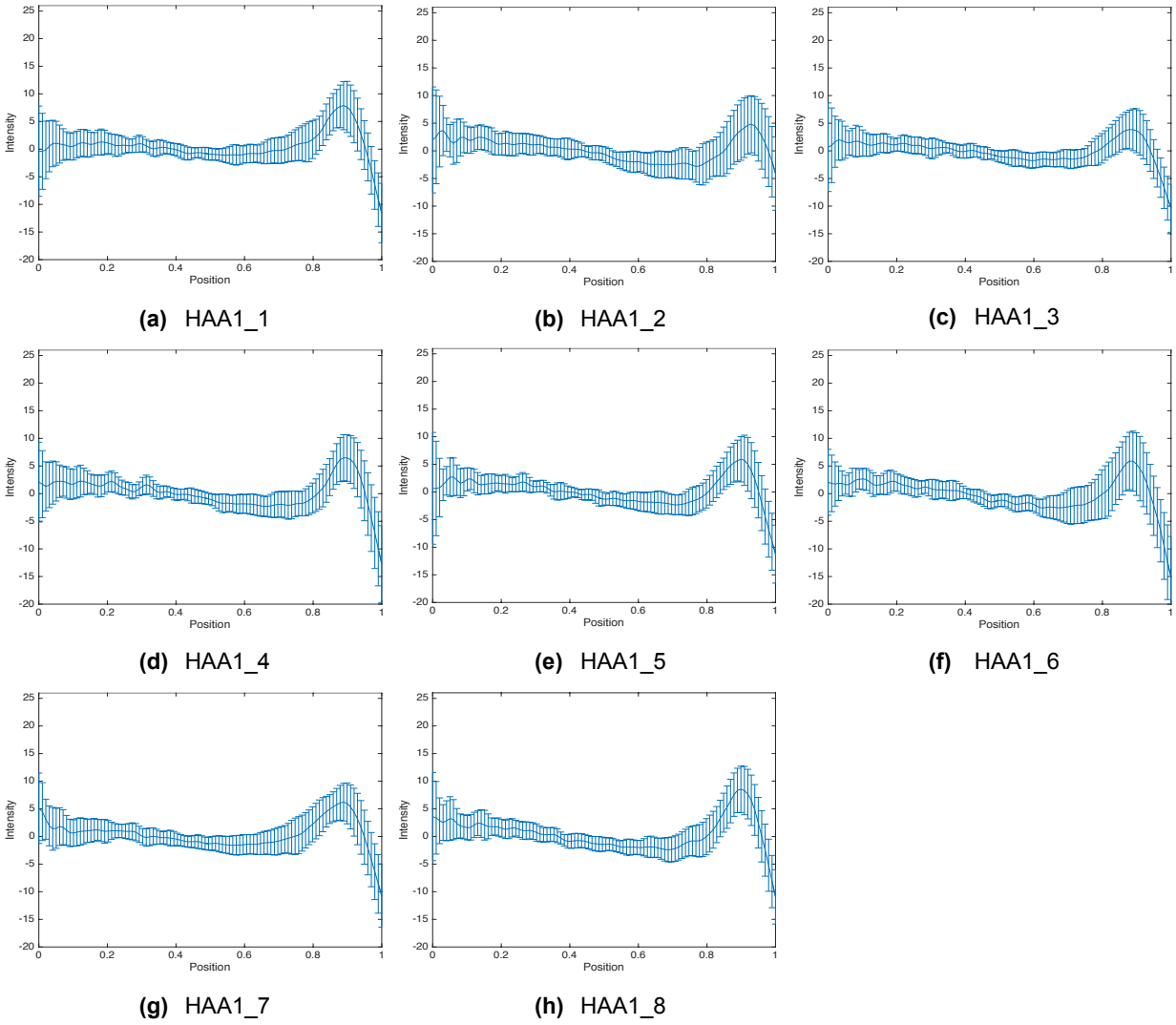

(a) HAA1_1 **(b)** HAA1_2 **(c)** HAA1_3

(d) HAA1_4 **(e)** HAA1_5 **(f)** HAA1_6

(g) HAA1_7 **(h)** HAA1_8

Figure A.6 – Error bar profiles for all replicas of *HAA1* strain after 1 hour in incubation in the absence of acetic acid.

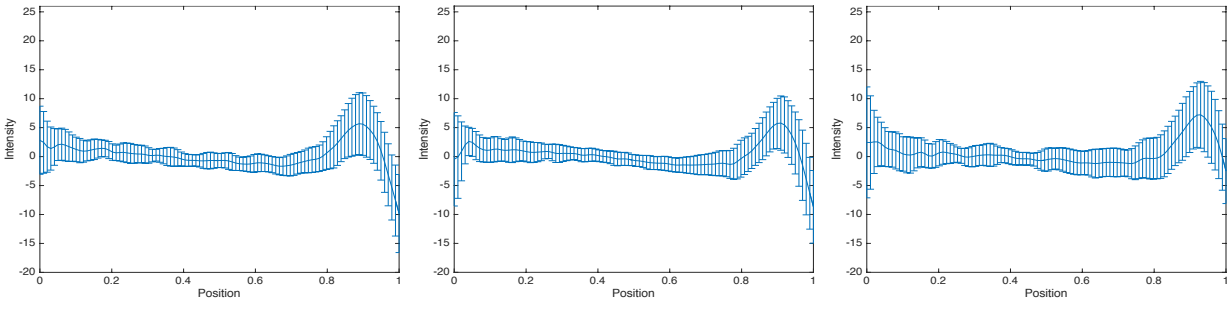

(a) HAA1_1 **(b)** HAA1_2 **(c)** HAA1_3

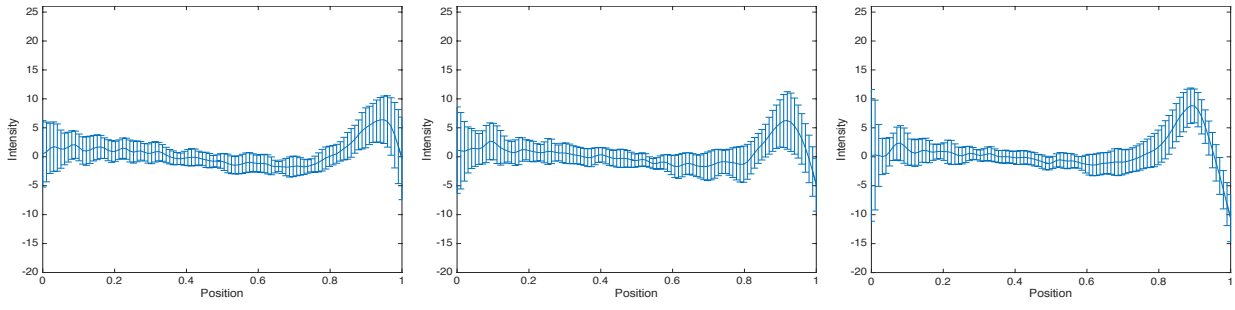

(d) HAA1_4 **(e)** HAA1_5 **(f)** HAA1_6

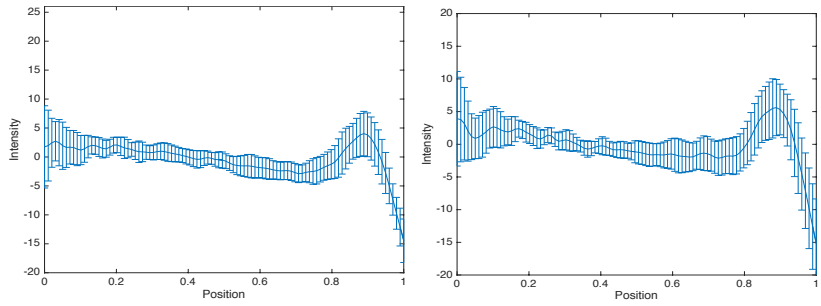

(g) HAA1_7 **(h)** HAA1_8

Figure A.7 – Error bar profiles for all replicas of *HAA1* strain after 1 hour in incubation in the presence of acetic acid.

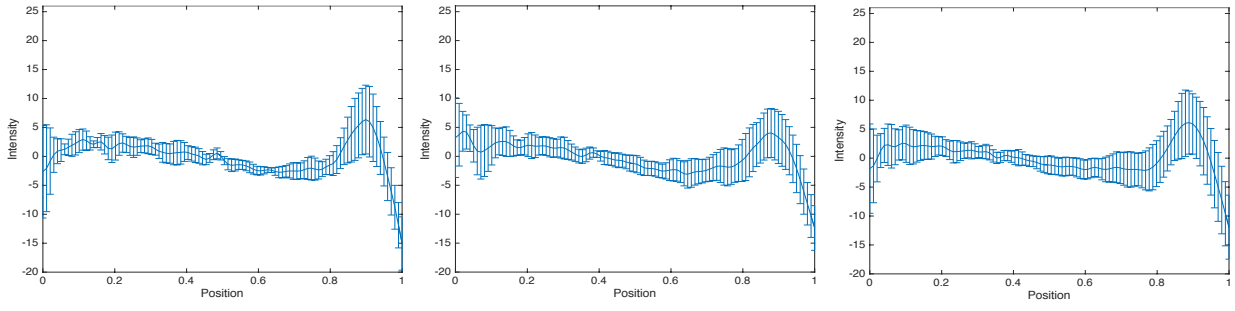

(a) HRK1_1 **(b)** HRK1_2 **(c)** HRK1_3

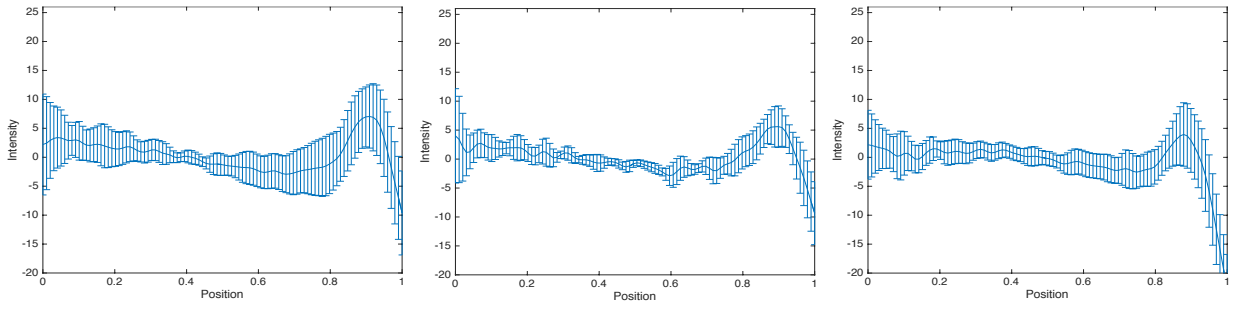

(d) HRK1_4 **(e)** HRK1_5 **(f)** HRK1_6

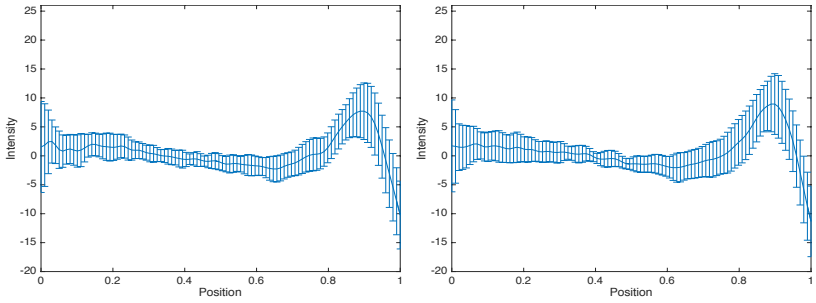

(g) HRK1_7 **(h)** HRK1_8

Figure A.9 – Error bar profiles for all replicas of *HRK1* strain after 1 hour in incubation in the absence of acetic acid.

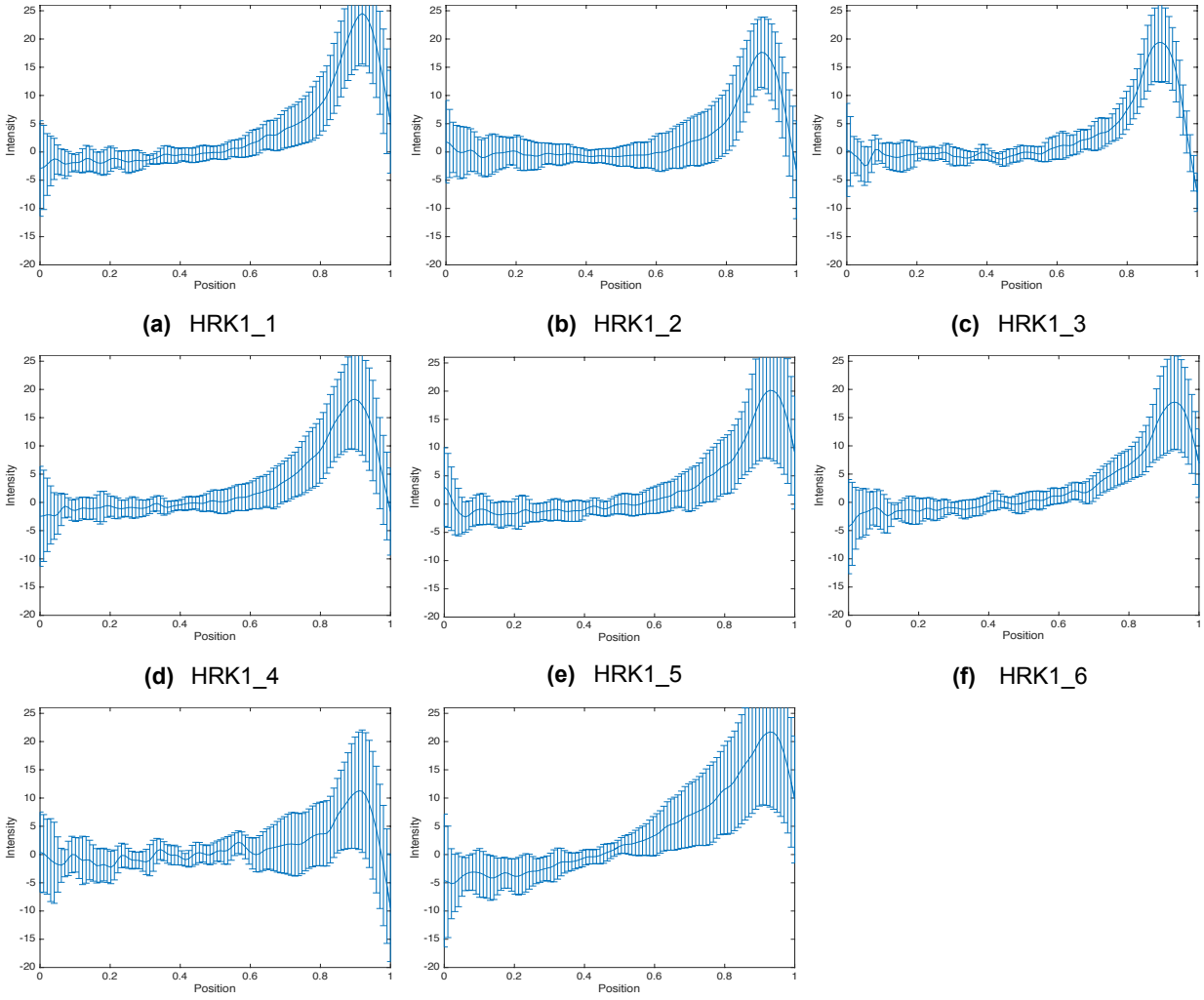

(a) HRK1_1 **(b)** HRK1_2 **(c)** HRK1_3

(d) HRK1_4 **(e)** HRK1_5 **(f)** HRK1_6

(g) HRK1_7 **(h)** HRK1_8

Figure A.8 – Error bar profiles for all replicas of *HRK1* strain after 1 hour in incubation in the presence of acetic acid.

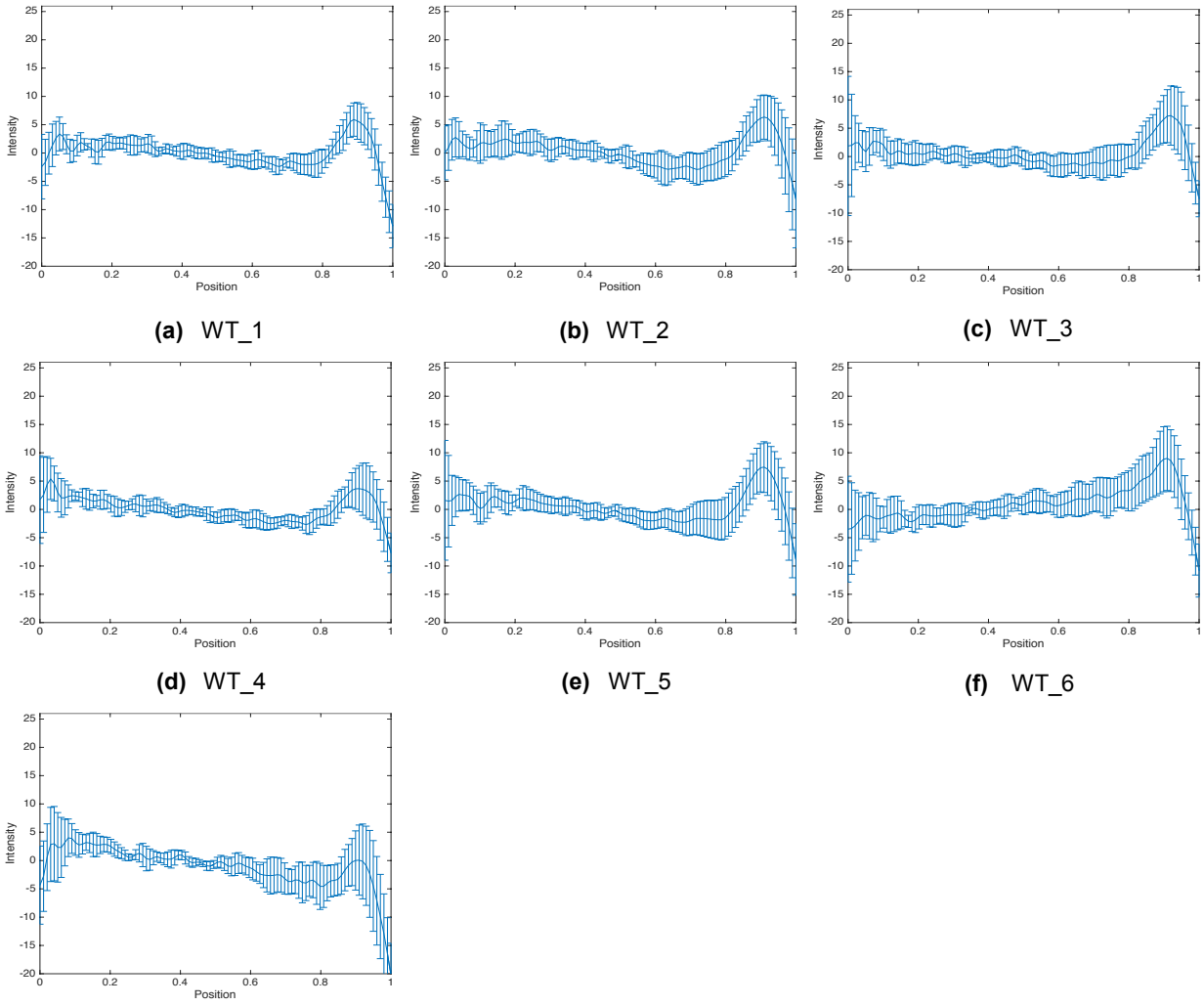

(a) WT_1 **(b)** WT_2 **(c)** WT_3

(d) WT_4 **(e)** WT_5 **(f)** WT_6

(g) WT_7

Figure A.10 – Error bar profiles for all replicas of *WT* strain after 2 hours in incubation in the absence of acetic acid.

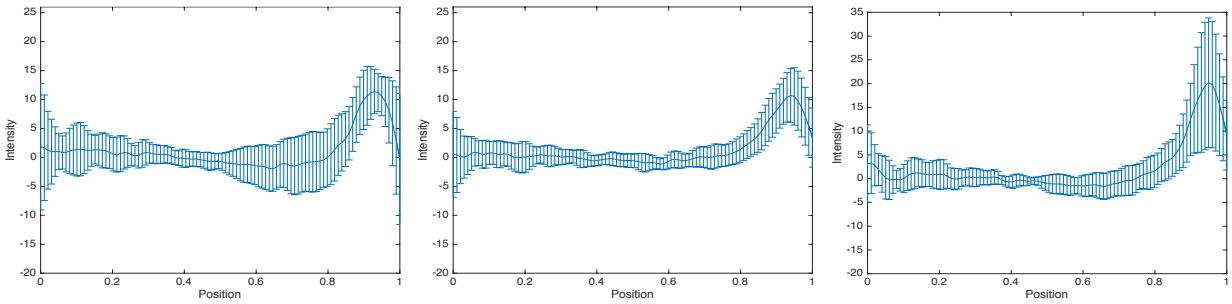

(a) WT_1 **(b)** WT_2 **(c)** WT_3

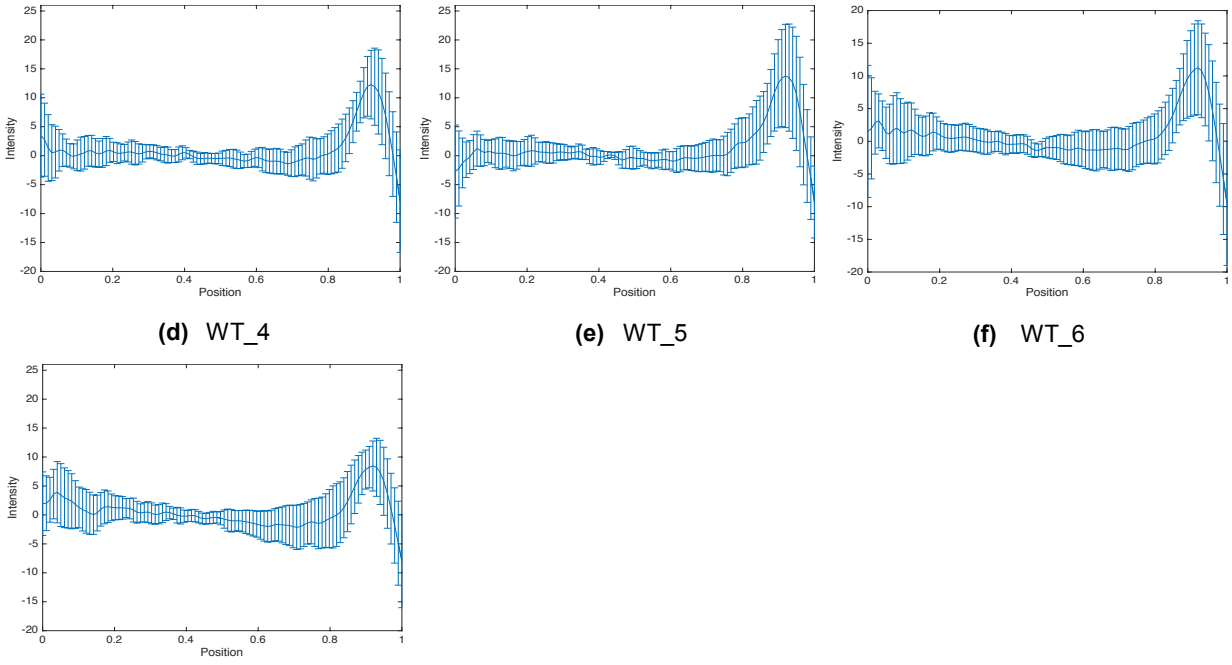

(d) WT_4 **(e)** WT_5 **(f)** WT_6

(g) WT_7

Figure A.11 – Error bar profiles for all replicas of *WT* strain after 2 hours in incubation in the presence of acetic acid.

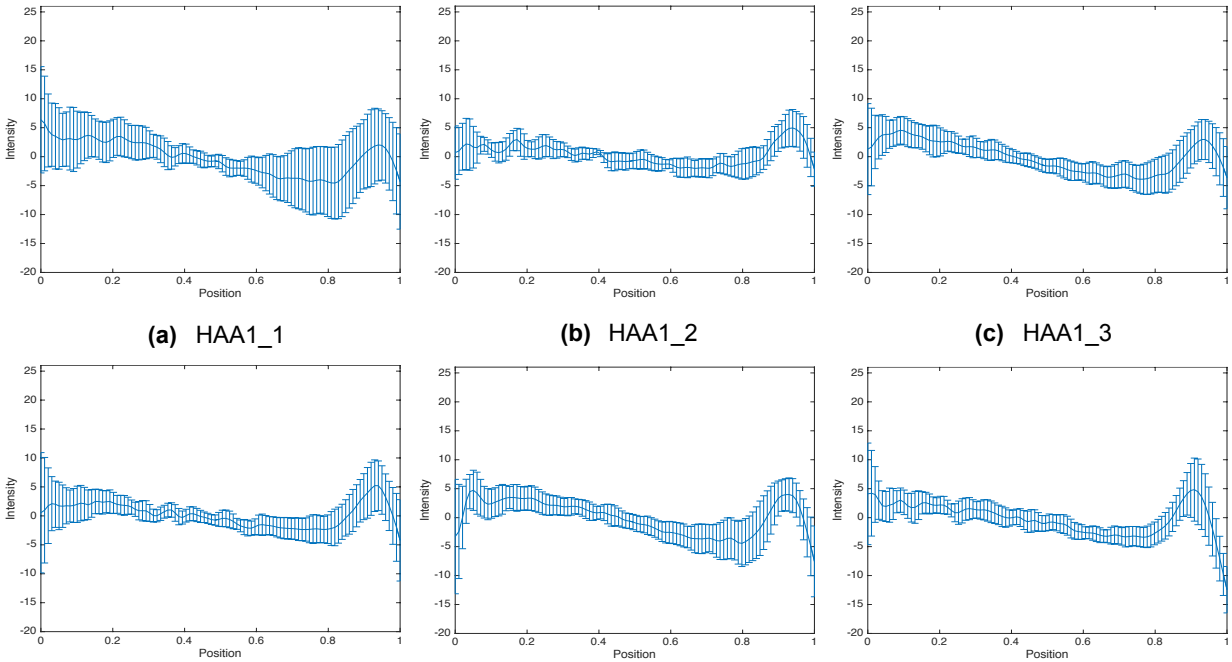

(a) HAA1_1 **(b)** HAA1_2 **(c)** HAA1_3

(d) HAA1_4 **(e)** HAA1_5 **(f)** HAA1_6

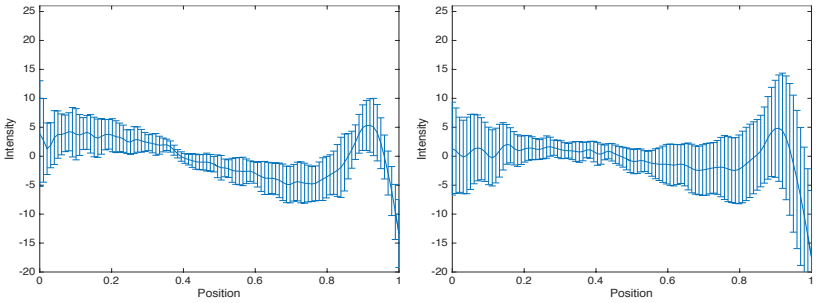

(g) HAA1_7 **(h)** HAA1_8

Figure A.13 – Error bar profiles for all replicas of *HAA1* strain after 2 hours in incubation in the absence of acetic acid.

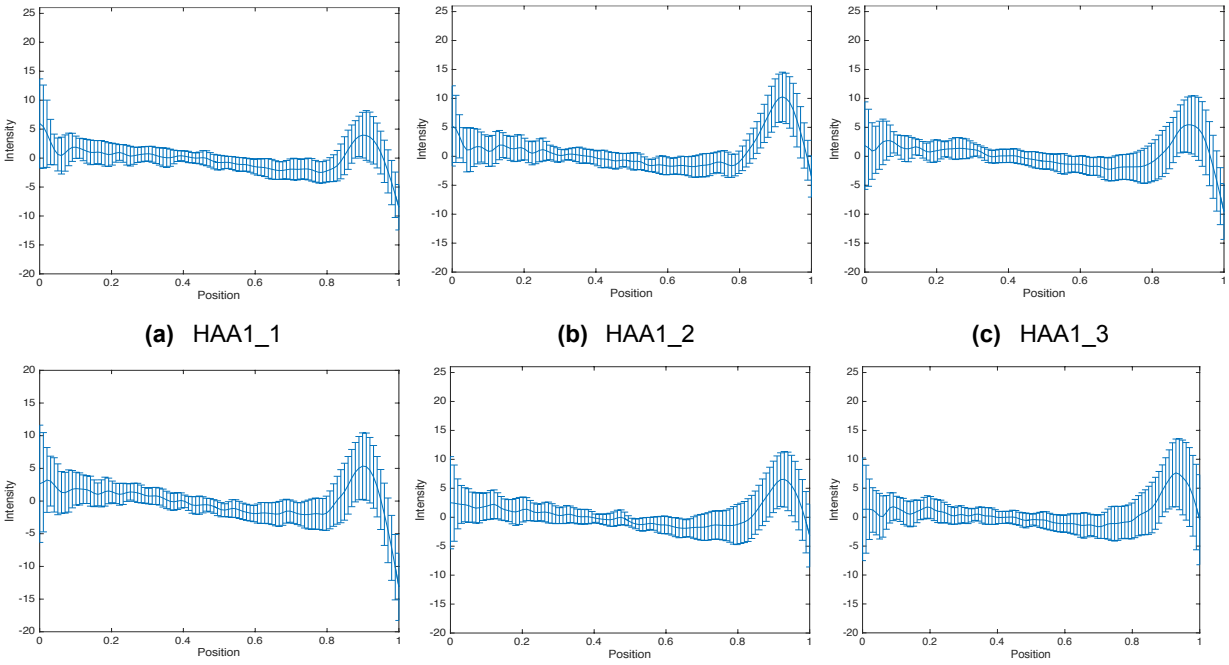

(a) HAA1_1 **(b)** HAA1_2 **(c)** HAA1_3

(d) HAA1_4 **(e)** HAA1_5 **(f)** HAA1_6

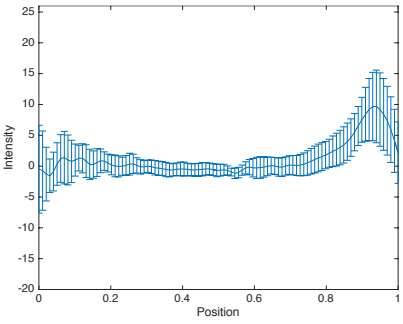

(g) HAA1_7

Figure A.12 – Error bar profiles for all replicas of *HAA1* strain after 2 hours in incubation in the presence of acetic acid.

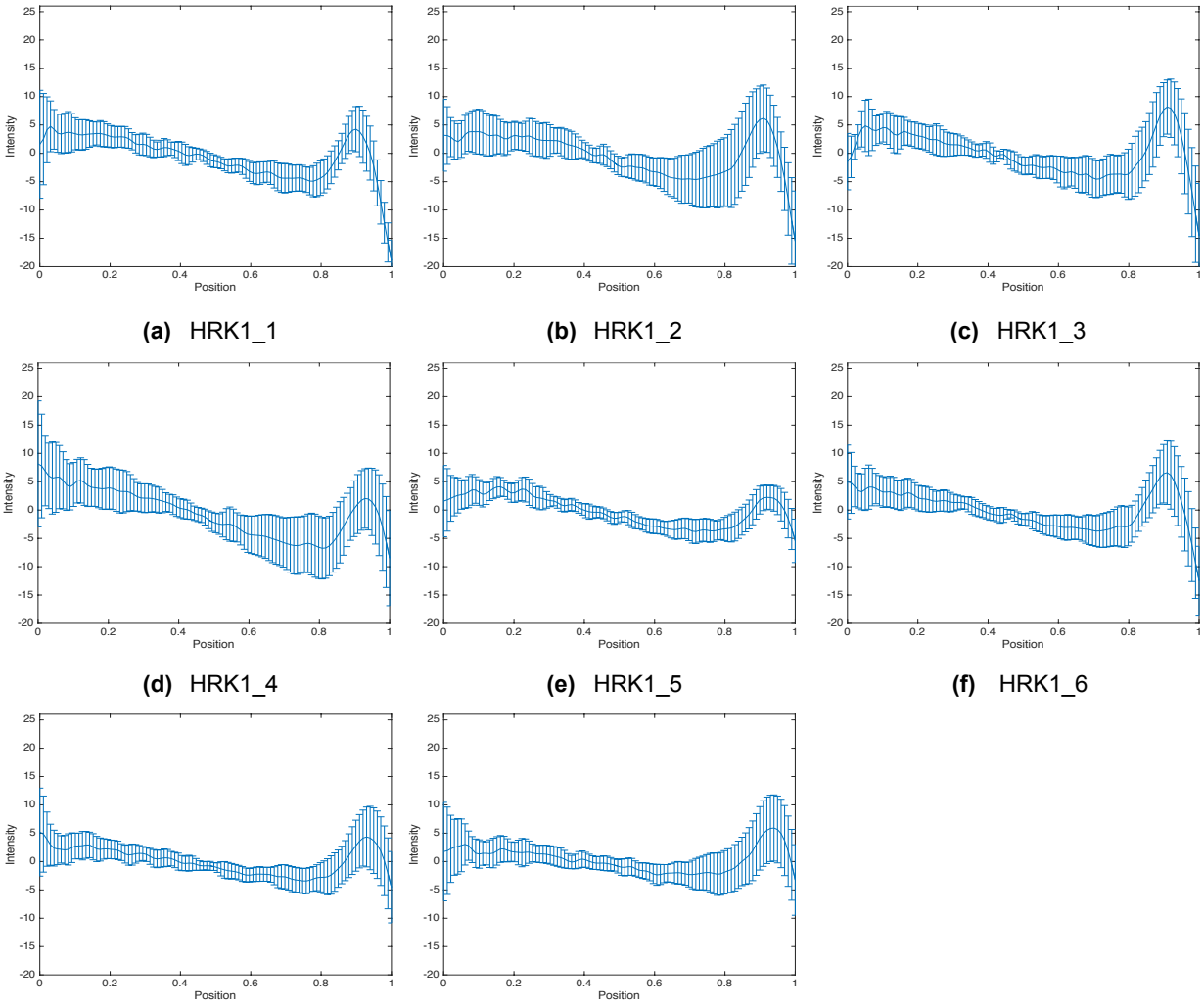

(a) HRK1_1 **(b)** HRK1_2 **(c)** HRK1_3

(d) HRK1_4 **(e)** HRK1_5 **(f)** HRK1_6

(g) HRK1_7 **(h)** HRK1_8

Figure A.14 – Error bar profiles for all replicas of *HRK1* strain after 2 hours in incubation in the absence of acetic acid.

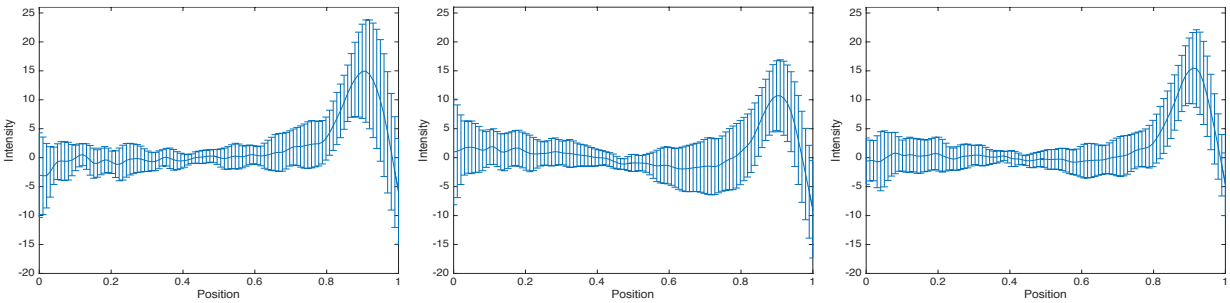

(a) HRK1_1 **(b)** HRK1_2 **(c)** HRK1_3

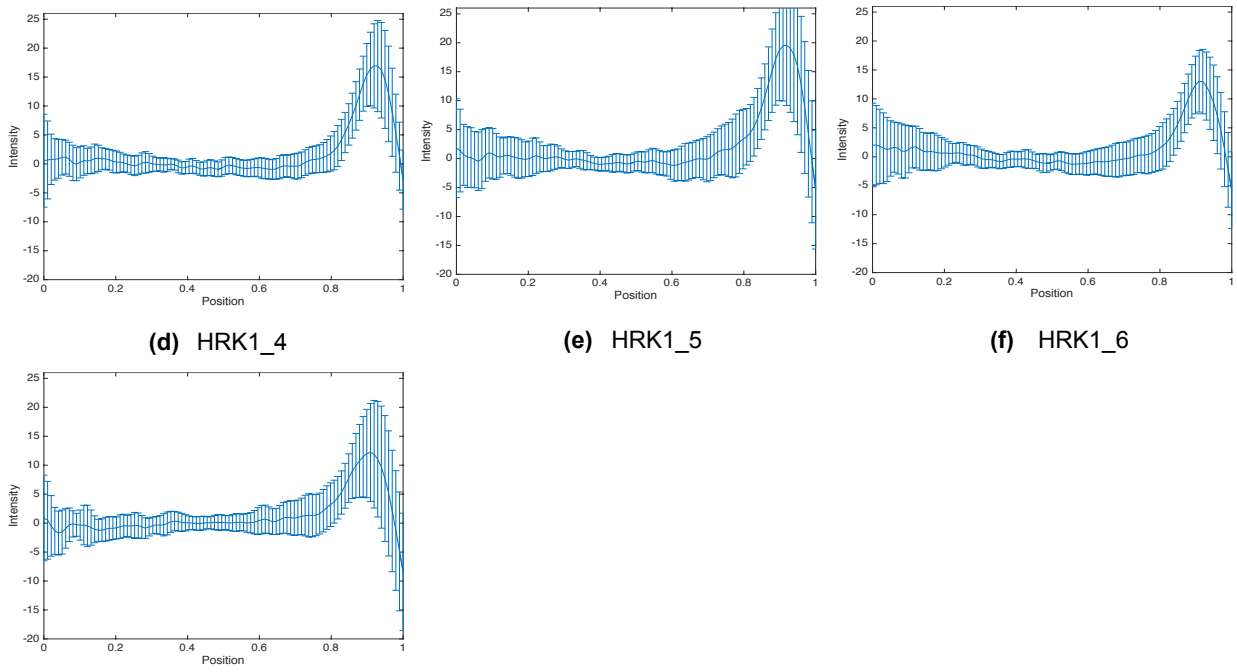

(d) HRK1_4 **(e)** HRK1_5 **(f)** HRK1_6

(g) HRK1_7

Figure A.15 – Error bar profiles for all replicas of *HRK1* strain after 2 hours in incubation in the presence of acetic acid.

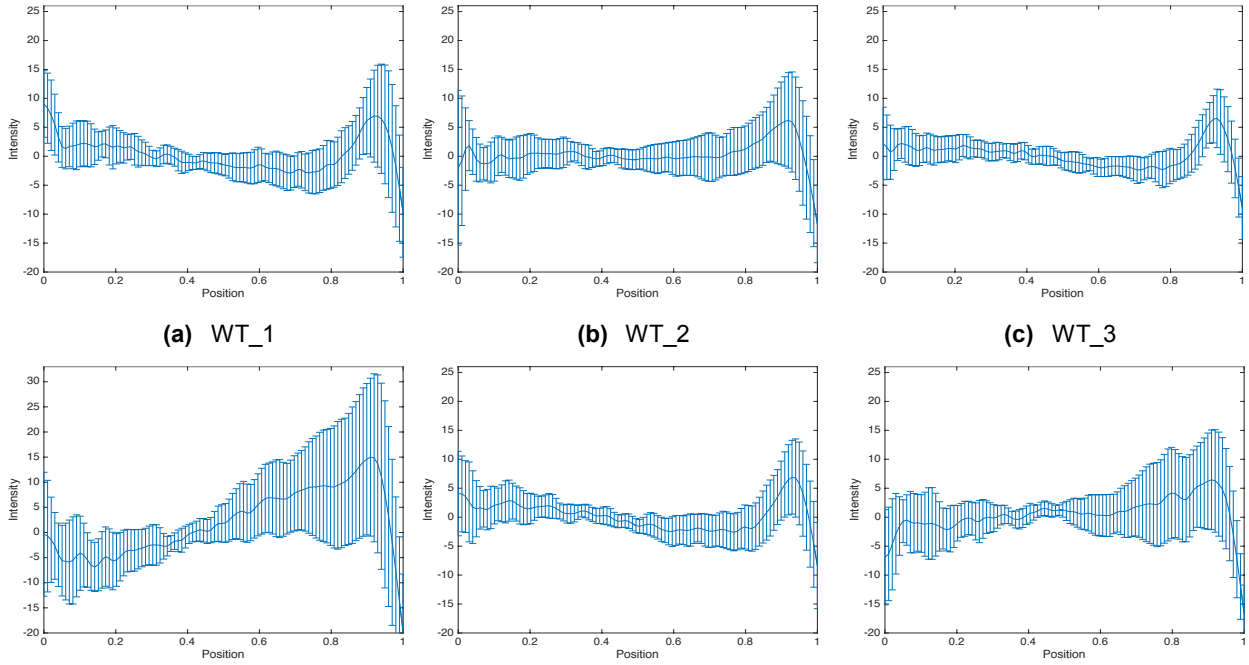

(a) WT_1 **(b)** WT_2 **(c)** WT_3

(d) WT_4 **(e)** WT_5 **(f)** WT_6

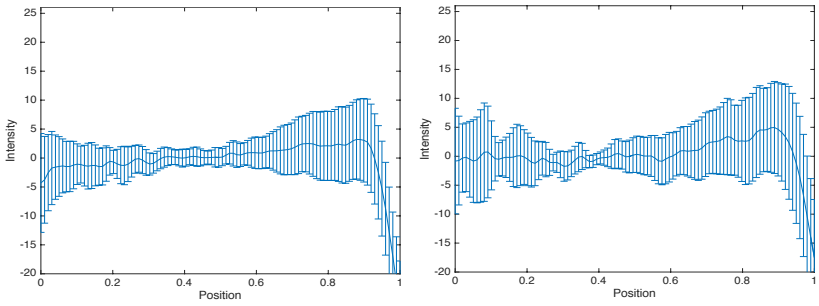

(g) WT_7 **(h)** WT_8

Figure A.17 – Error bar profiles for all replicas of *WT* strain after 4 hours in incubation in the absence of acetic acid.

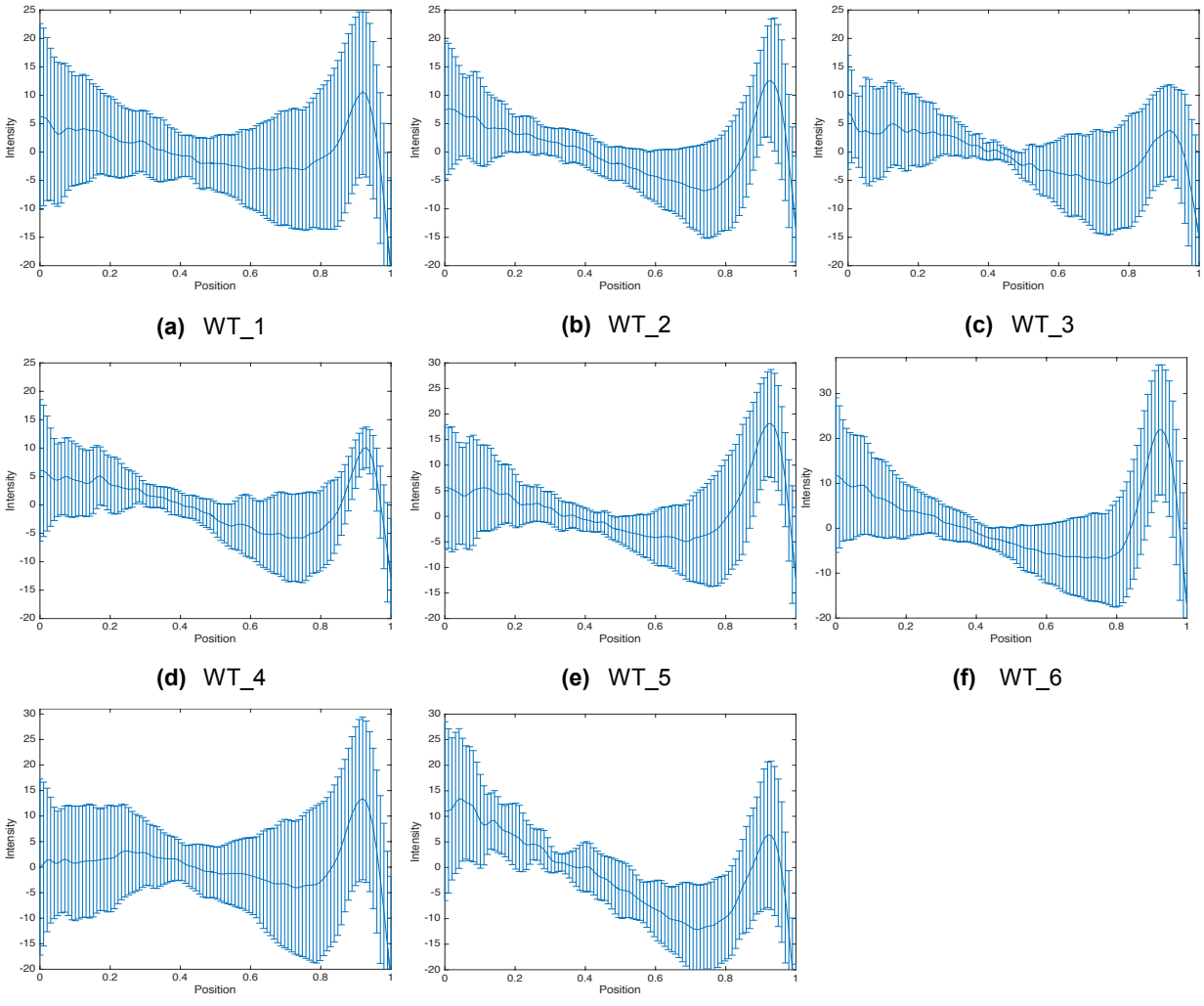

(a) WT_1 **(b)** WT_2 **(c)** WT_3

(d) WT_4 **(e)** WT_5 **(f)** WT_6

(g) WT_7 **(h)** WT_8

Figure A.16 – Error bar profiles for all replicas of *WT* strain after 4 hours in incubation in the presence of acetic acid.

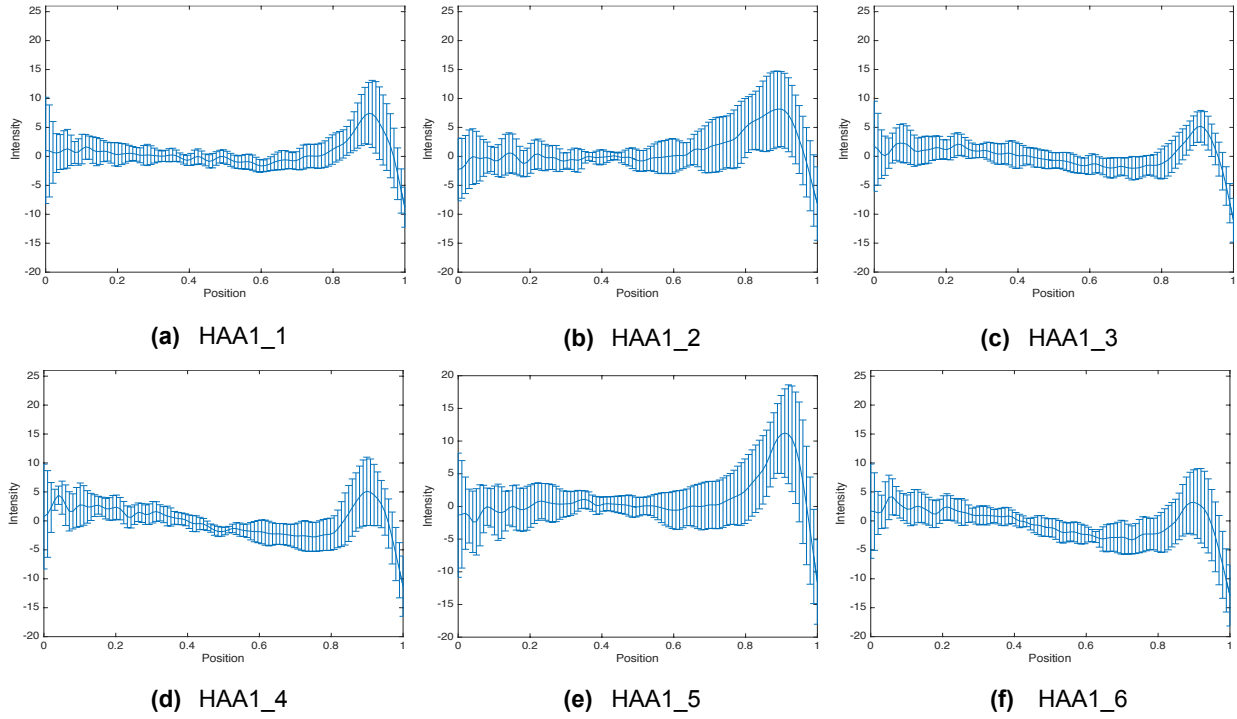

(a) HAA1_1 **(b)** HAA1_2 **(c)** HAA1_3

(d) HAA1_4 **(e)** HAA1_5 **(f)** HAA1_6

Figure A.19 – Error bar profiles for all replicas of *HAA1* strain after 4 hours in incubation in the absence of acetic acid.

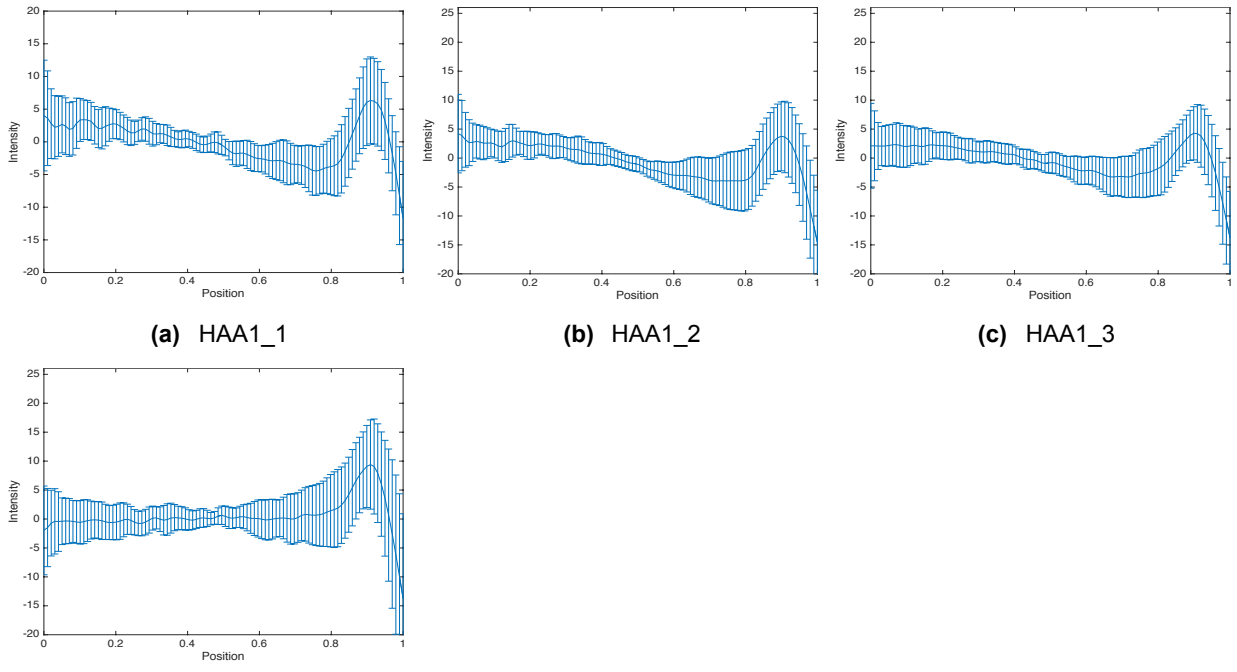

(a) HAA1_1 **(b)** HAA1_2 **(c)** HAA1_3

(d) HAA1_4

Figure A.18 – Error bar profiles for all replicas of *HAA1* strain after 4 hours in incubation in the presence of acetic acid.

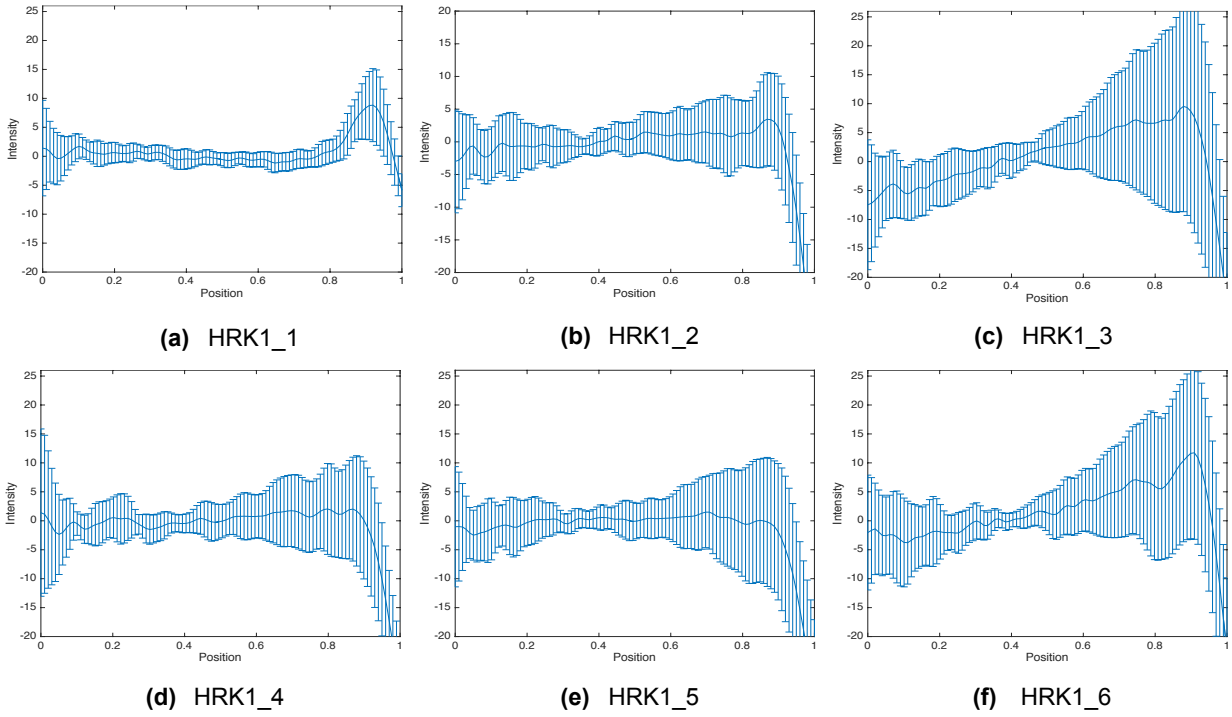

(a) HRK1_1 **(b)** HRK1_2 **(c)** HRK1_3

(d) HRK1_4 **(e)** HRK1_5 **(f)** HRK1_6

Figure A.20 – Error bar profiles for all replicas of *HRK1* strain after 4 hours in incubation in the absence of acetic acid.

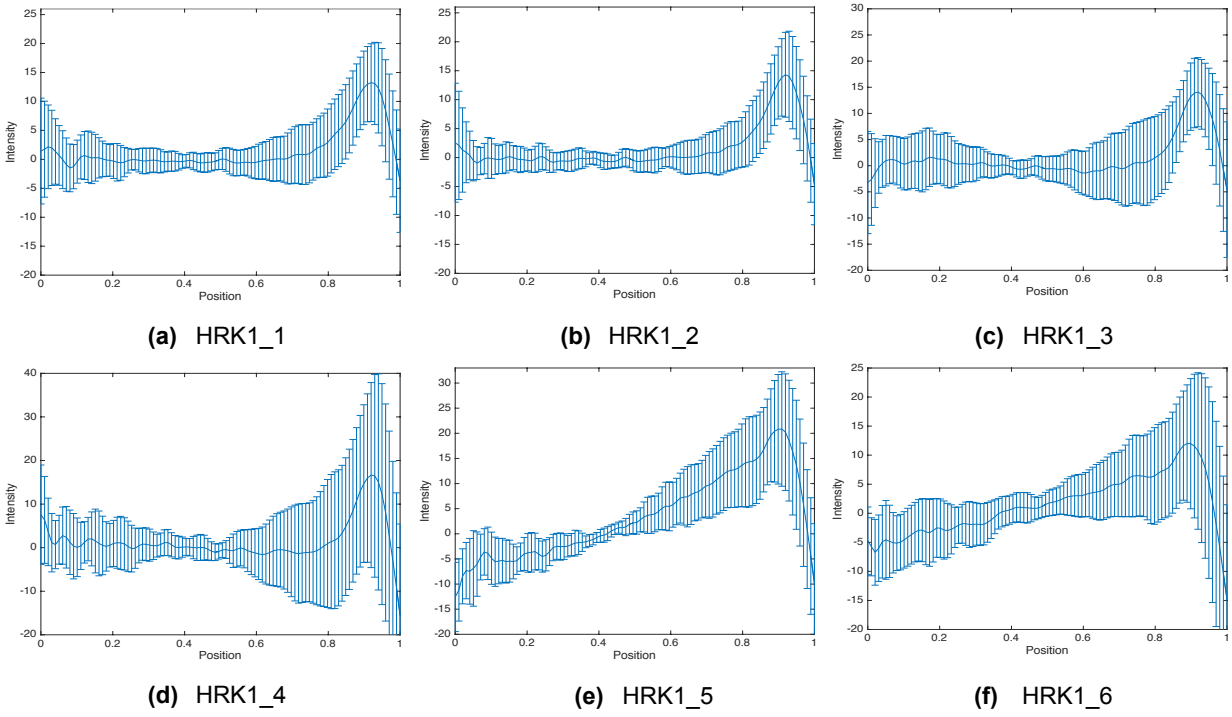

(a) HRK1_1 **(b)** HRK1_2 **(c)** HRK1_3

(d) HRK1_4 **(e)** HRK1_5 **(f)** HRK1_6

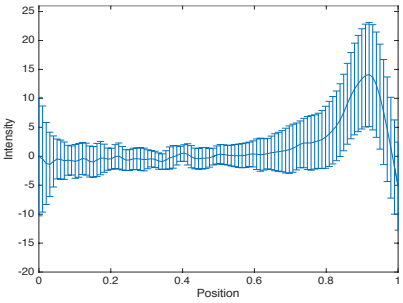

(g) HRK1_7

Figure A.21 – Error bar profiles for all replicas of *HRK1* strain after 4 hours in incubation in the presence of acetic acid.

A.2. Radial Profiles

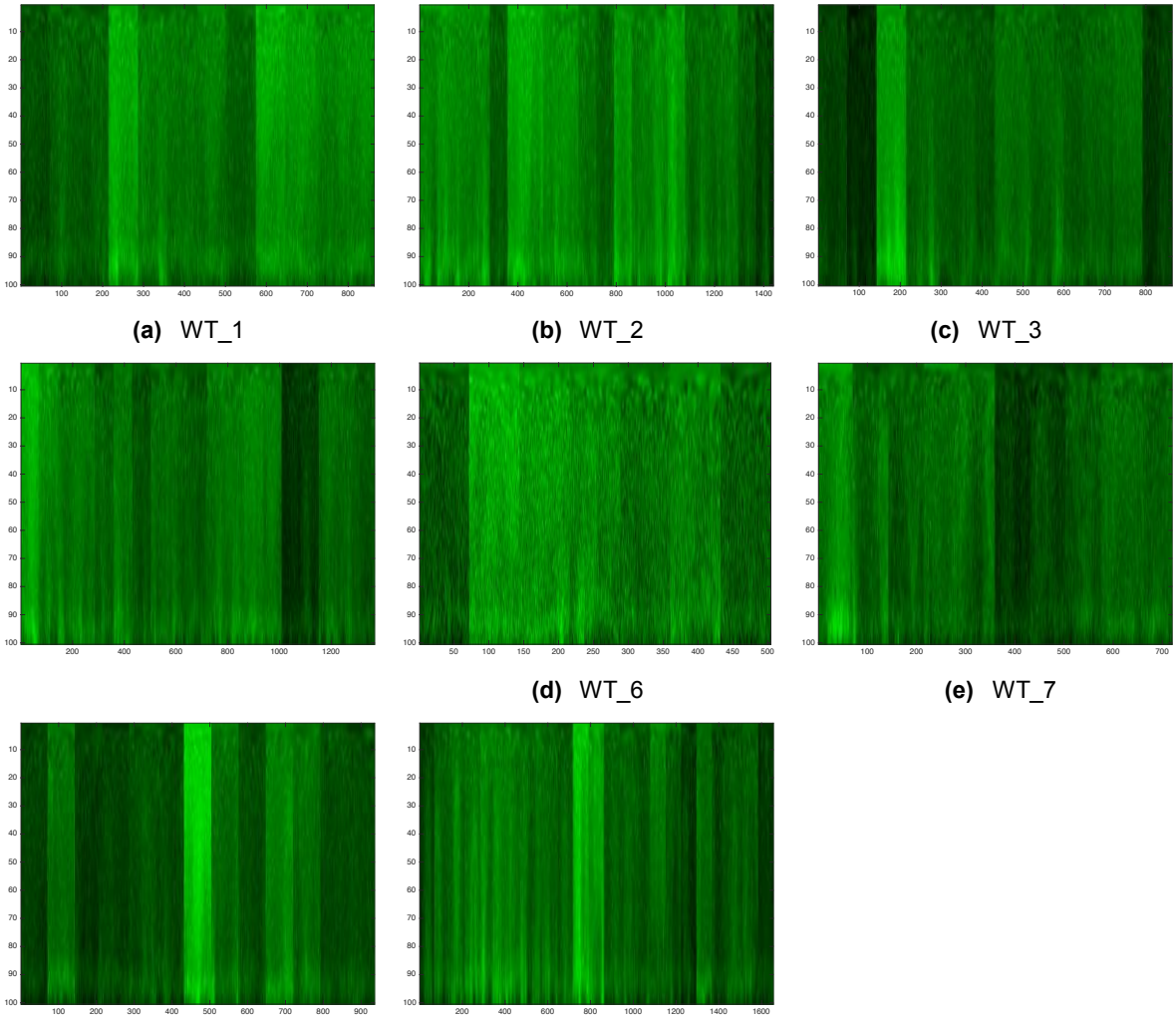

(a) WT_1 **(b)** WT_2 **(c)** WT_3

(d) WT_6 **(e)** WT_7

(f) WT_8 **(g)** WT_9

Figure A.22 – Radial profiles for all replicas of *WT* strain after 0 hours in incubation.

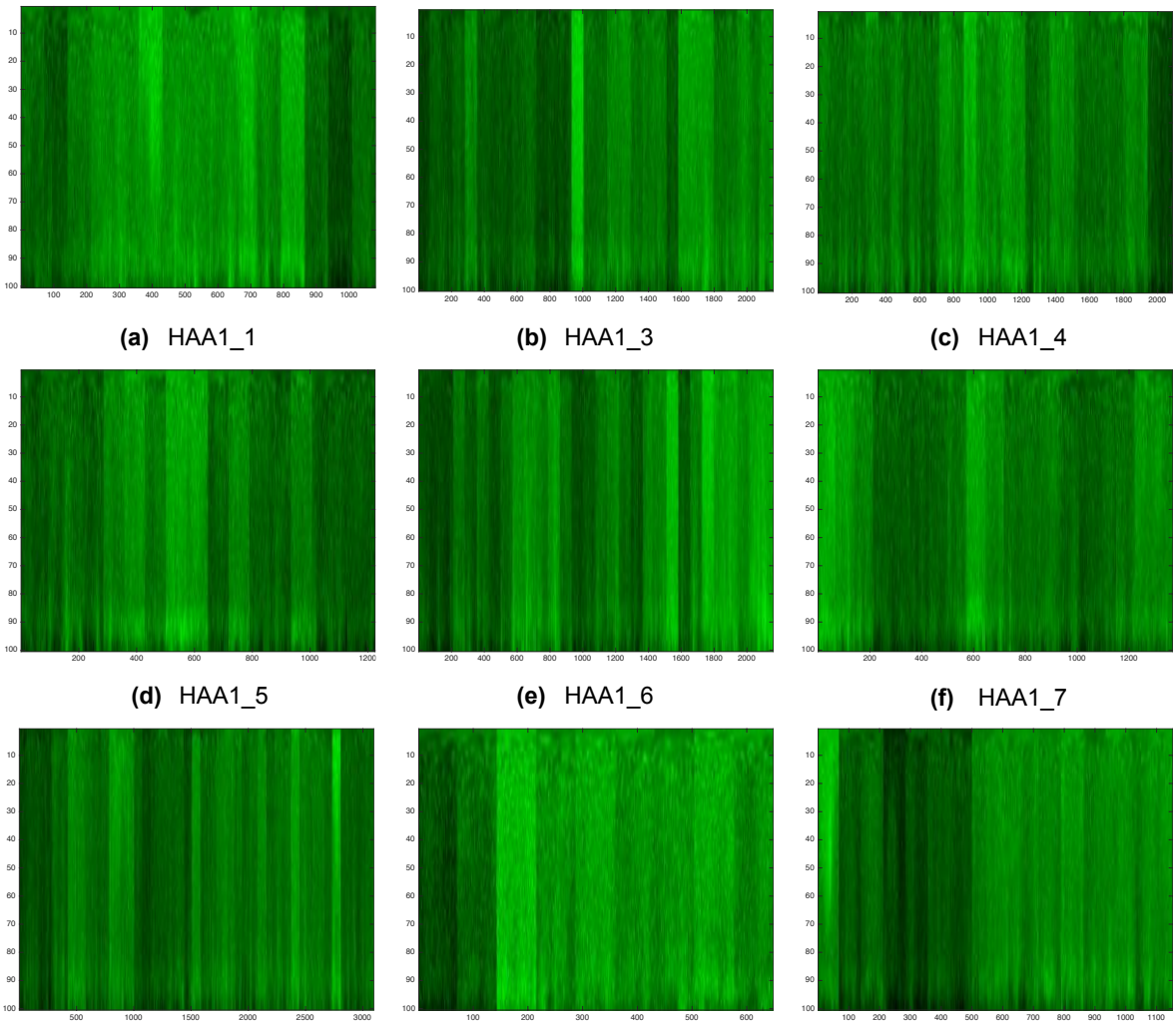

(a) HAA1_1 **(b)** HAA1_3 **(c)** HAA1_4

(d) HAA1_5 **(e)** HAA1_6 **(f)** HAA1_7

(g) HAA1_8 **(h)** HAA1_9 **(i)** HAA1_10

Figure A.23 – Radial profiles for all replicas of *HAA1* strain after 0 hours in incubation.

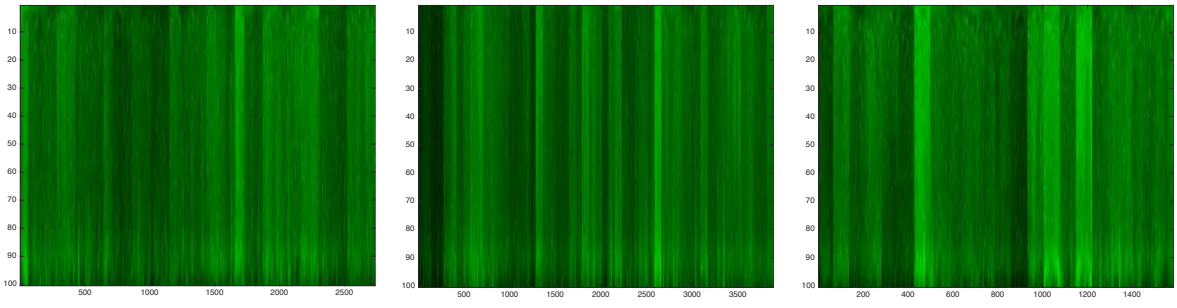

(a) HRK1_1 **(b)** HRK1_2 **(c)** HRK1_4

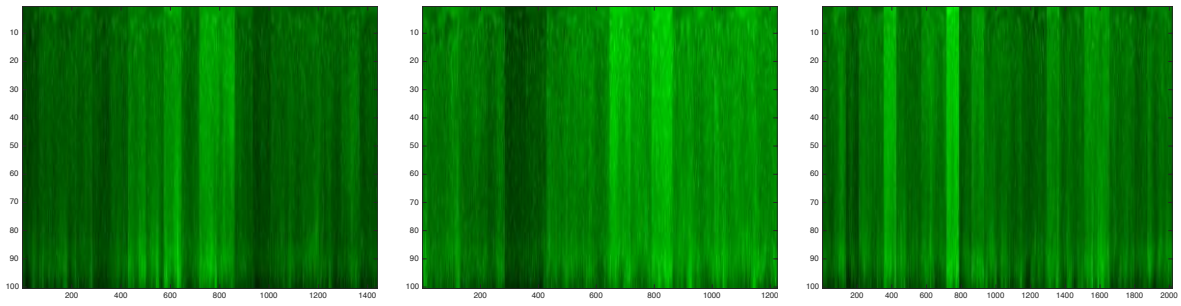

(d) HRK1_5 **(e)** HRK1_6 **(f)** HRK1_7

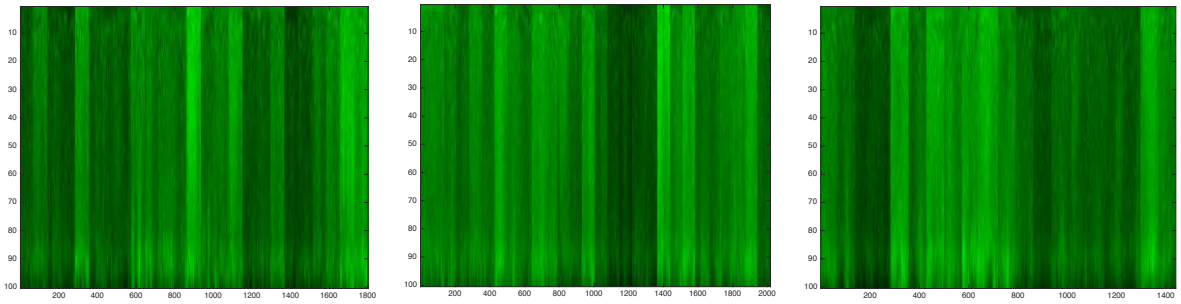

(g) HRK1_8 **(h)** HRK1_9 **(i)** HRK1_10

Figure A.24 – Radial profiles for all replicas of *HRK1* strain after 0 hours in incubation.

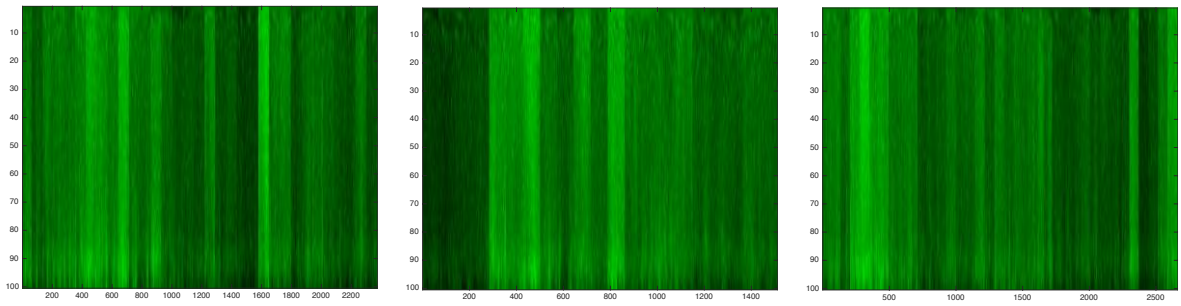

(a) WT_1 **(b)** WT_2 **(c)** WT_3

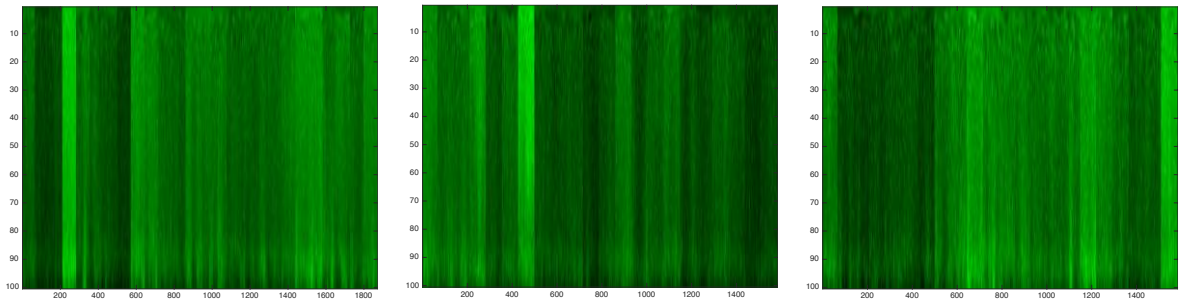

(d) WT_4 **(e)** WT_5 **(f)** WT_6

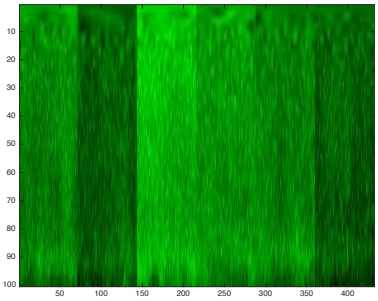

(g) WT_8

Figure A.25 – Radial profiles for all replicas of *WT* strain after 1 hour in incubation in the absence of acetic acid.

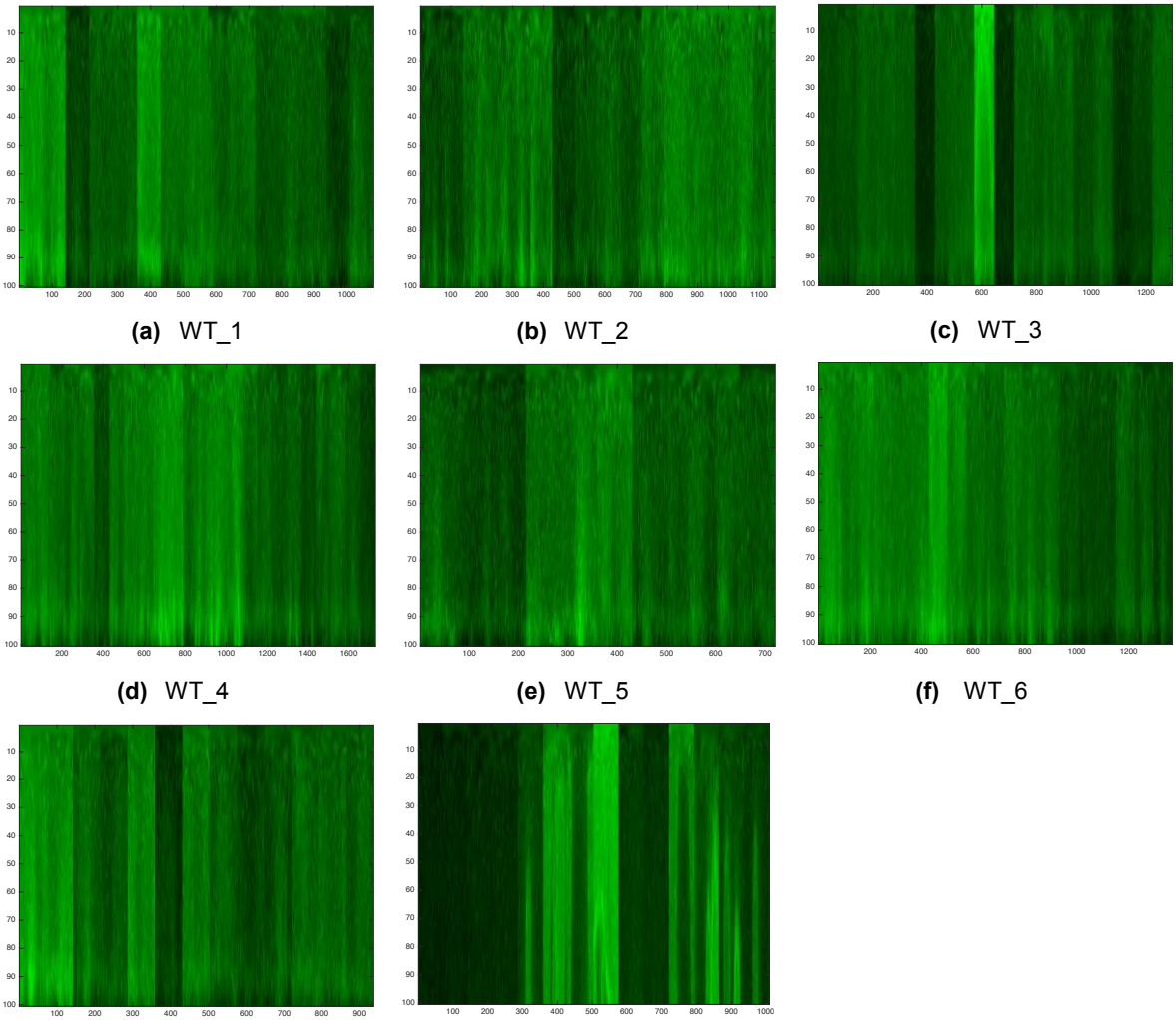

(a) WT_1 **(b)** WT_2 **(c)** WT_3

(d) WT_4 **(e)** WT_5 **(f)** WT_6

(g) WT_7 **(h)** WT_8

Figure A.26 – Radial profiles for all replicas of *WT* strain after 1 hour in incubation in the presence of acetic acid.

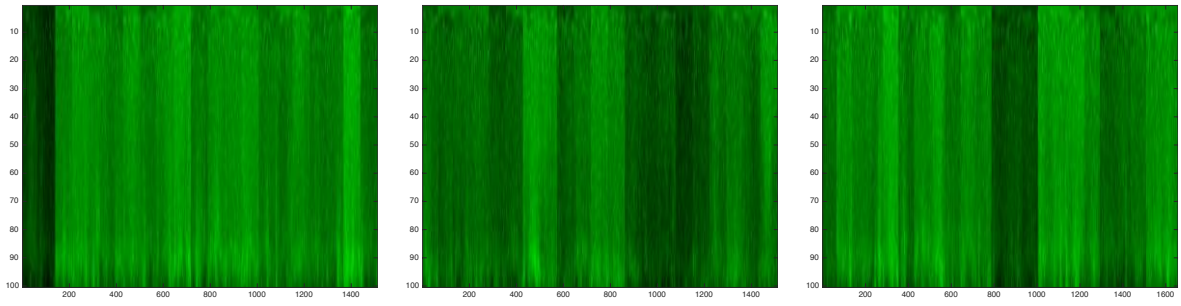

(a) HAA1_1 **(b)** HAA1_2 **(c)** HAA1_3

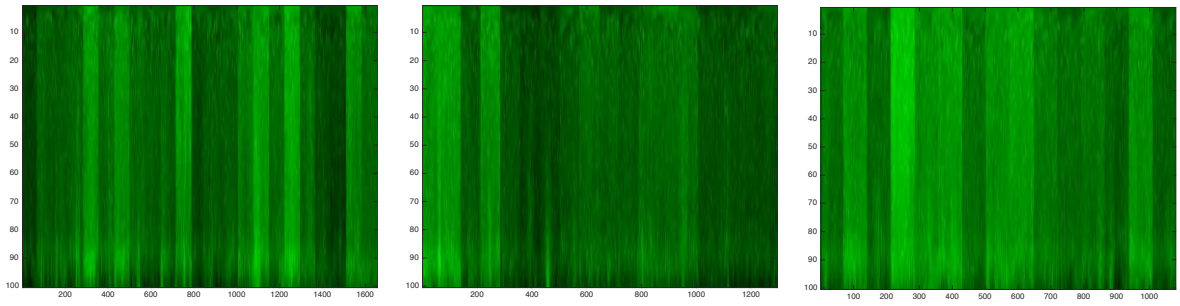

(d) HAA1_4 **(e)** HAA1_5 **(f)** HAA1_6

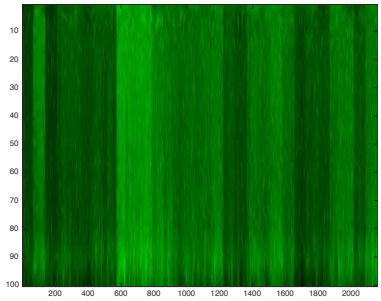

(g) HAA1_8

Figure A.27 – Radial profiles for all replicas of *HAA1* strain after 1 hour in incubation in the absence of acetic acid.

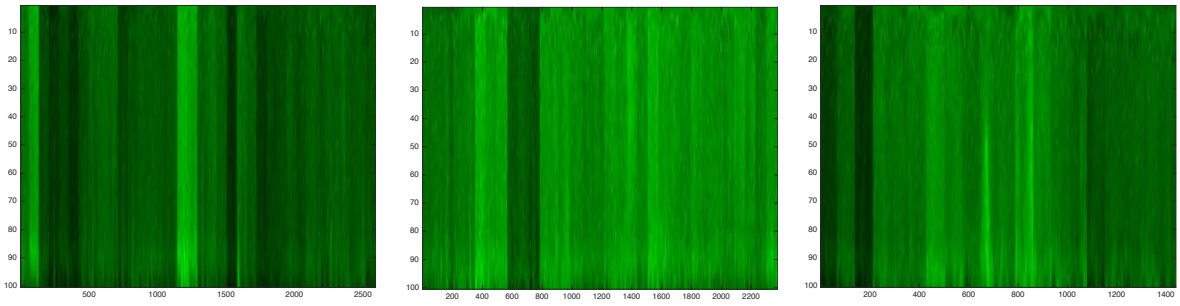

(a) HAA1_1 **(b)** HAA1_2 **(c)** HAA1_3

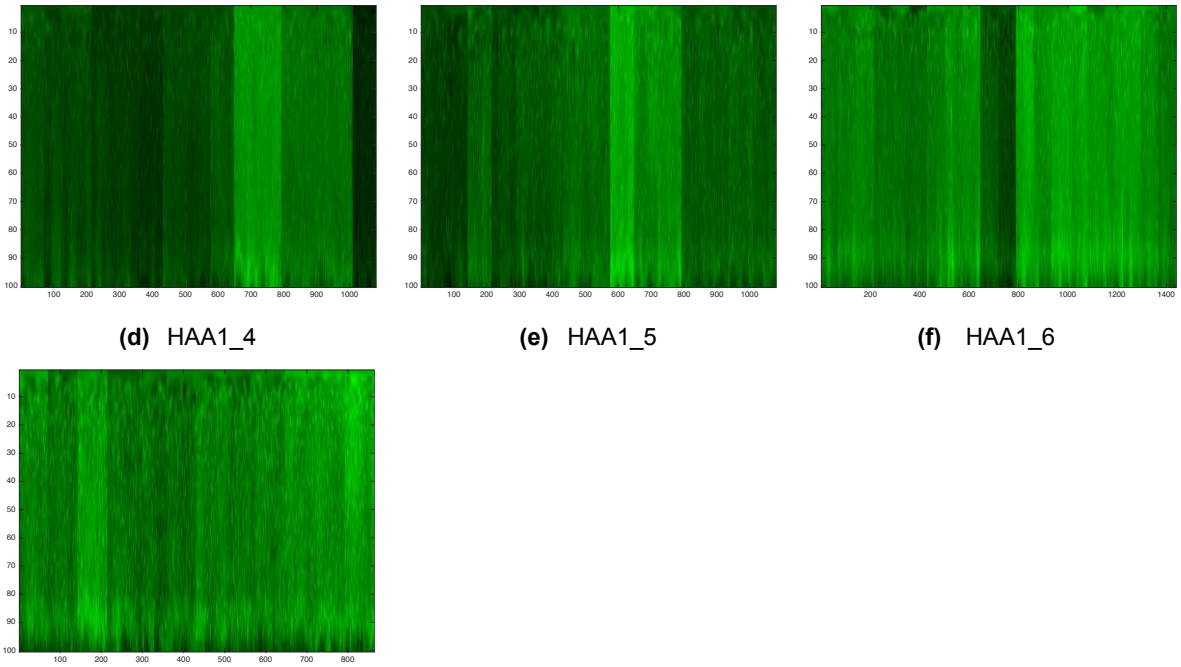

(d) HAA1_4 **(e)** HAA1_5 **(f)** HAA1_6

(g) HAA1_8

Figure A.28 – Radial profiles for all replicas of *HAA1* strain after 1 hour in incubation in the presence of acetic acid.

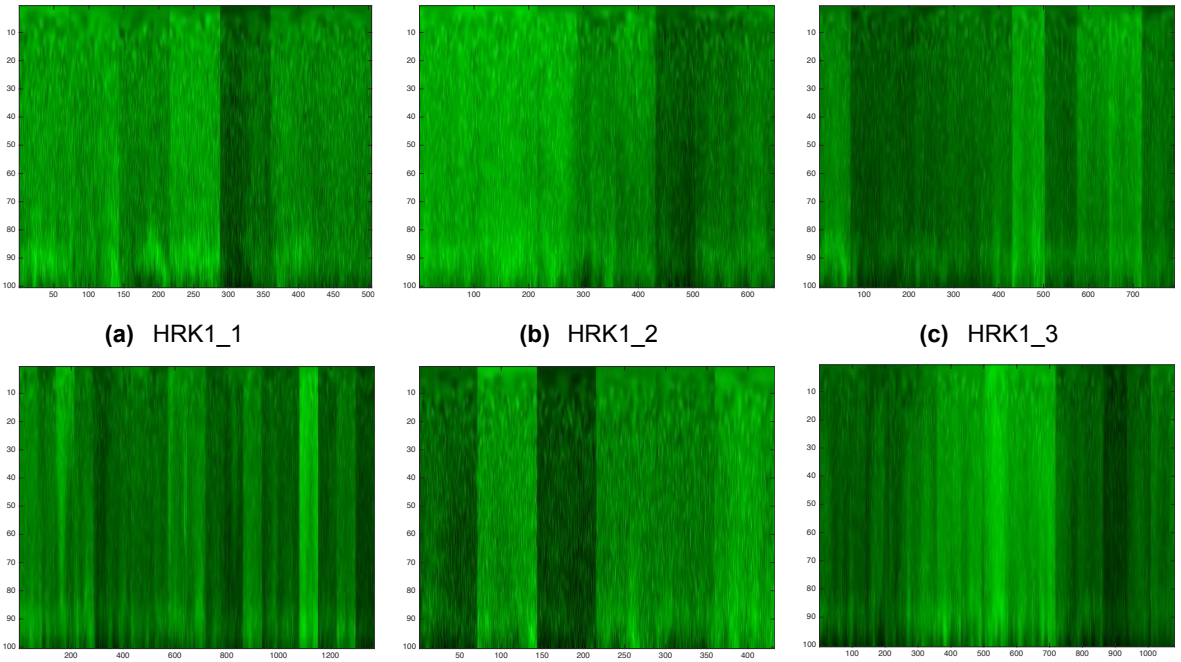

(a) HRK1_1 **(b)** HRK1_2 **(c)** HRK1_3

(d) HRK1_4 **(e)** HRK1_5 **(f)** HRK1_6

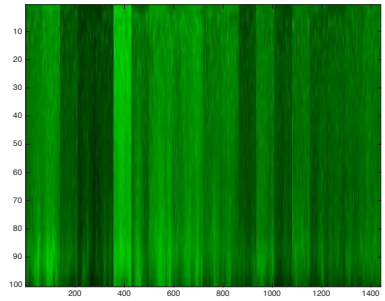

(g) HRK1_8

Figure A.30 – Radial profiles for all replicas of *HRK1* strain after 1 hour in incubation in the absence of acetic acid.

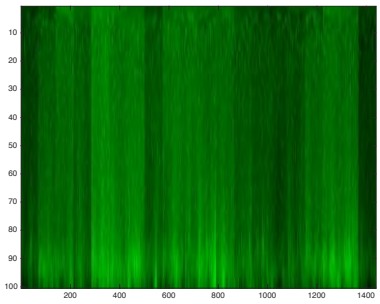

(a) HRK1_1

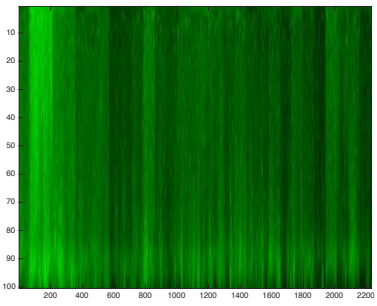

(b) HRK1_2

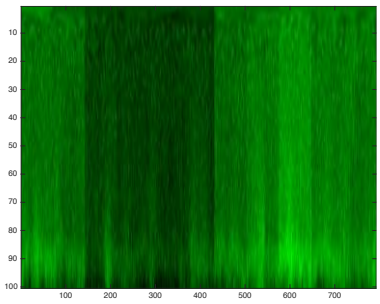

(c) HRK1_3

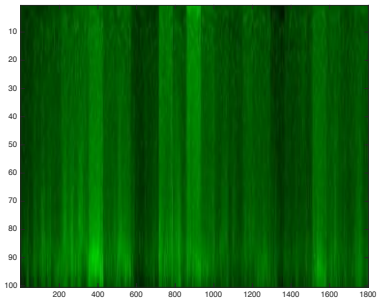

(d) HRK1_4

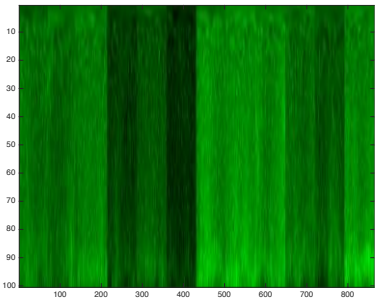

(e) HRK1_6

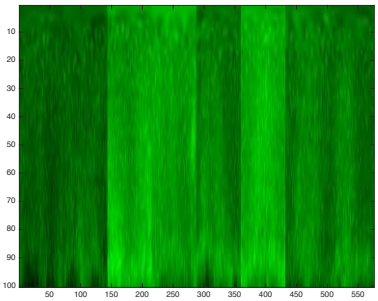

(f) HRK1_7

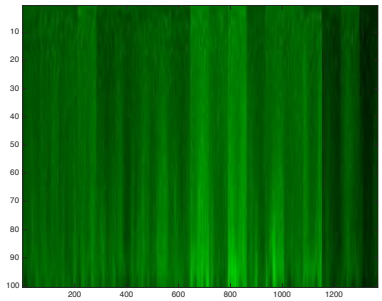

(g) HRK1_8

Figure A.29 – Radial profiles for all replicas of *HRK1* strain after 1 hour in incubation in the presence of acetic acid.

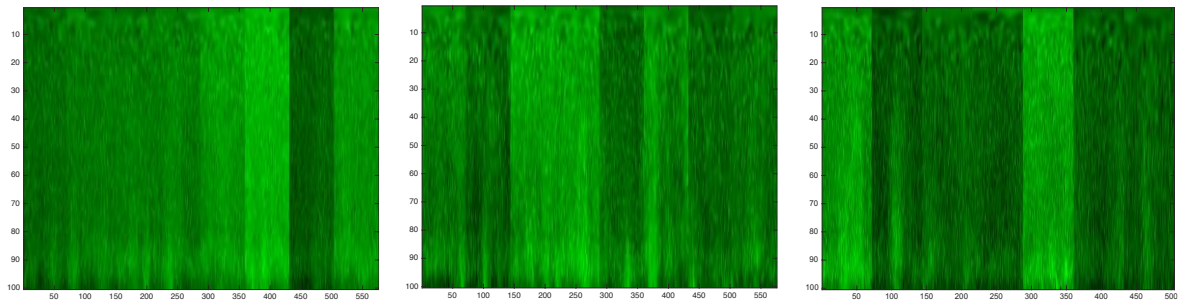

(a) WT_1 **(b)** WT_2 **(c)** WT_3

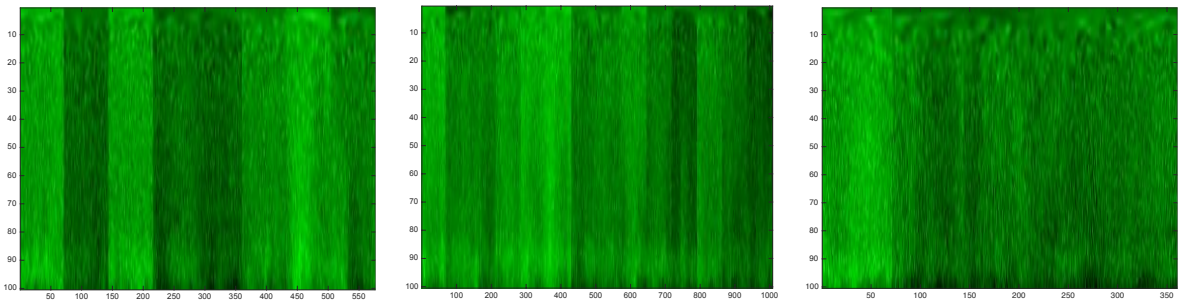

(d) WT_4 **(e)** WT_5 **(f)** WT_7

Figure A.31 – Radial profiles for all replicas of *WT* strain after 2 hours in incubation in the absence of acetic acid.

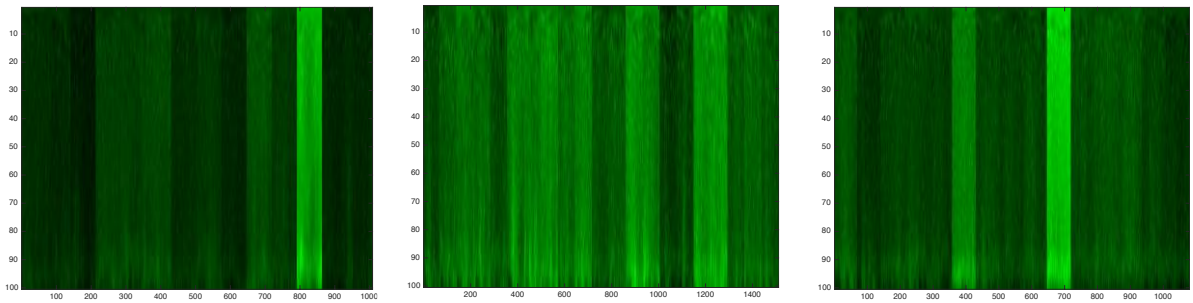

(a) WT_1 **(b)** WT_2 **(c)** WT_4

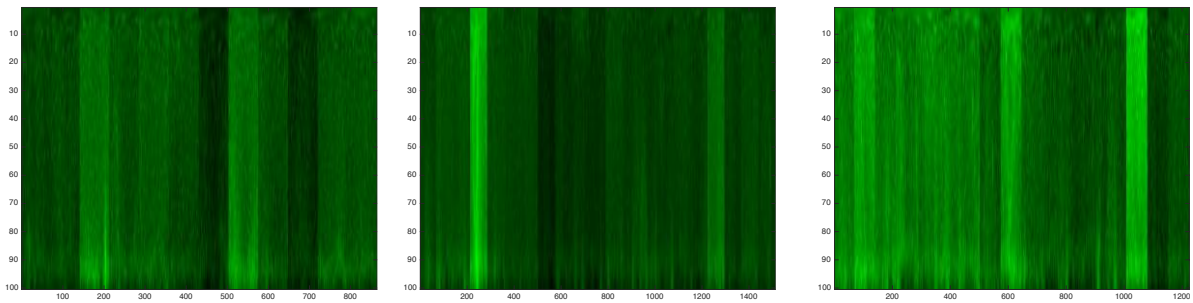

(d) WT_5 **(e)** WT_6 **(f)** WT_7

Figure A.32 – Radial profiles for all replicas of *WT* strain after 2 hours in incubation in the presence of acetic acid.

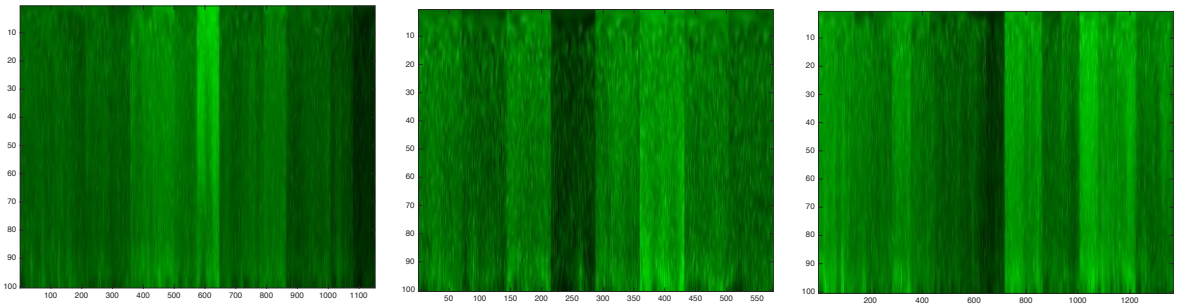

(a) HAA1_1 **(b)** HAA1_2 **(c)** HAA1_3

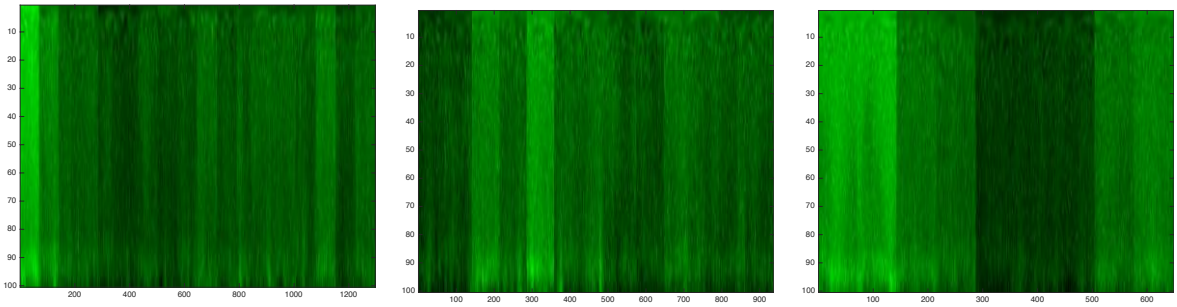

(d) HAA1_5 **(e)** HAA1_6 **(f)** HAA1_7

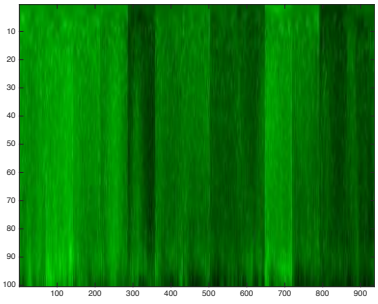

(g) HAA1_8

Figure A.33 – Radial profiles for all replicas of *HAA1* strain after 2 hours in incubation in the absence of acetic acid.

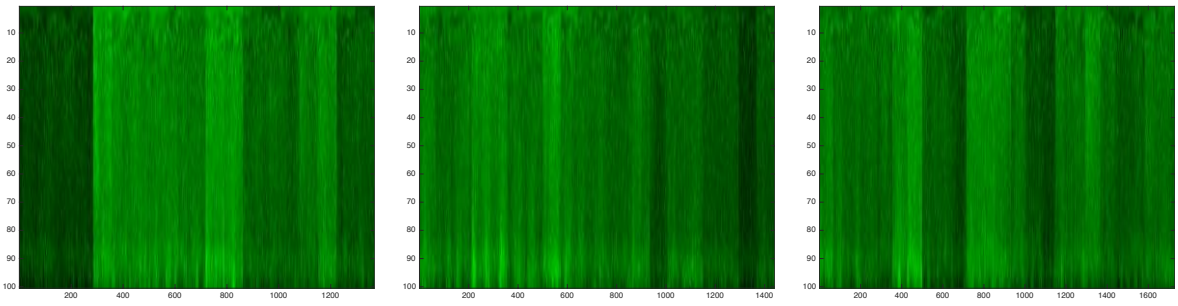

(a) HAA1_1 **(b)** HAA1_2 **(c)** HAA1_3

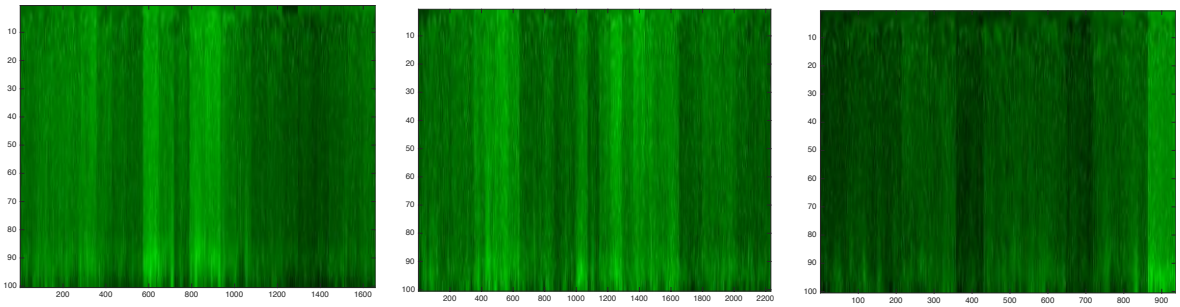

(d) HAA1_4 **(e)** HAA1_5 **(f)** HAA1_7

Figure A.34 – Radial profiles for all replicas of *HAA1* strain after 2 hours in incubation in the presence of acetic acid.

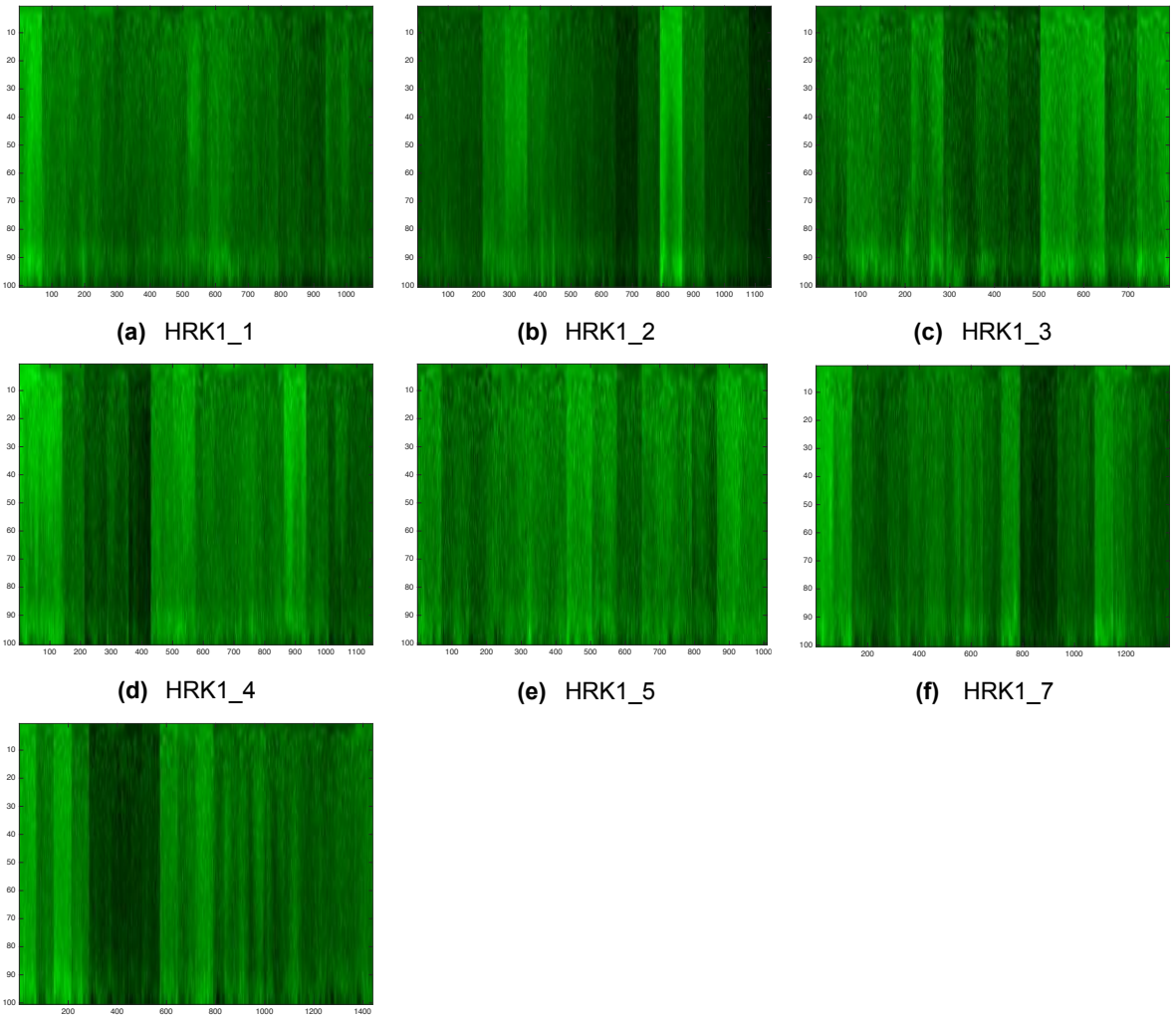

(a) HRK1_1 **(b)** HRK1_2 **(c)** HRK1_3

(d) HRK1_4 **(e)** HRK1_5 **(f)** HRK1_7

(g) HRK1_8

Figure A.35 – Radial profiles for all replicas of *HRK1* strain after 2 hours in incubation in the absence of acetic acid.

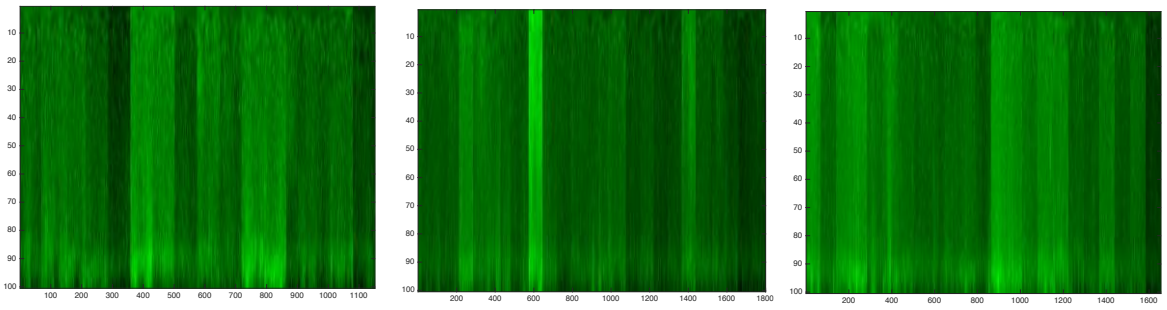

(a) HRK1_1 **(b)** HRK1_2 **(c)** HRK1_4

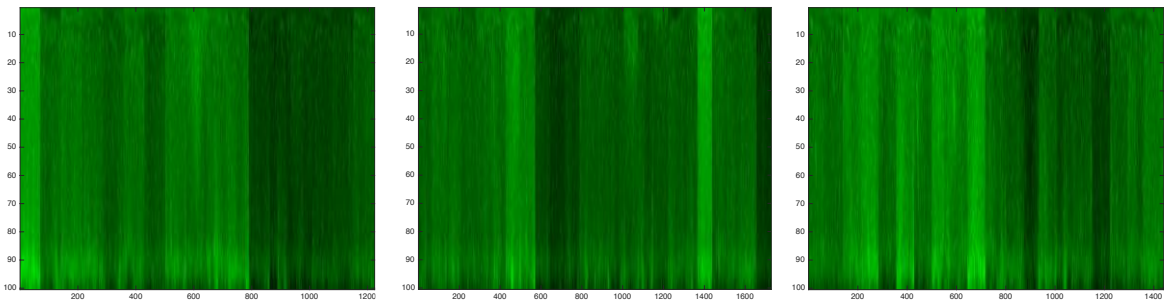

(d) HRK1_5 **(e)** HRK1_6 **(f)** HRK1_7

Figure A.36 – Radial profiles for all replicas of *HRK1* strain after 2 hours in incubation in the presence of acetic acid.

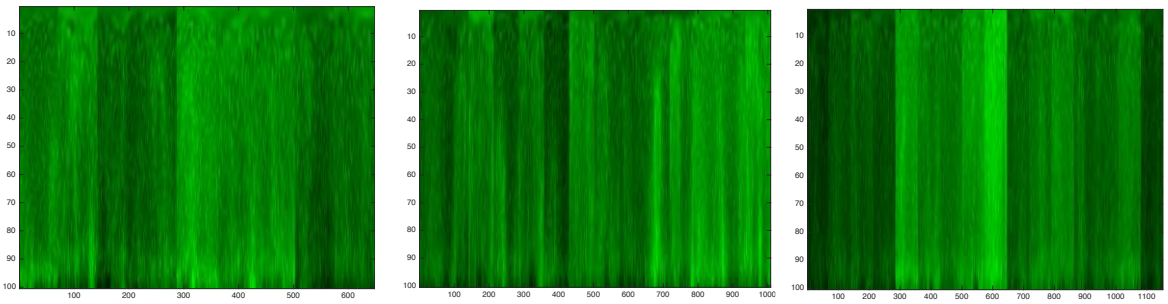

(a) WT_1 **(b)** WT_2 **(c)** WT_3

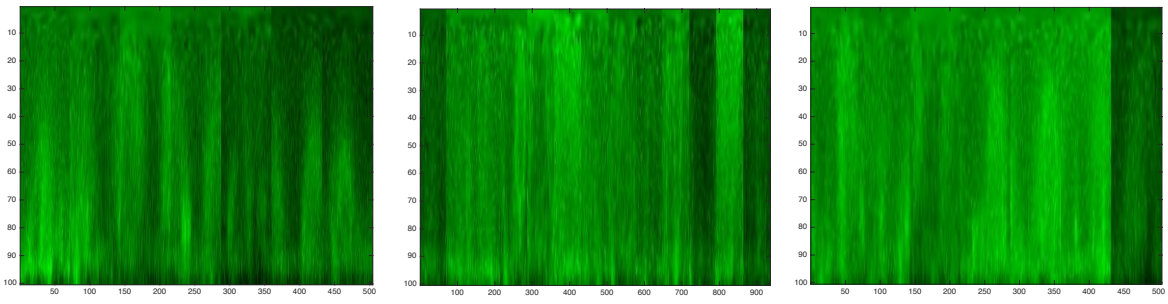

(f) WT_4 **(e)** WT_5 **(d)** WT_6

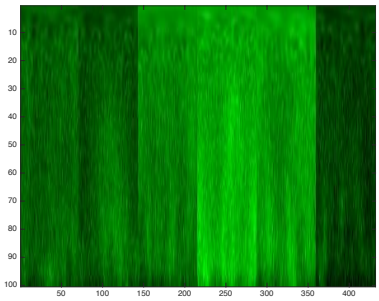

(g) WT_8

Figure A.37– Radial profiles for all replicas of *WT* strain after 4 hours in incubation in the absence of acetic acid.

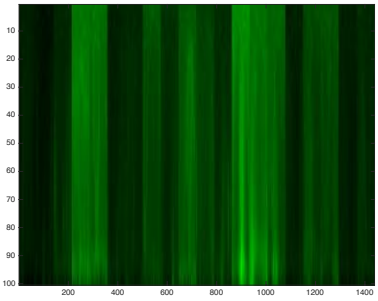

(a) WT_1

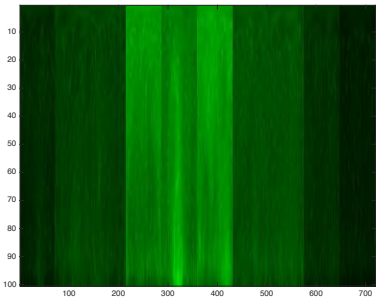

(b) WT_3

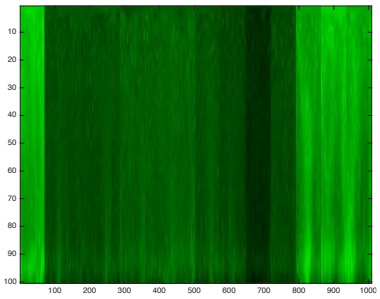

(c) WT_4

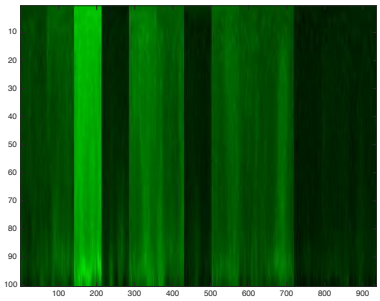

(d) WT_5

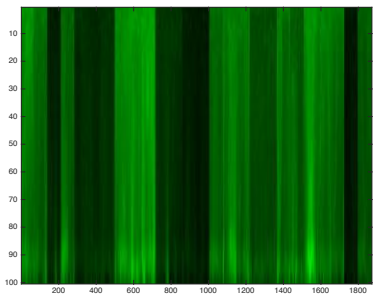

(e) WT_6

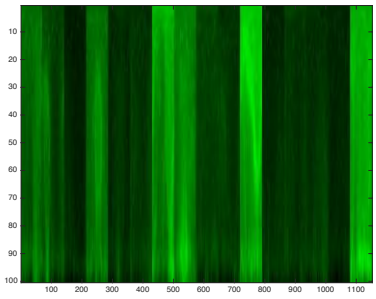

(f) WT_7

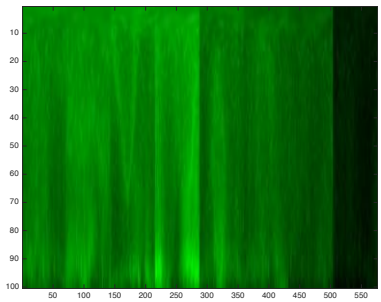

(g) WT_8

Figure A.38 – Radial profiles for all replicas of *WT* strain after 4 hours in incubation in the presence of acetic acid.

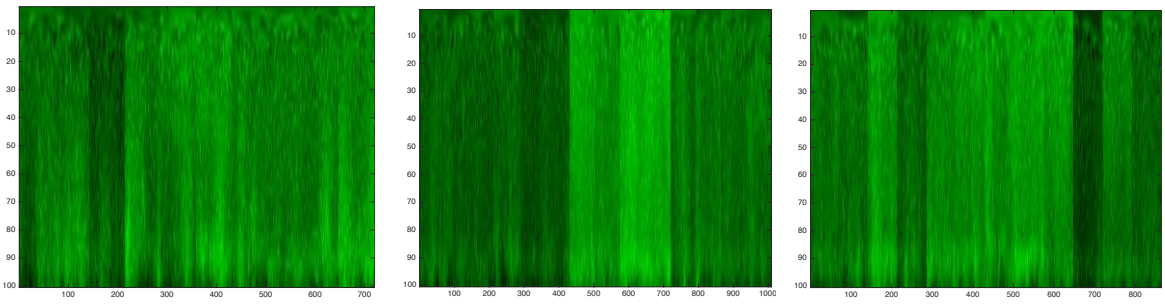

(a) HAA1_2

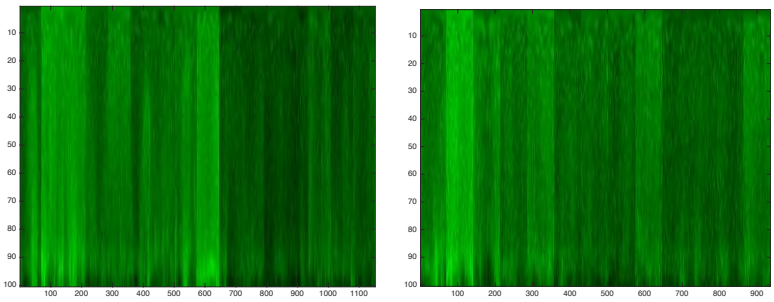

(b) HAA1_5 **(c)** HAA1_6

Figure A.40 – Radial profiles for all replicas of *HAA1* strain after 4 hours in incubation in the absence of acetic acid.

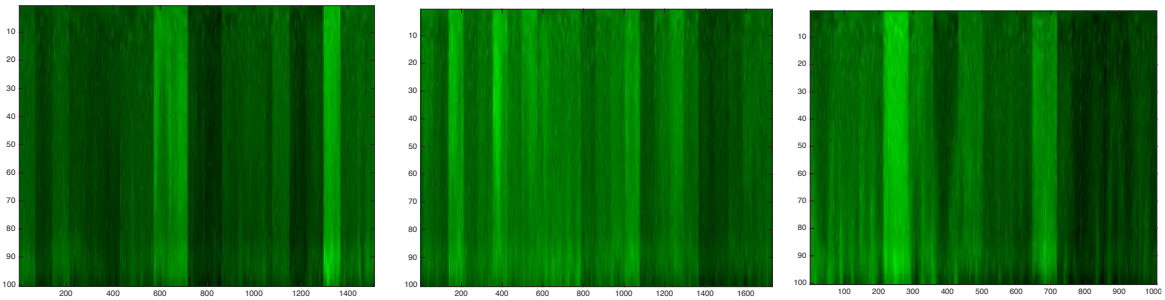

(b) HAA1_1 **(a)** HAA1_2 **(c)** HAA1_4

Figure A.39 – Radial profiles for all replicas of *HAA1* strain after 4 hours in incubation in the presence of acetic acid.

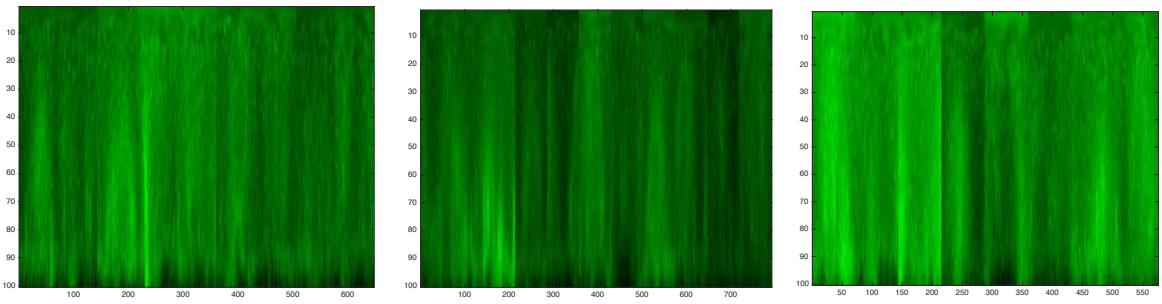

(a) HRK1_2 **(b)** HRK1_3 **(c)** HRK1_4

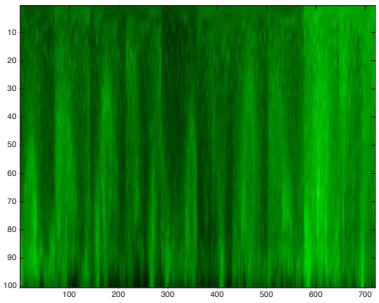

(d) HRK1_6

Figure A.41 – Radial profiles for all replicas of *HRK1* strain after 4 hours in incubation in the absence of acetic acid.

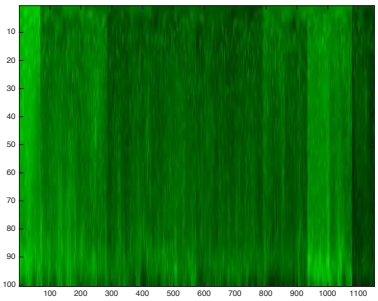

(f) HRK_1

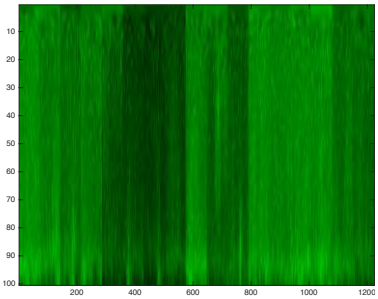

(e) HRK_2

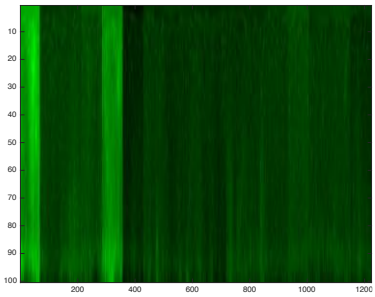

(d) HRK_3

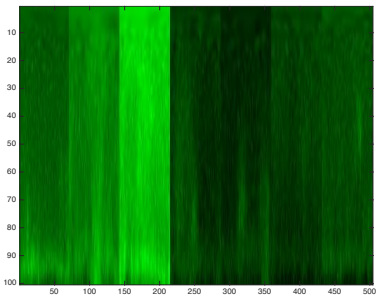

(c) HRK_4

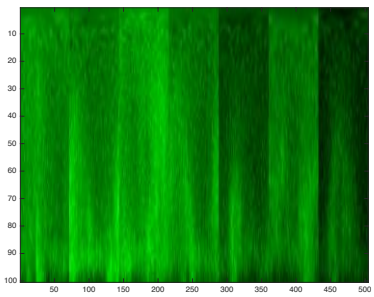

(b) HRK_5

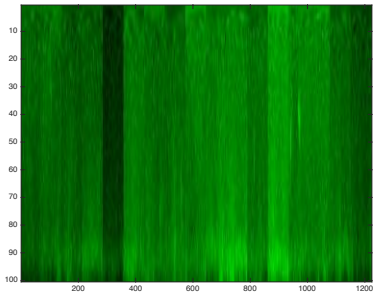

(a) HRK_7

Figure A.42 – Radial profiles for all replicas of *HRK1* strain after 4 hours in incubation in the presence of acetic acid.

A.3. Mean Profiles

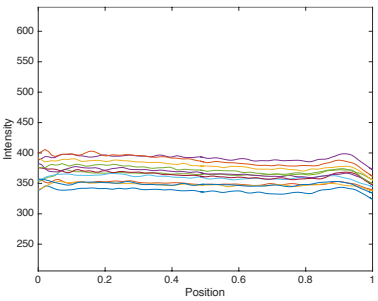

(c) WT_1

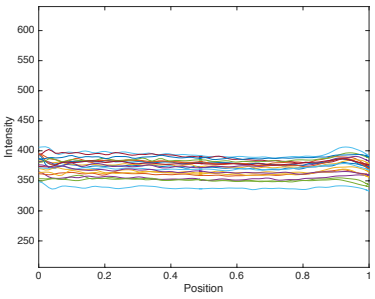

(b) WT_3

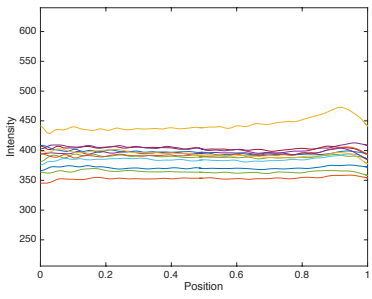

(a) WT_4

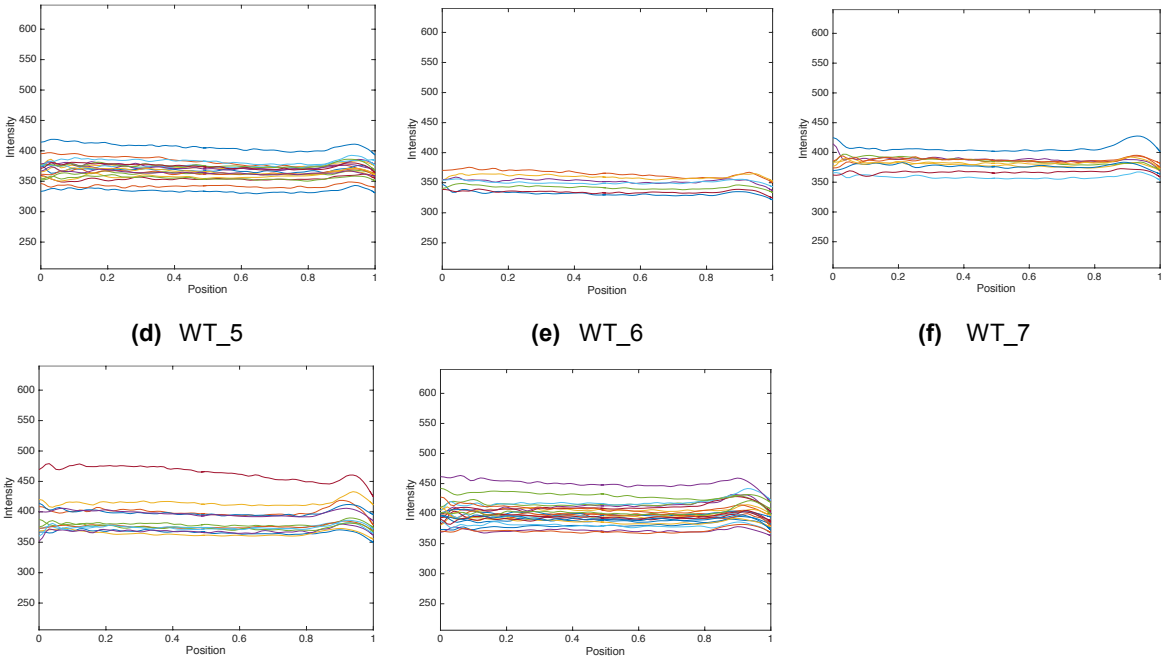

(d) WT_5 **(e)** WT_6 **(f)** WT_7

(g) WT_8 **(h)** WT_9

Figure A.43 – Mean profiles for all replicas of *WT* strain after 0 hours in incubation.

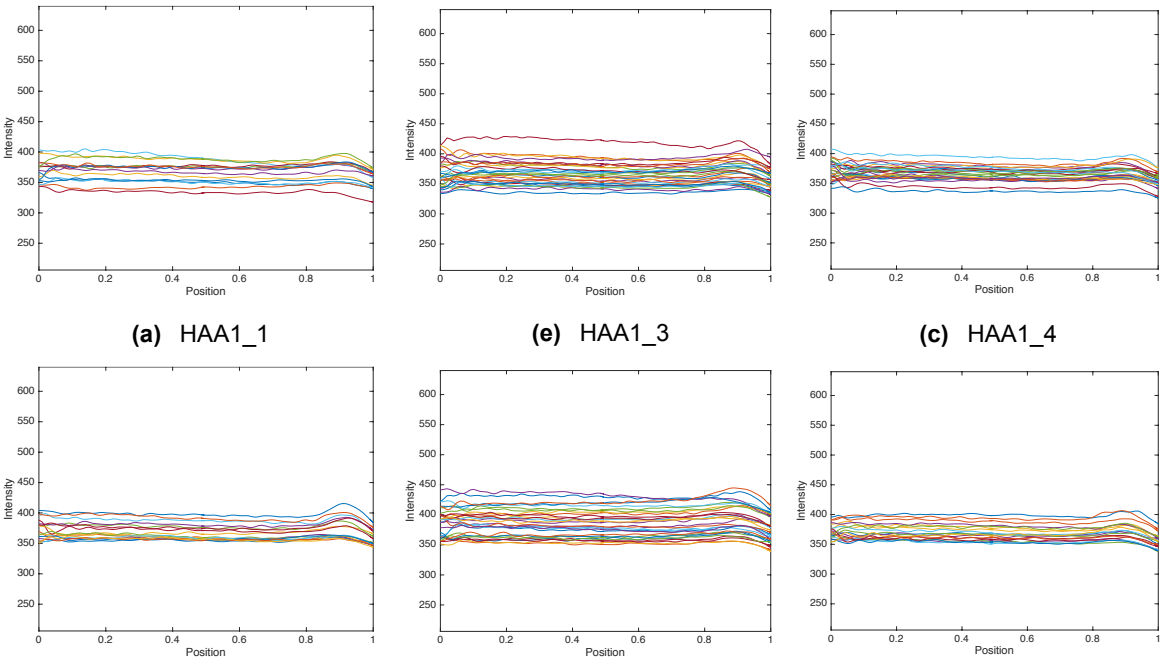

(a) HAA1_1 **(e)** HAA1_3 **(c)** HAA1_4

(b) HAA1_5 **(d)** HAA1_6 **(f)** HAA1_7

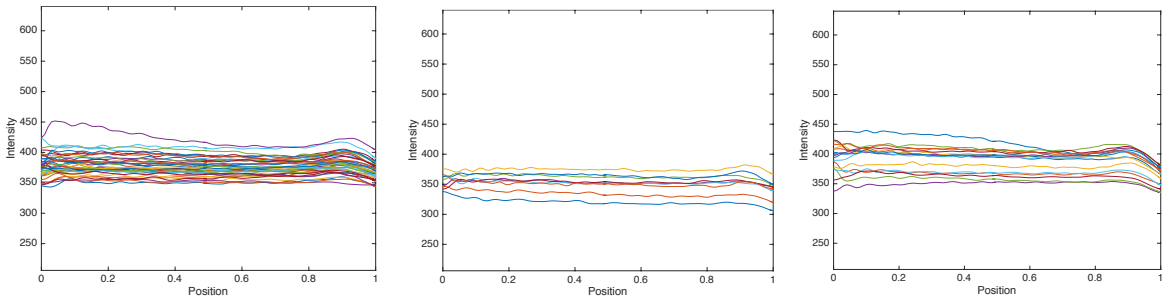

(g) HAA1_8 **(h)** HAA1_9 **(i)** HAA1_10

Figure A.44 – Mean profiles for all replicas of *HAA1* strain after 0 hours in incubation.

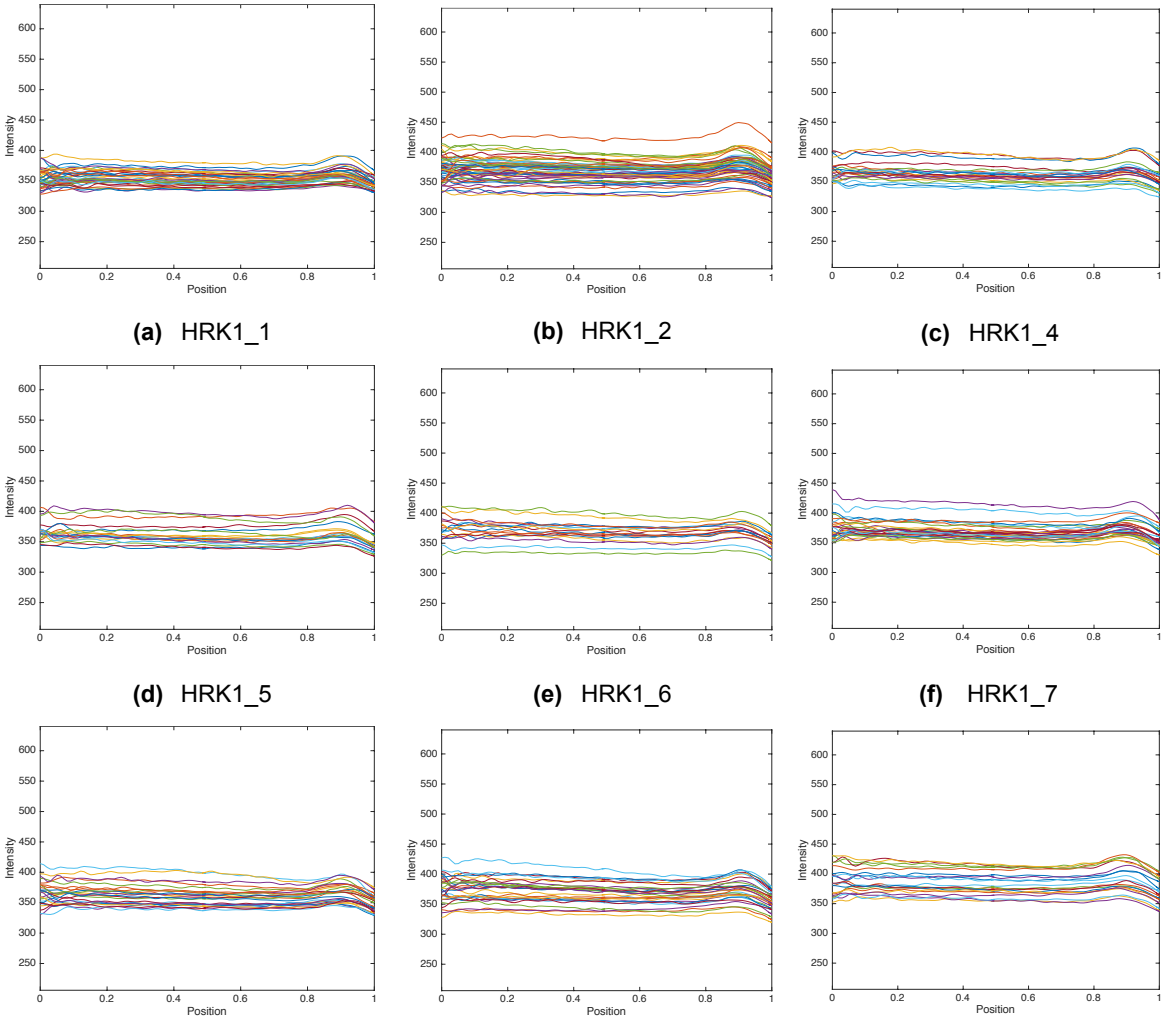

(a) HRK1_1 **(b)** HRK1_2 **(c)** HRK1_4

(d) HRK1_5 **(e)** HRK1_6 **(f)** HRK1_7

(g) HRK1_8 **(i)** HRK1_9 **(h)** HRK1_10

Figure A.45 – Mean profiles for all replicas of *HRK1* strain after 0 hours in incubation.

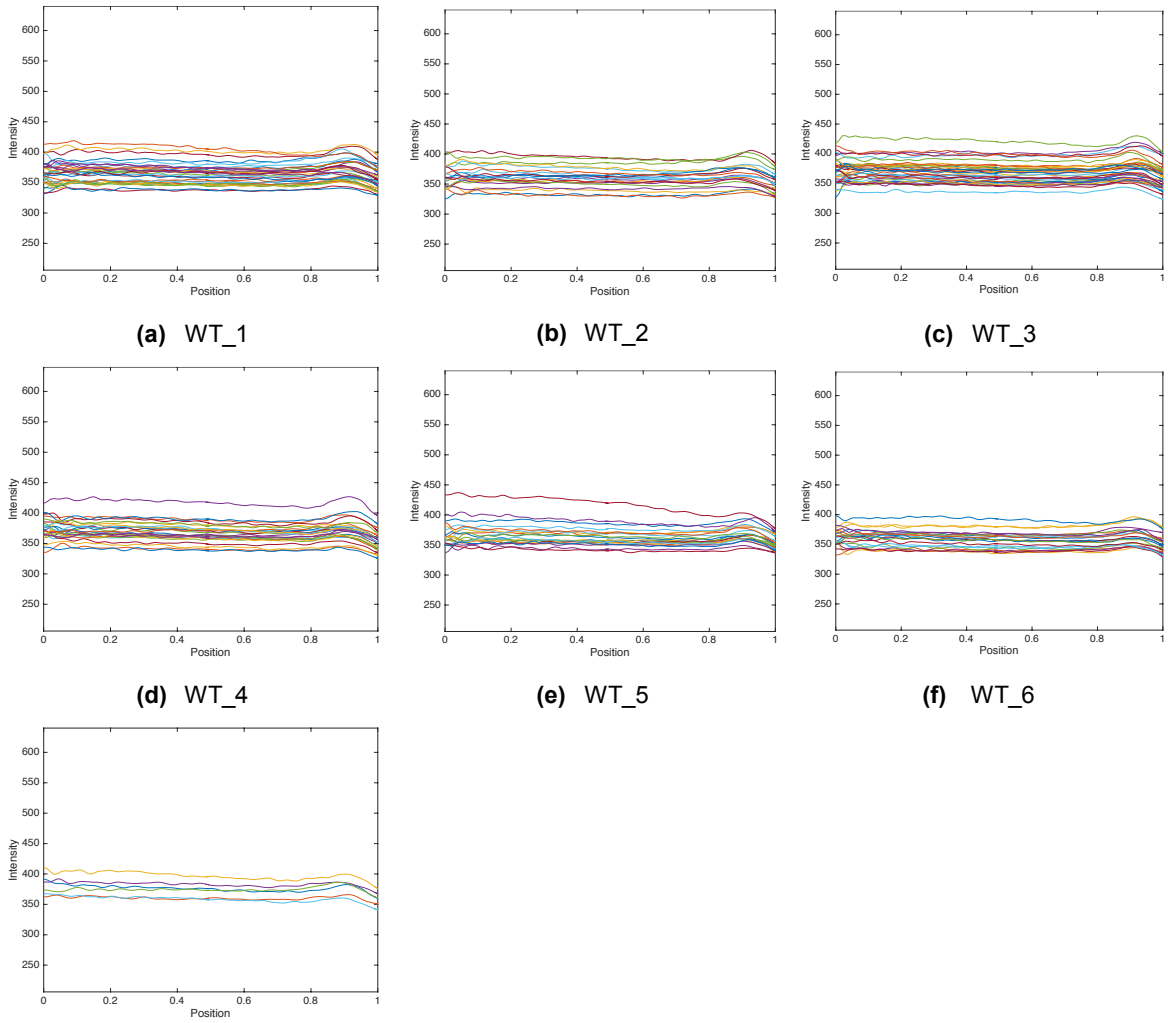

(a) WT_1 **(b)** WT_2 **(c)** WT_3

(d) WT_4 **(e)** WT_5 **(f)** WT_6

(g) WT_8

Figure A.46 – Mean profiles for all replicas of *WT* strain after 1 hour in incubation in the absence of acetic acid.

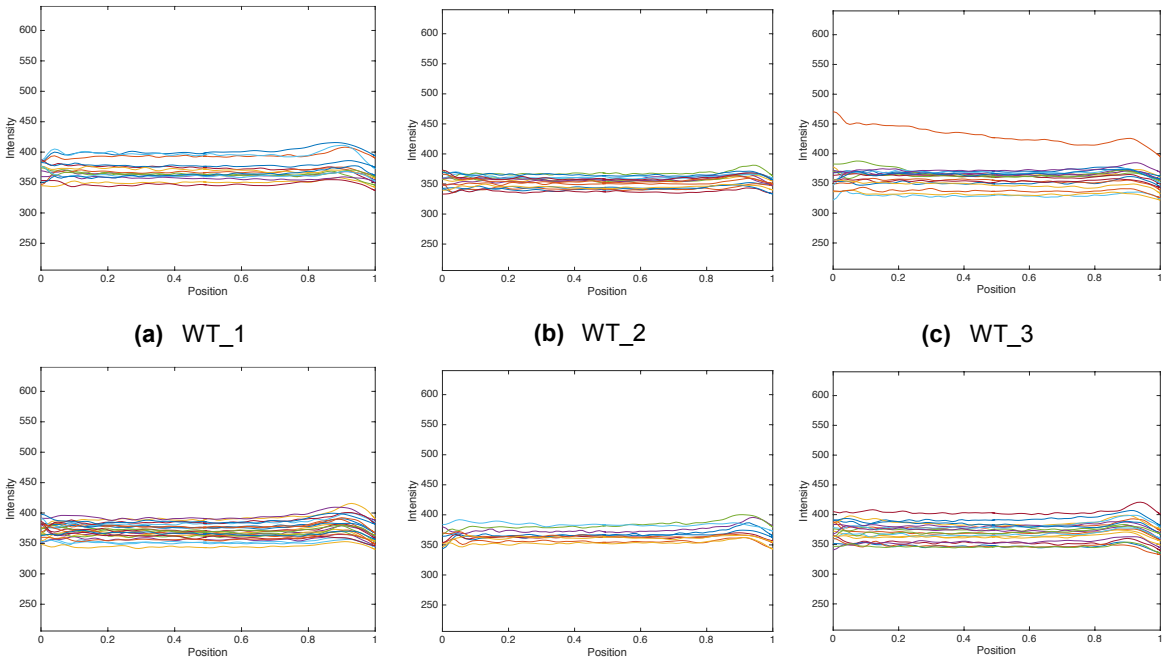

(a) WT_1 **(b)** WT_2 **(c)** WT_3

(d) WT_4 **(e)** WT_5 **(f)** WT_6

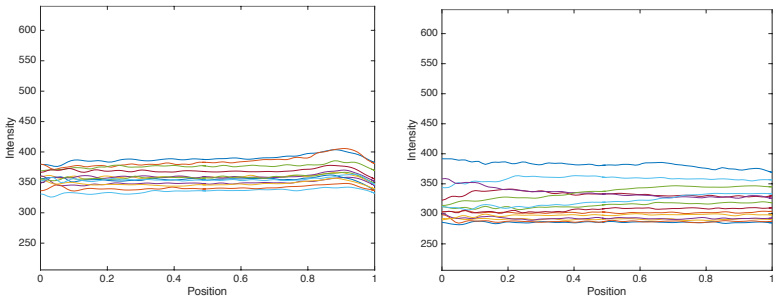

(g) WT_7 **(h)** WT_8

Figure A.47 – Mean profiles for all replicas of *WT* strain after 1 hour in incubation in the presence of acetic acid.

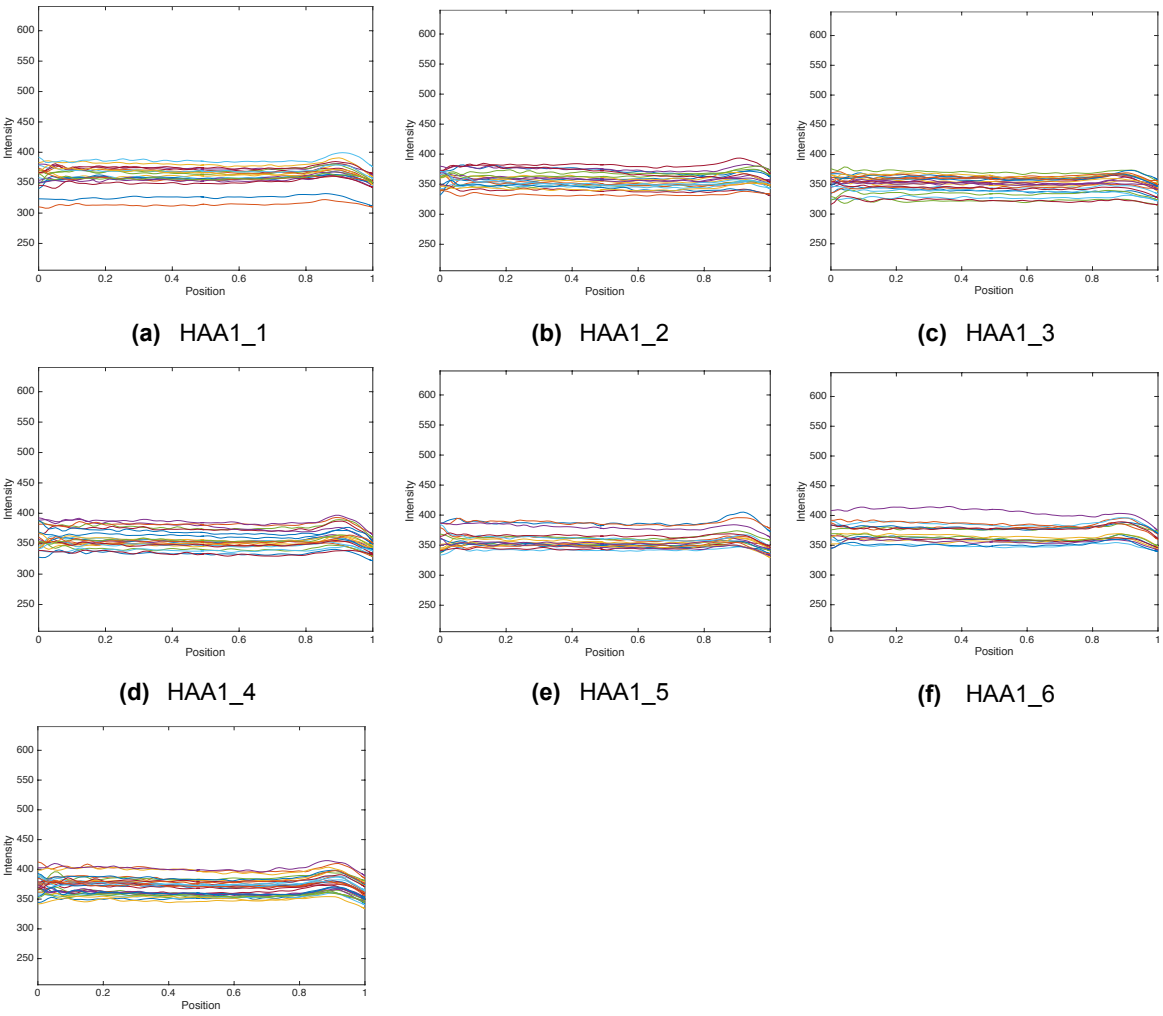

(a) HAA1_1 **(b)** HAA1_2 **(c)** HAA1_3

(d) HAA1_4 **(e)** HAA1_5 **(f)** HAA1_6

(g) HAA1_8

Figure A.48 – Mean profiles for all replicas of *HAA1* strain after 1 hour in incubation in the absence of acetic acid.

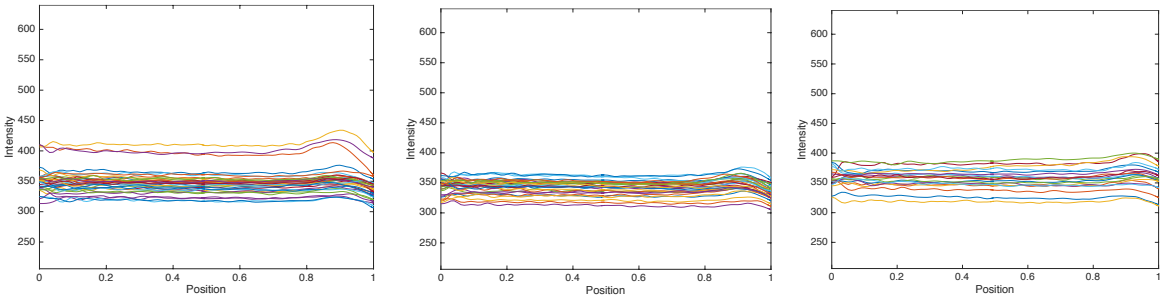

(a) HAA1_1 **(b)** HAA1_2 **(c)** HAA1_3

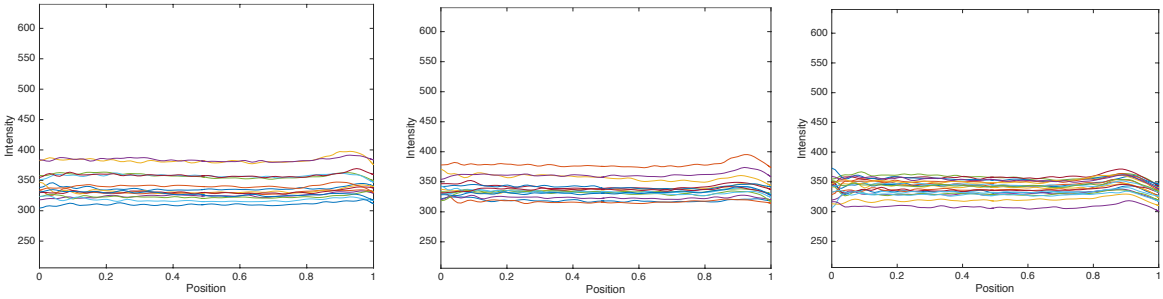

(d) HAA1_4 **(e)** HAA1_5 **(f)** HAA1_6

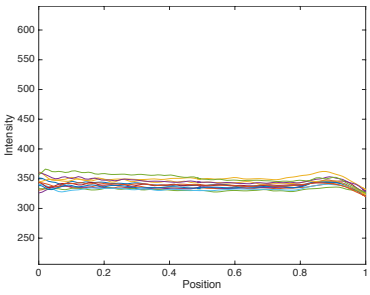

(g) HAA1_8

Figure A.49 – Mean profiles for all replicas of *HAA1* strain after 1 hour in incubation in the presence of acetic acid.

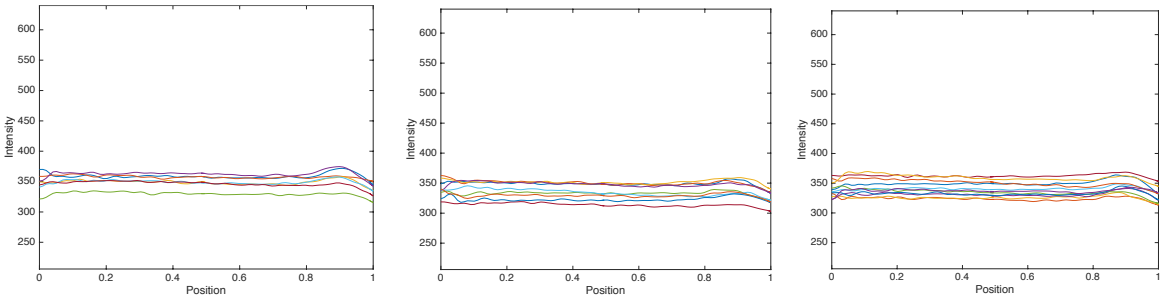

(a) HRK1_1 **(b)** HRK1_2 **(c)** HRK1_3

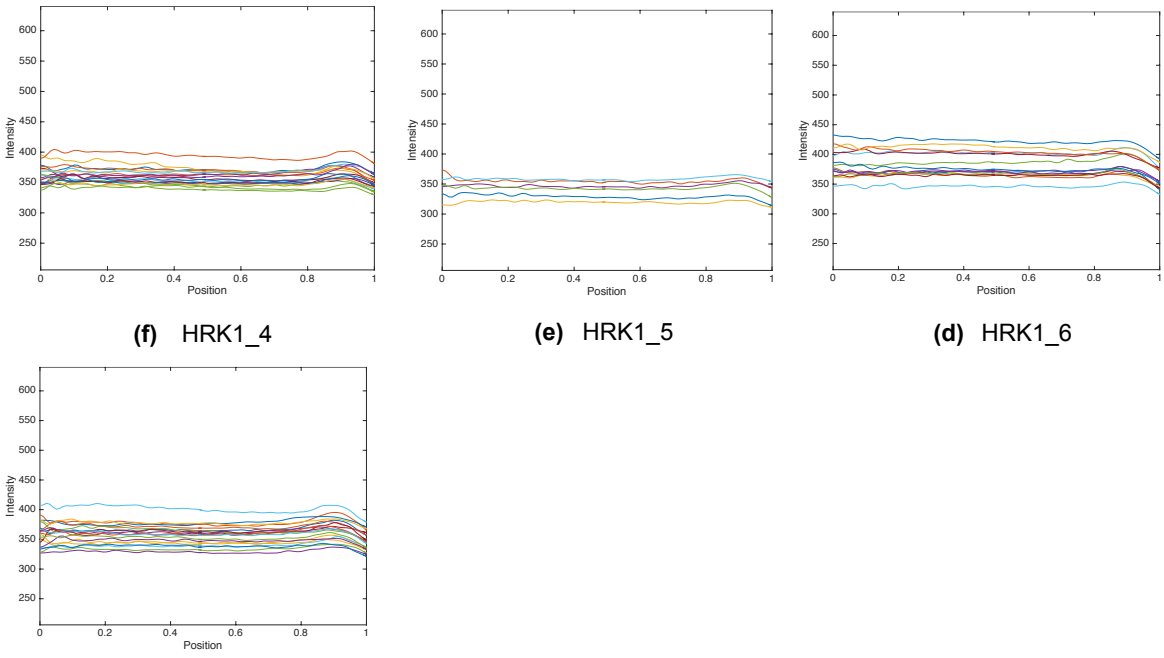

(f) HRK1_4 **(e)** HRK1_5 **(d)** HRK1_6

(g) HRK1_8

Figure A.50 – Mean profiles for all replicas of *HRK1* strain after 1 hour in incubation in the absence of acetic acid.

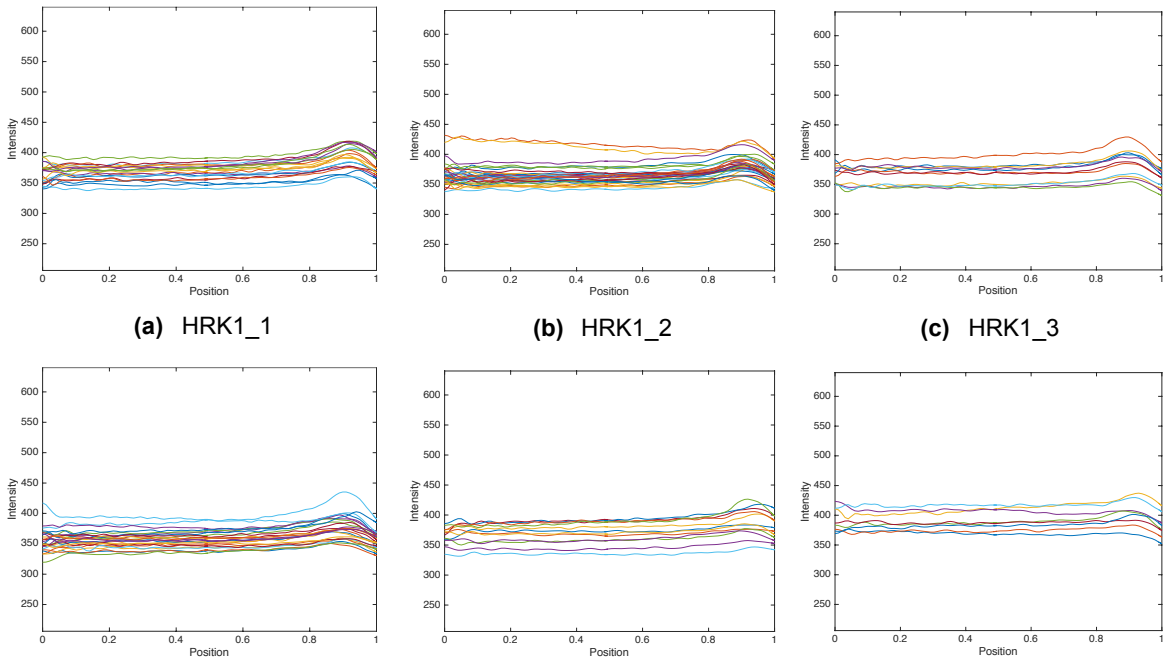

(a) HRK1_1 **(b)** HRK1_2 **(c)** HRK1_3

(d) HRK1_4 **(e)** HRK1_6 **(f)** HRK1_7

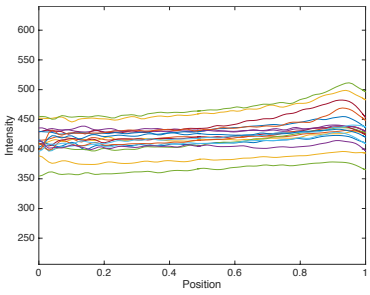

(g) HRK1_8

Figure A.51 – Mean profiles for all replicas of *HRK1* strain after 1 hour in incubation in the presence of acetic acid.

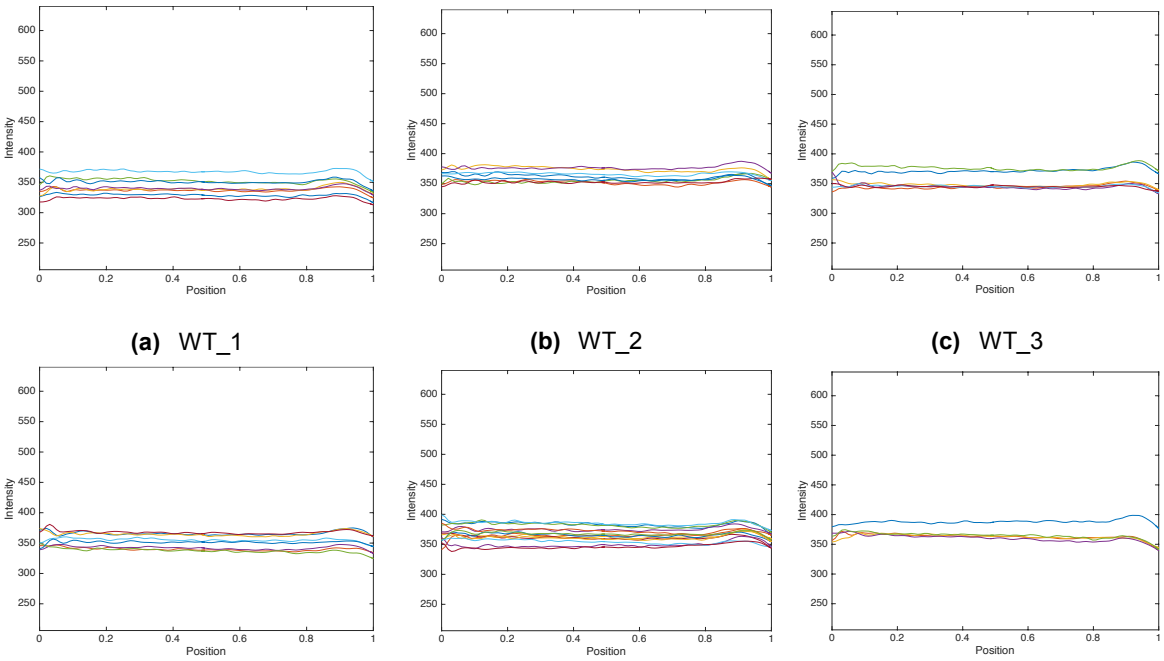

(a) WT_1 **(b)** WT_2 **(c)** WT_3

(d) WT_4 **(e)** WT_5 **(f)** WT_7

Figure A.52 – Mean profiles for all replicas of *WT* strain after 2 hour in incubation in the absence of acetic acid.

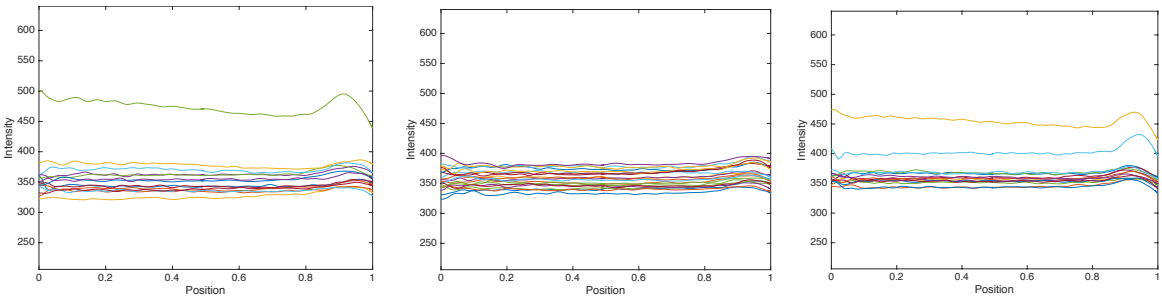

(a) WT_1 **(b)** WT_2 **(c)** WT_4

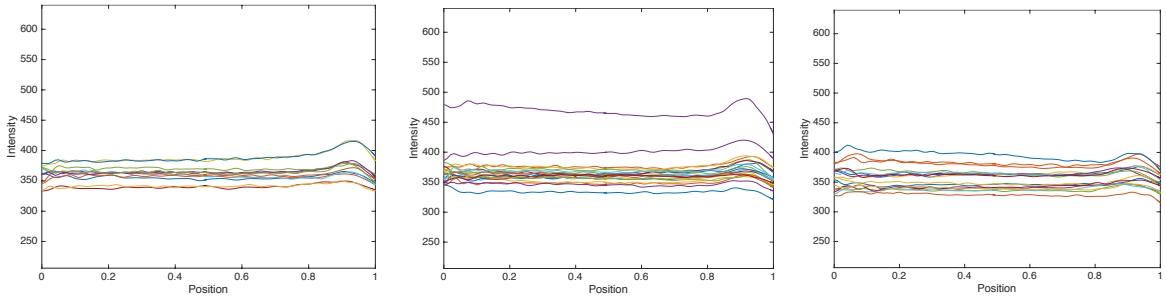

(d) WT_5 **(e)** WT_6 **(f)** WT_7

Figure A.53 – Mean profiles for all replicas of *WT* strain after 2 hour in incubation in the presence of acetic acid.

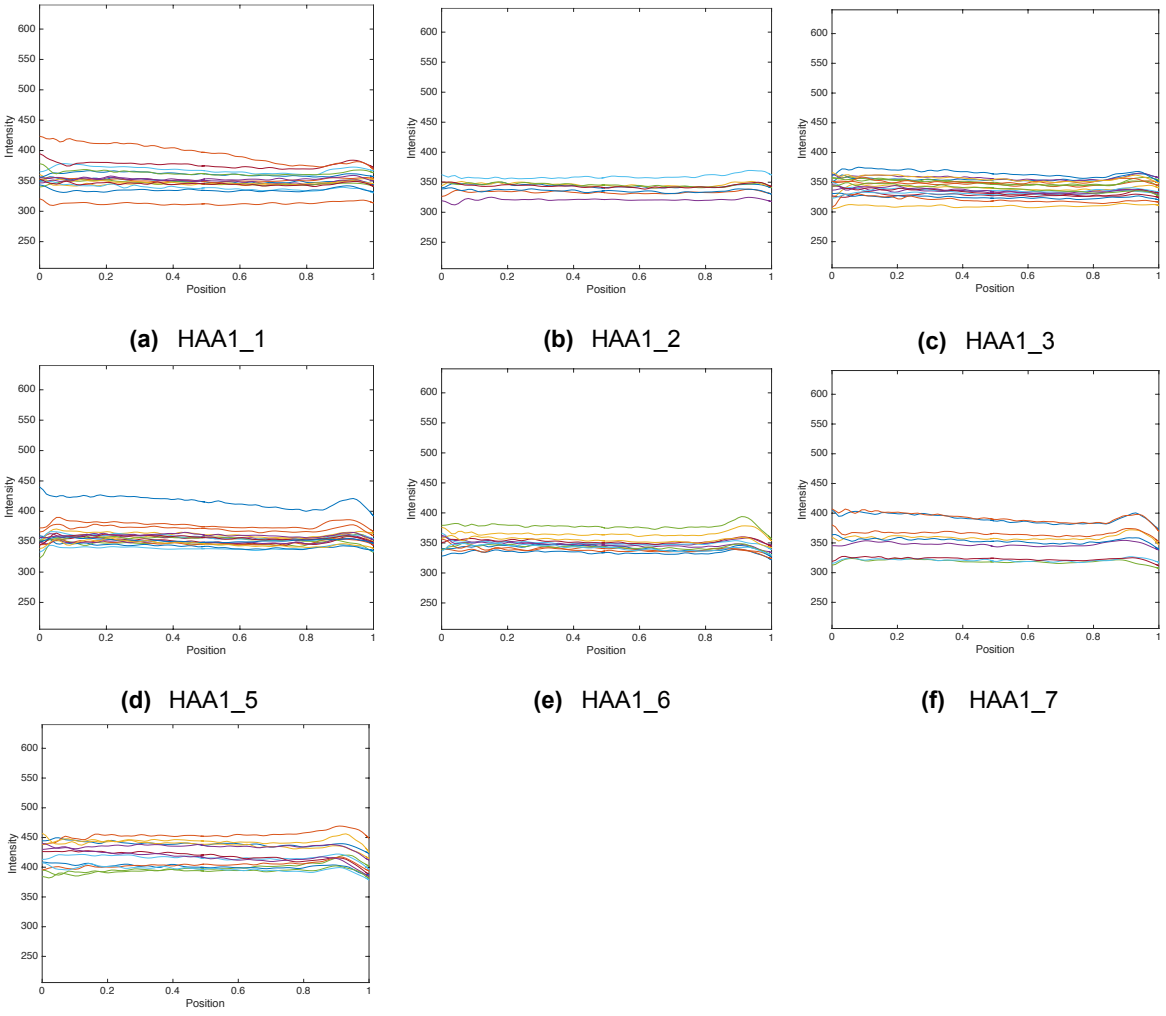

(a) HAA1_1 **(b)** HAA1_2 **(c)** HAA1_3

(d) HAA1_5 **(e)** HAA1_6 **(f)** HAA1_7

(g) HAA1_8

Figure A.54 – Mean profiles for all replicas of *HAA1* strain after 2 hour in incubation in the absence of acetic acid.

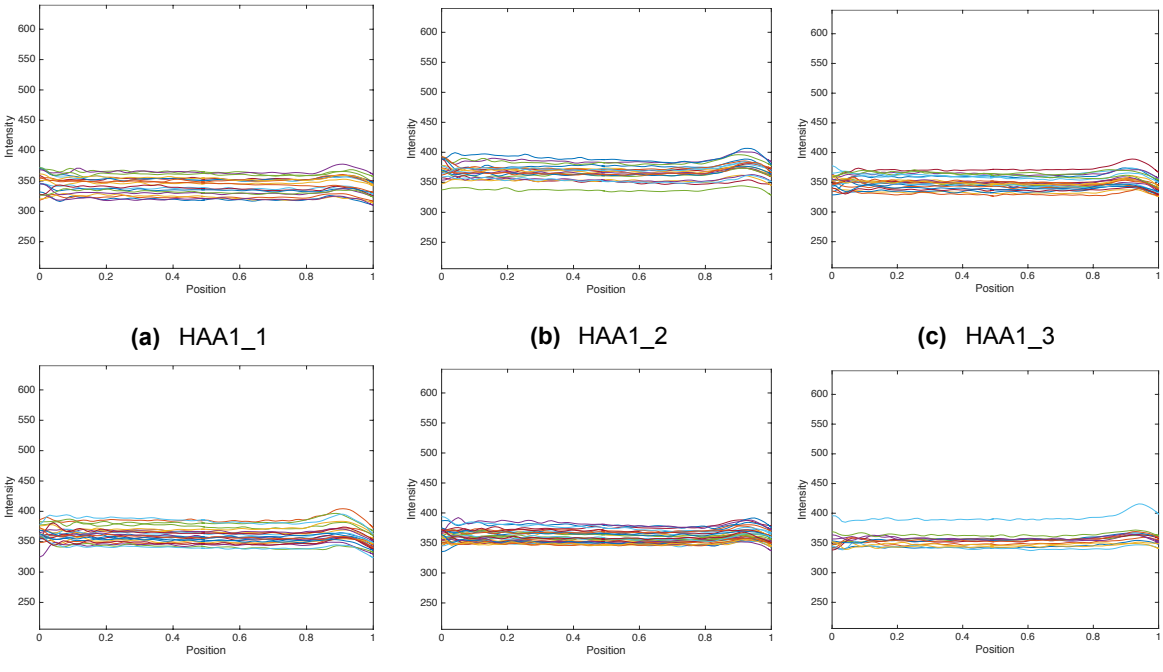

(a) HAA1_1 **(b)** HAA1_2 **(c)** HAA1_3

(d) HAA1_4 **(e)** HAA1_5 **(f)** HAA1_7

Figure A.55 – Mean profiles for all replicas of *HAA1* strain after 2 hour in incubation in the presence of acetic acid.

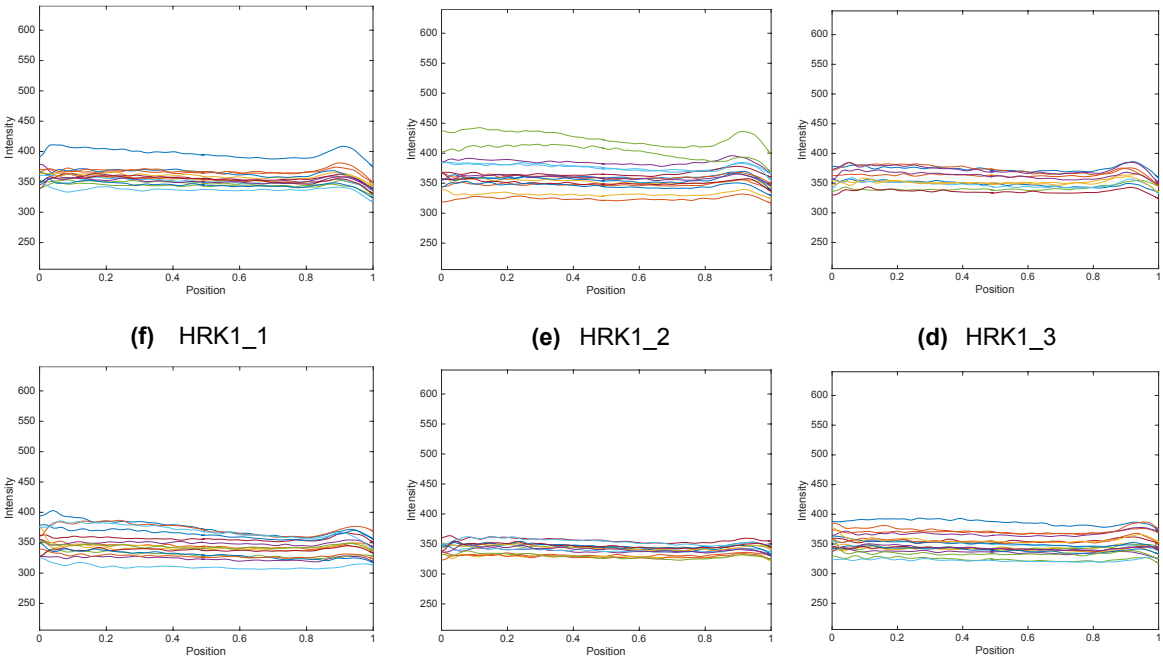

(f) HRK1_1 **(e)** HRK1_2 **(d)** HRK1_3

(c) HRK1_4 **(b)** HRK1_5 **(a)** HRK1_7

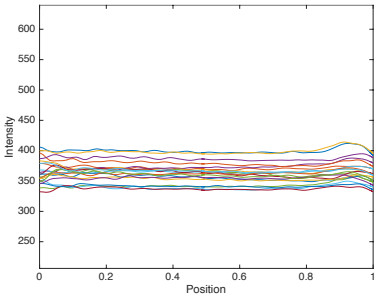

(g) HRK1_8

Figure A.56 – Mean profiles for all replicas of *HRK1* strain after 2 hour in incubation in the absence of acetic acid.

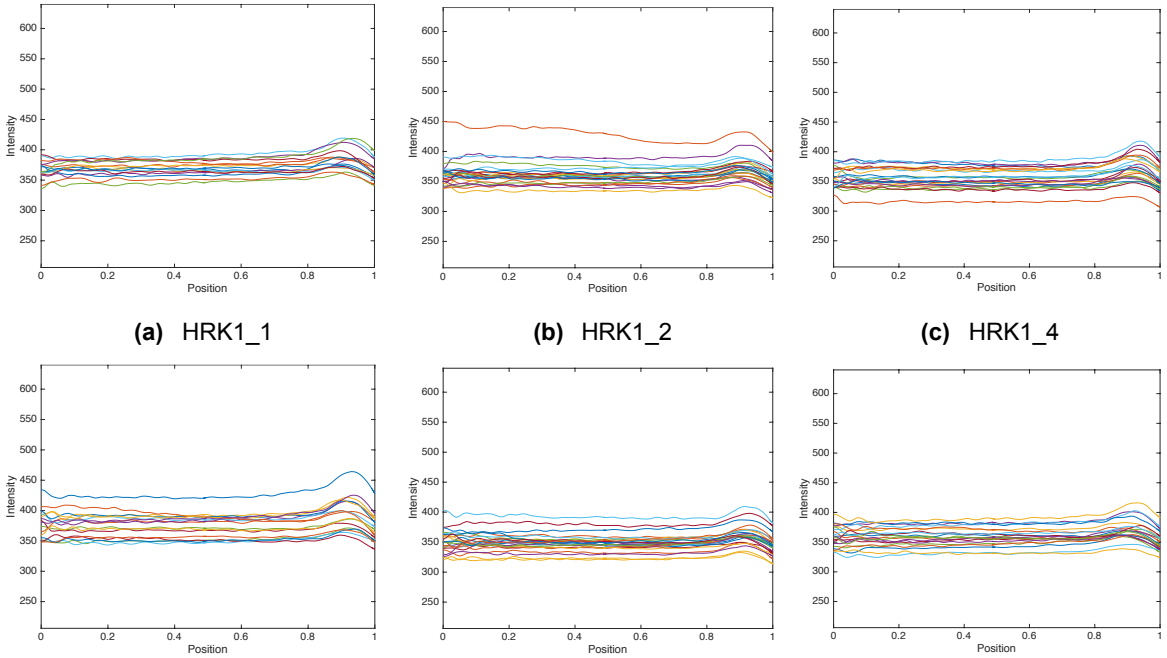

(a) HRK1_1 **(b)** HRK1_2 **(c)** HRK1_4

(d) HRK1_5 **(e)** HRK1_6 **(f)** HRK1_7

Figure A.57 – Mean profiles for all replicas of *HRK1* strain after 2 hour in incubation in the presence of acetic acid.

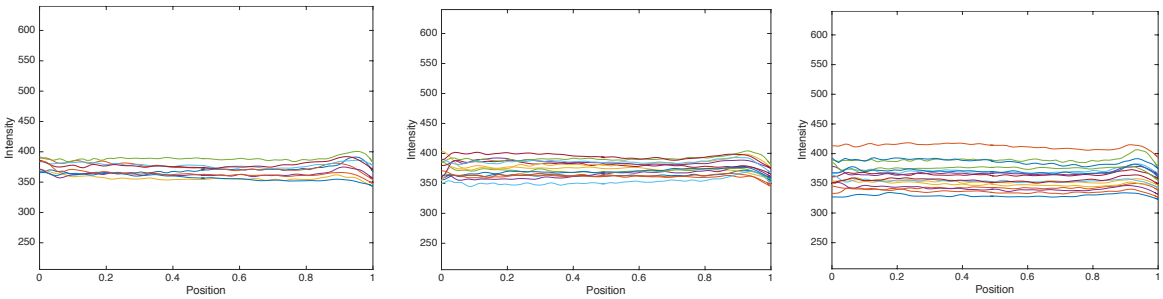

(a) WT_1 **(b)** WT_2 **(c)** WT_3

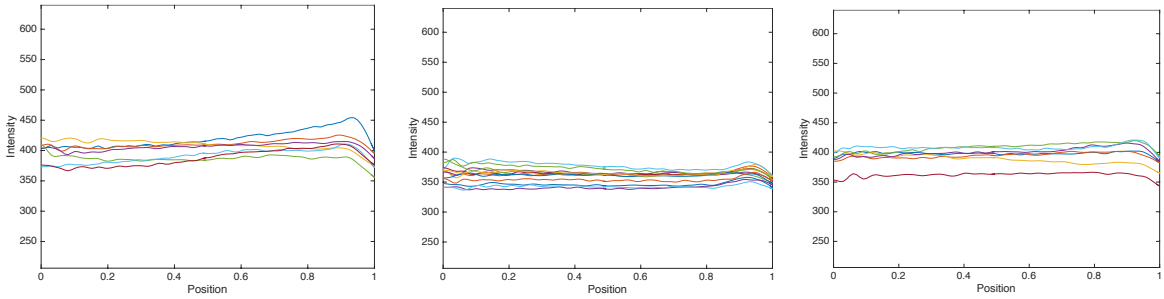

(d) WT_4 **(e)** WT_5 **(f)** WT_6

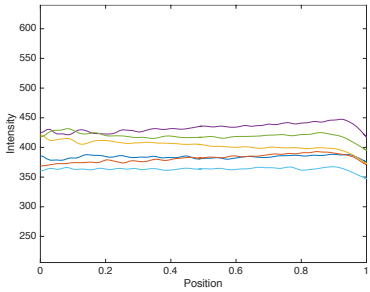

(g) WT_8

Figure A.58 – Mean profiles for all replicas of *WT* strain after 4 hour in incubation in the absence of acetic acid.

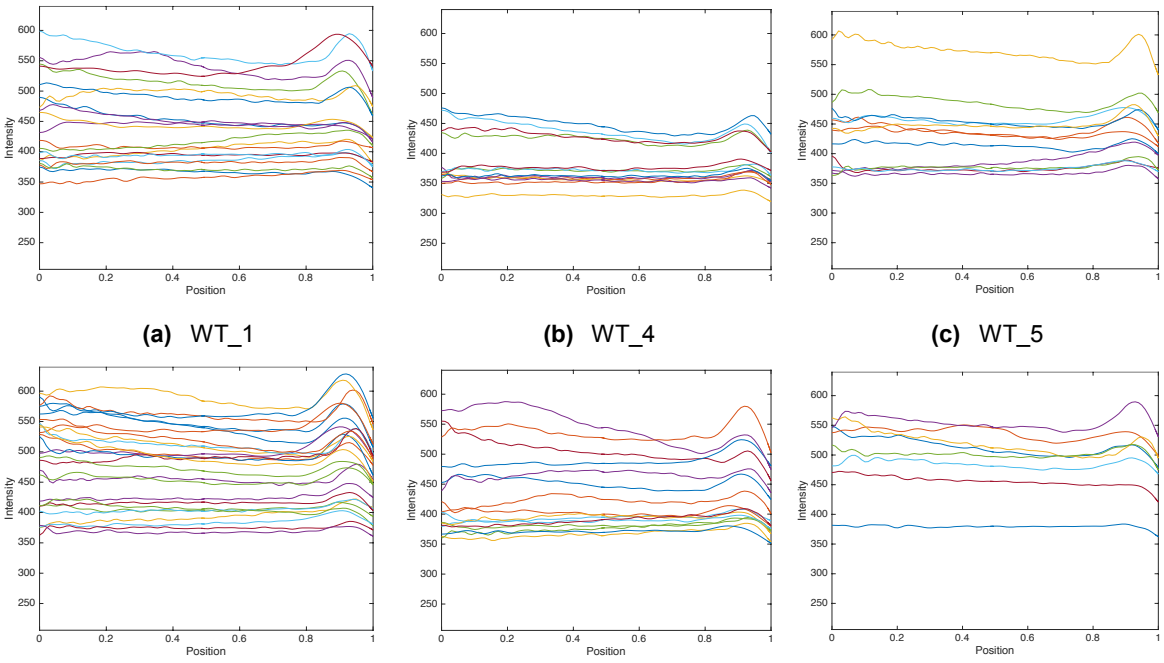

(a) WT_1 **(b)** WT_4 **(c)** WT_5

(d) WT_6 **(e)** WT_7 **(f)** WT_8

Figure A.59 – Mean profiles for all replicas of *WT* strain after 4 hour in incubation in the presence of acetic acid.

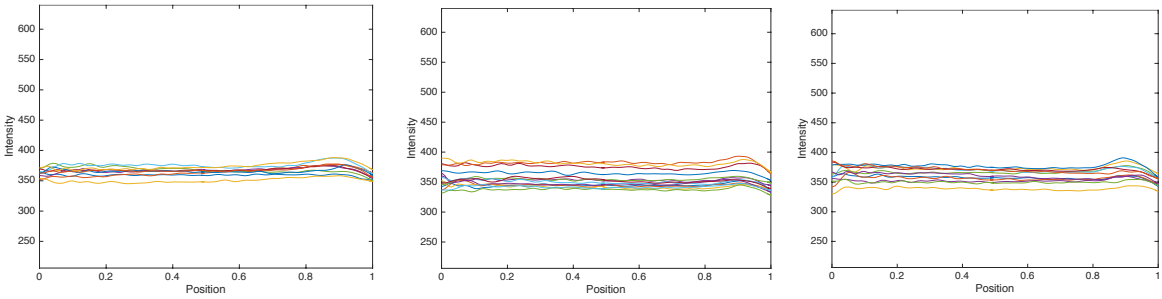

(a) HAA1_2 **(b)** HAA1_3 **(c)** HAA1_4

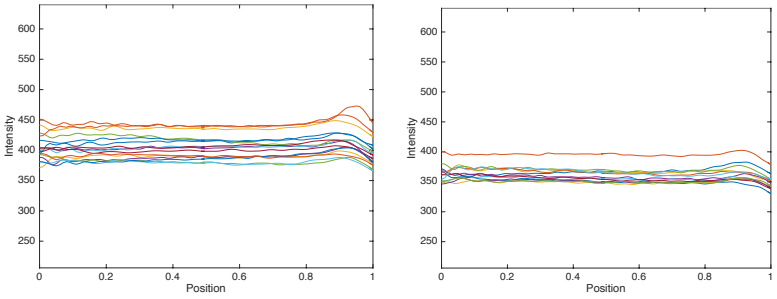

(d) HAA1_5 **(e)** HAA1_6

Figure A.60 – Mean profiles for all replicas of *HAA1* strain after 4 hour in incubation in the absence of acetic acid.

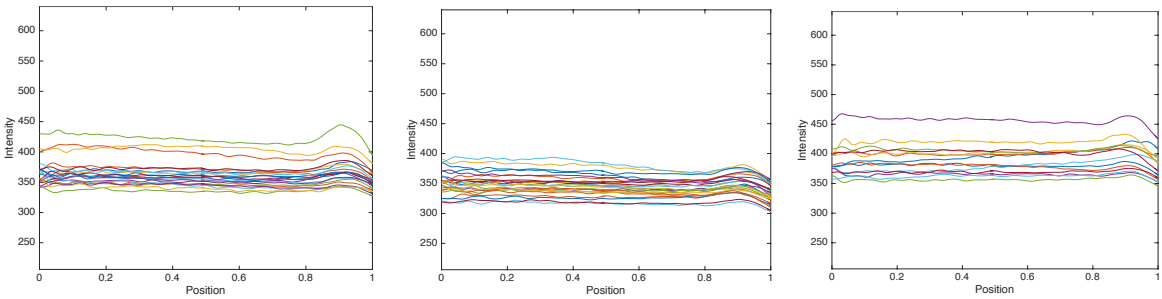

(a) HAA1_1 **(b)** HAA1_2 **(c)** HAA1_4

Figure A.61 – Mean profiles for all replicas of *HAA1* strain after 4 hour in incubation in the presence of acetic acid.

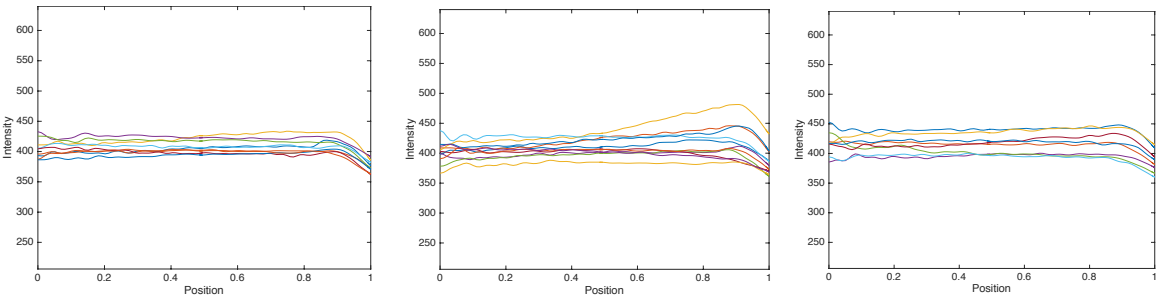

(a) HRK1_2 **(b)** HRK1_3 **(c)** HRK1_4

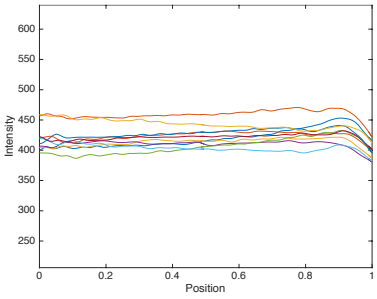

(d) HRK1_6

Figure A.62 – Mean profiles for all replicas of *HRK1* strain after 4 hour in incubation in the absence of acetic acid.

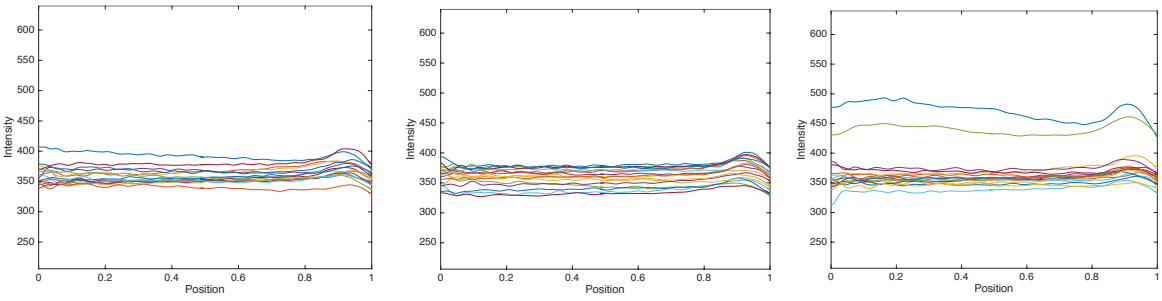

(a) HRK1_1 **(b)** HRK1_2 **(c)** HRK1_3

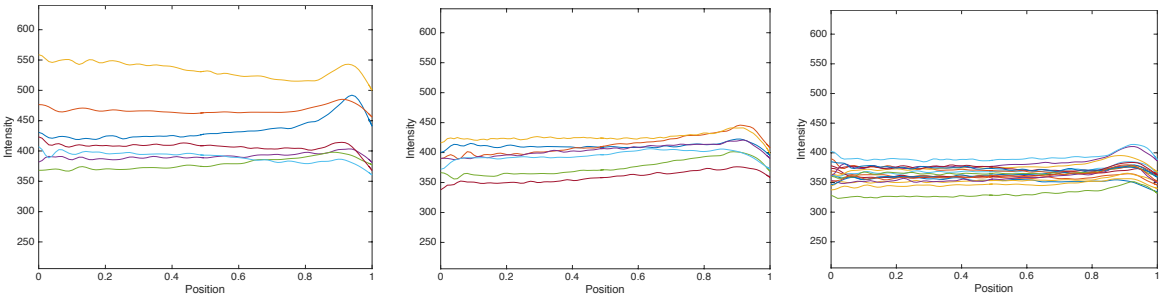

(d) HRK1_4 **(e)** HRK1_5 **(f)** HRK1_7

Figure A.63 – Mean profiles for all replicas of *HRK1* strain after 4 hour in incubation in the presence of acetic acid.

A.4. Standard Deviation Profiles

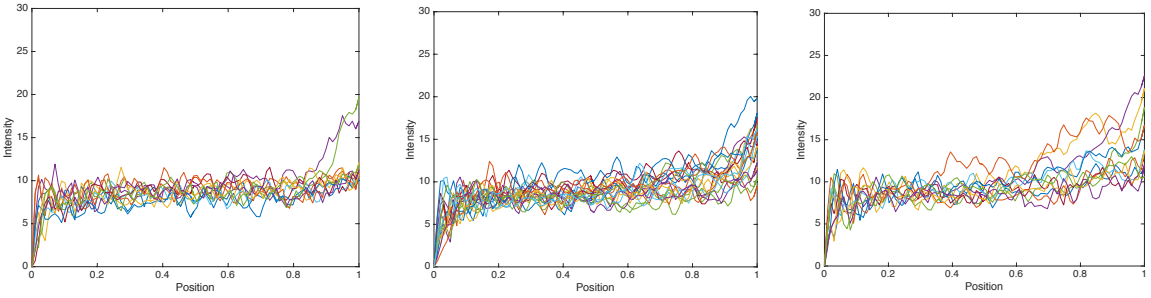

(a) WT_1 **(b)** WT_3 **(c)** WT_4

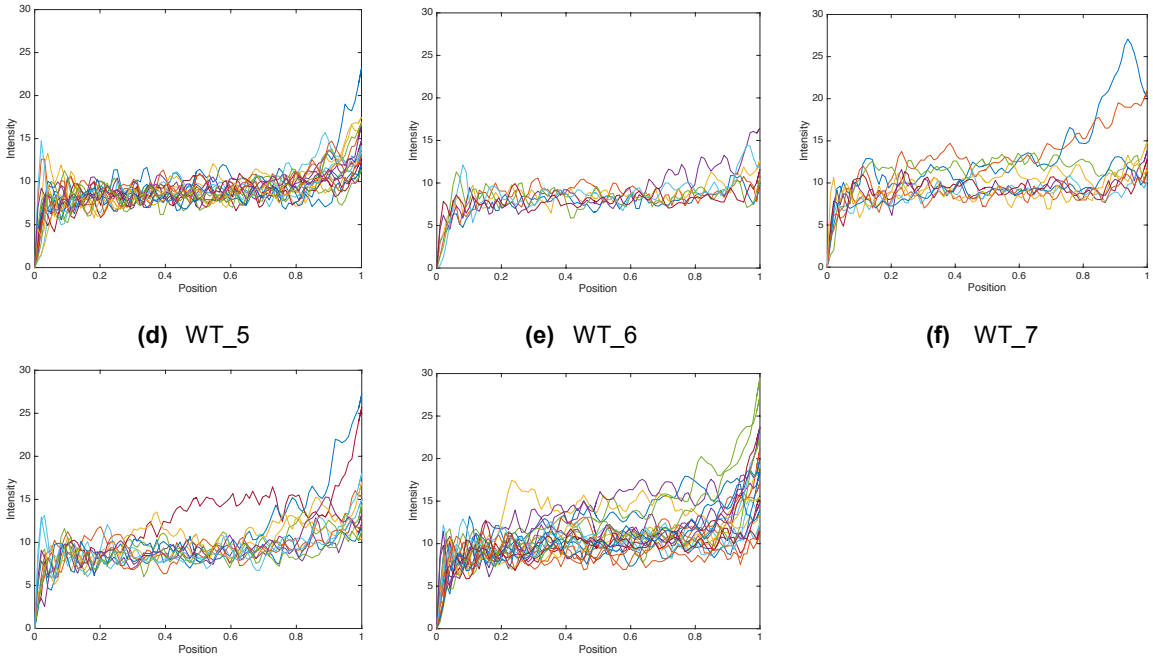

(d) WT_5 **(e)** WT_6 **(f)** WT_7

(g) WT_8 **(h)** WT_9

Figure A.64 – Standard Deviation Profiles for all replicas of *WT* strain after 0 hours in incubation.

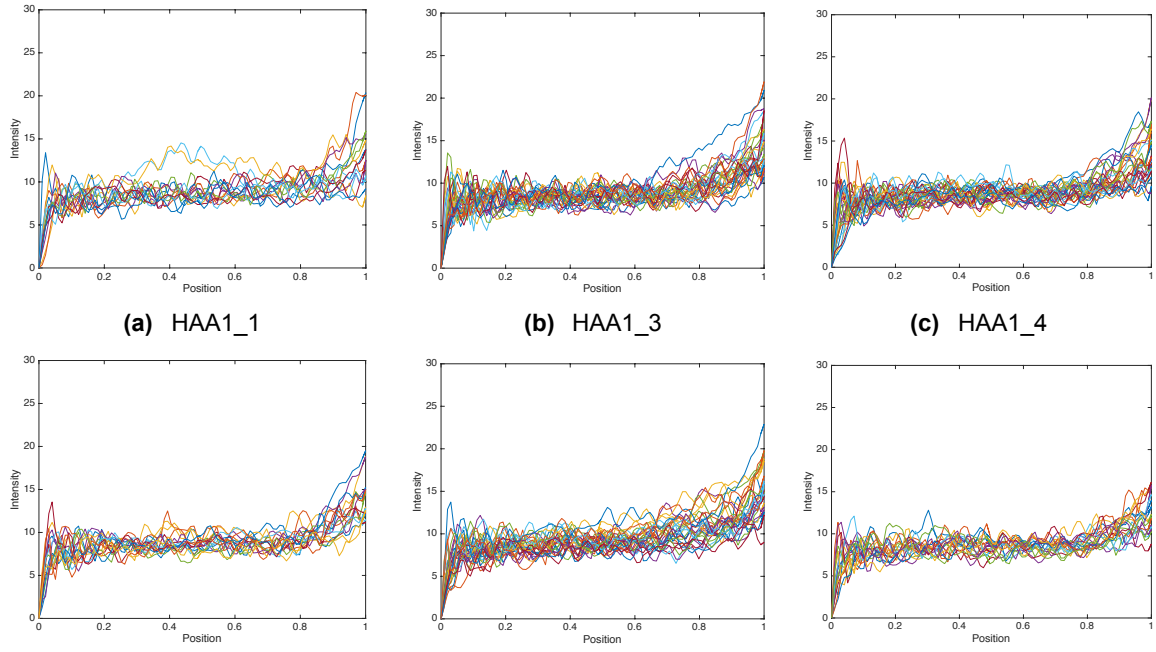

(a) HAA1_1 **(b)** HAA1_3 **(c)** HAA1_4

(d) HAA1_5 **(e)** HAA1_6 **(f)** HAA1_7

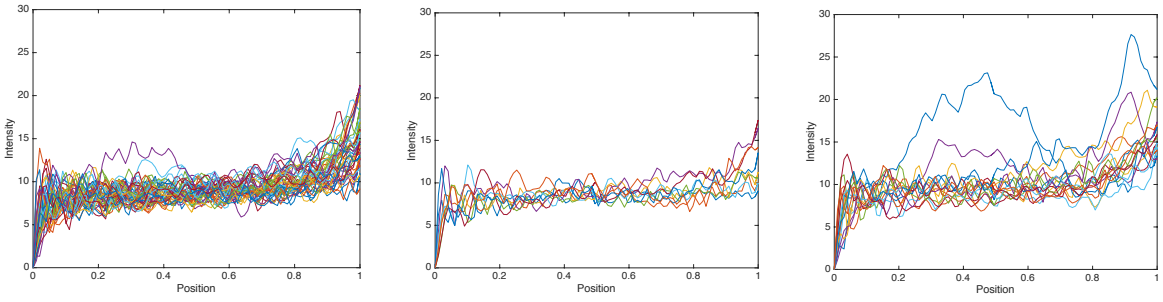

(g) HAA1_8 **(h)** HAA1_9 **(i)** HAA1_10

Figure A.65 – Standard Deviation Profiles for all replicas of *HAA1* strain after 0 hours in incubation.

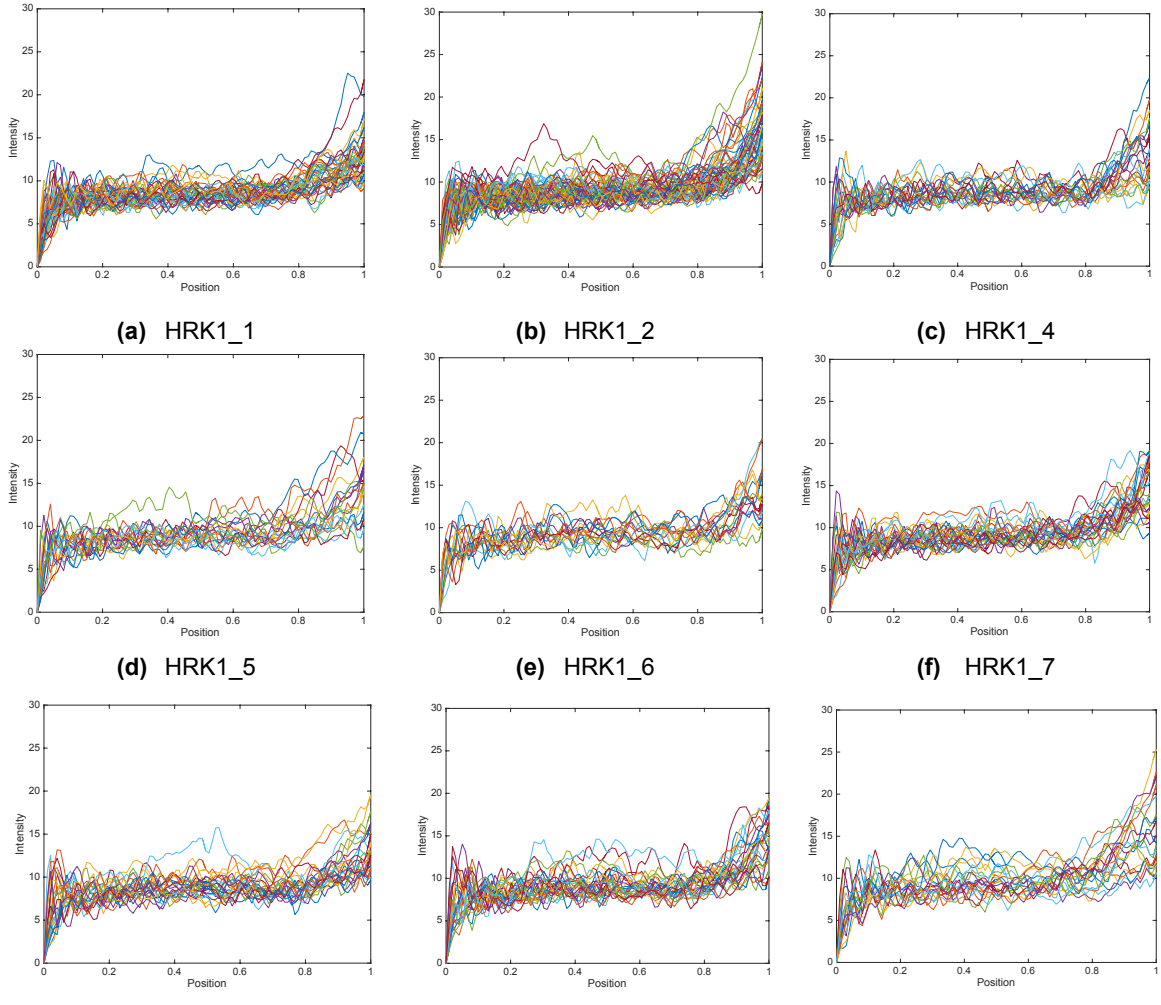

(a) HRK1_1 **(b)** HRK1_2 **(c)** HRK1_4

(d) HRK1_5 **(e)** HRK1_6 **(f)** HRK1_7

(g) HRK1_8 **(h)** HRK1_9 **(i)** HRK1_10

Figure A.66 – Standard Deviation Profiles for all replicas of *HRK1* strain after 0 hours in incubation.

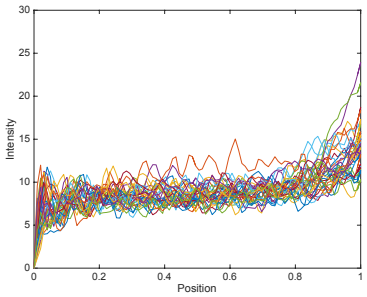

(a) WT_1

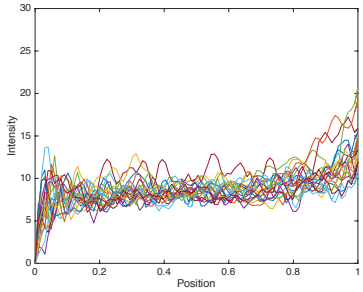

(b) WT_2

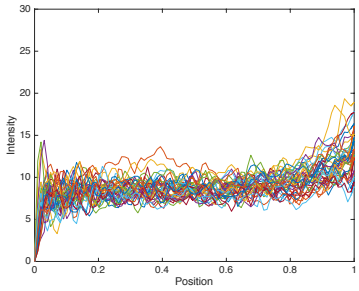

(c) WT_3

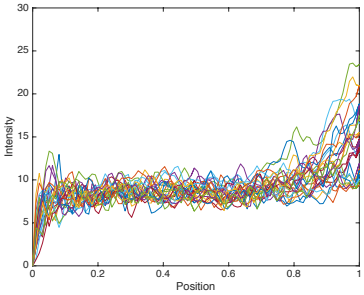

(d) WT_4

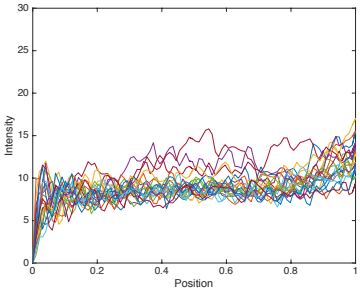

(e) WT_5

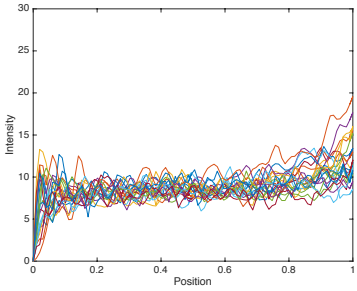

(f) WT_6

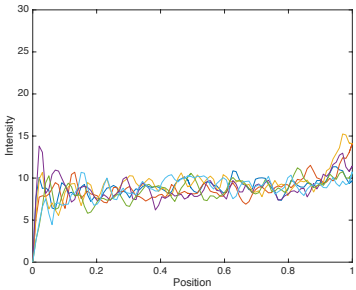

(g) WT_8

Figure A.67 – Standard Deviation Profiles for all replicas of *WT* strain after 1 hour in incubation in absence of acetic acid.

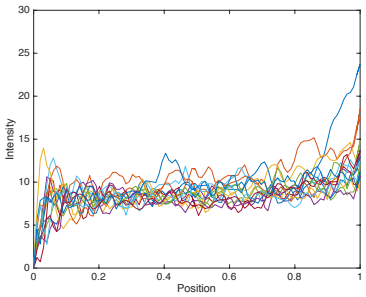

(a) WT_1

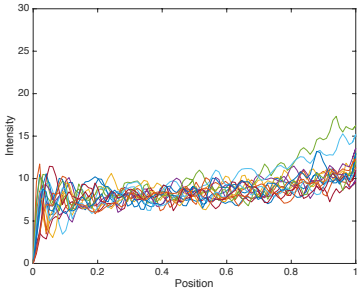

(b) WT_2

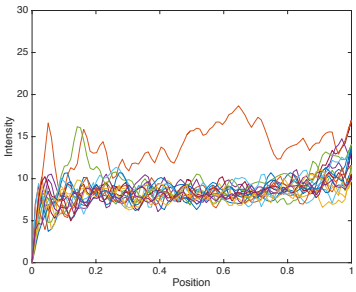

(c) WT_3

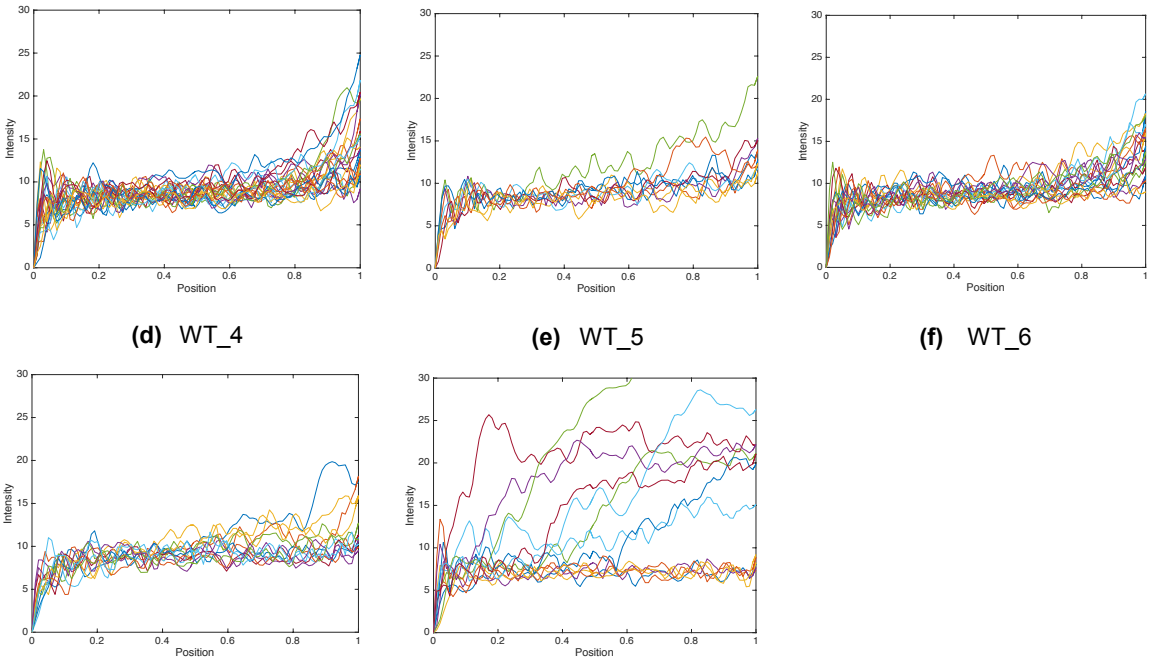

(d) WT_4 **(e)** WT_5 **(f)** WT_6

(g) WT_7 **(h)** WT_8

Figure A.68 – Standard Deviation Profiles for all replicas of *WT* strain after 1 hour in incubation in presence of acetic acid.

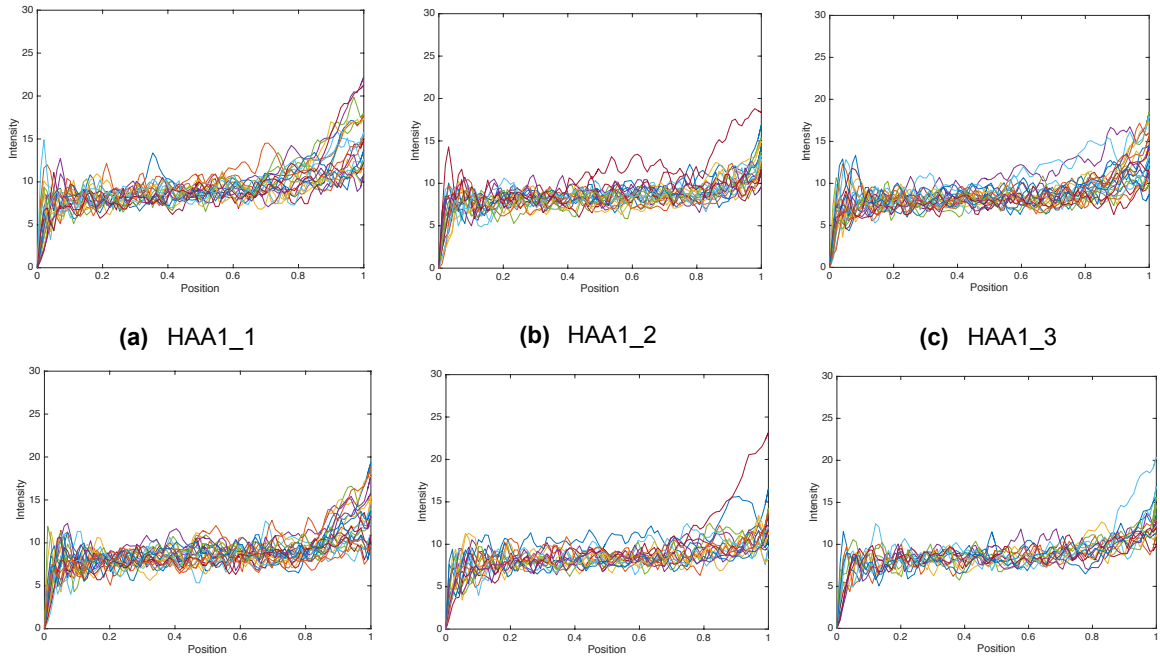

(a) HAA1_1 **(b)** HAA1_2 **(c)** HAA1_3

(d) HAA1_4 **(e)** HAA1_5 **(f)** HAA1_6

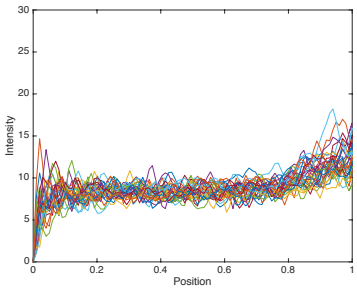

(g) HAA1_8

Figure A.69 – Standard Deviation Profiles for all replicas of *HAA1* strain after 1 hour in incubation in absence of acetic acid.

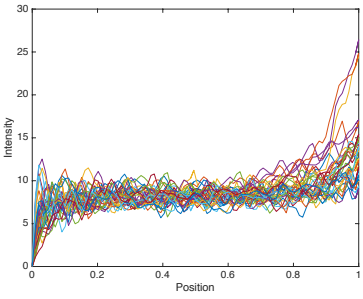

(a) HAA1_1

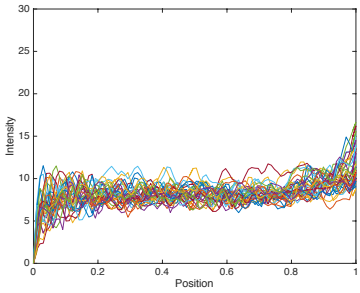

(b) HAA1_2

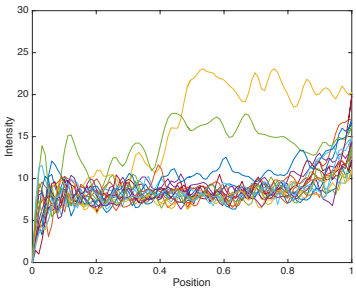

(c) HAA1_3

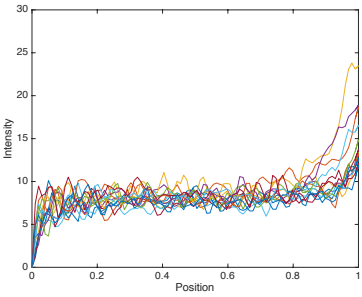

(g) HAA1_4

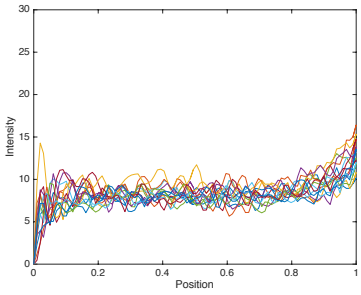

(f) HAA1_5

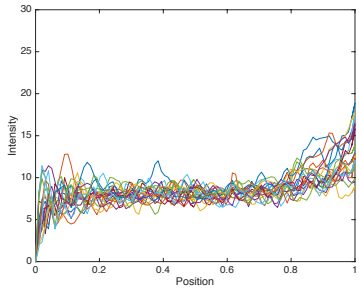

(e) HAA1_6

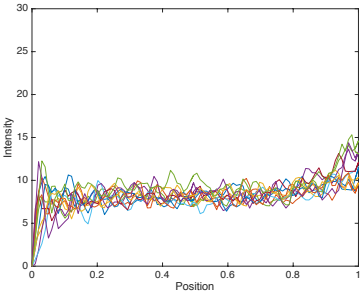

(d) HAA1_8

Figure A.70 – Standard Deviation Profiles for all replicas of *HAA1* strain after 1 hour in incubation in presence of acetic acid.

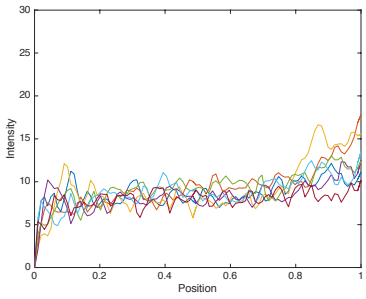

(a) HRK1_1

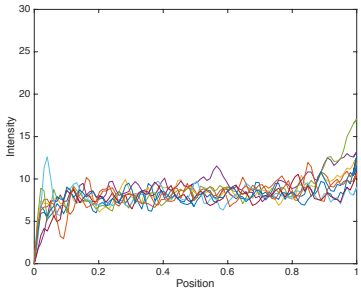

(b) HRK1_2

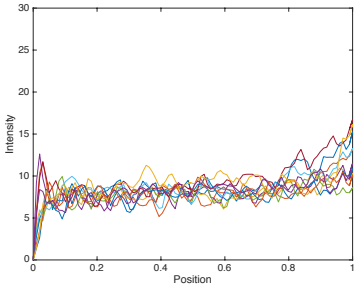

(c) HRK1_3

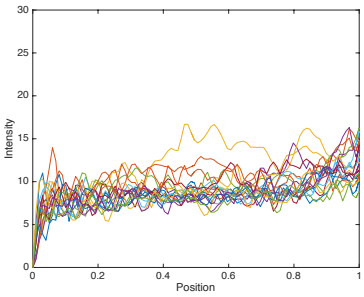

(d) HRK1_4

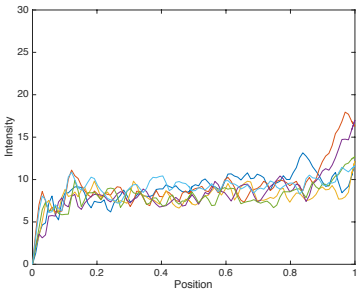

(e) HRK1_5

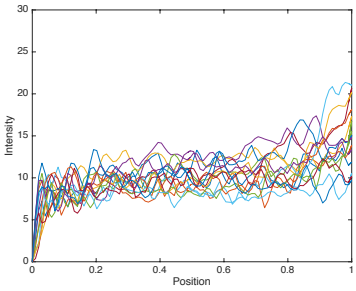

(f) HRK1_6

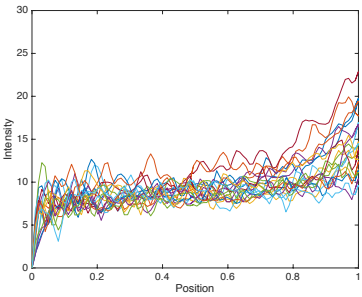

(g) HRK1_8

Figure A.71 – Standard Deviation Profiles for all replicas of *HRK1* strain after 1 hour in incubation in absence of acetic acid.

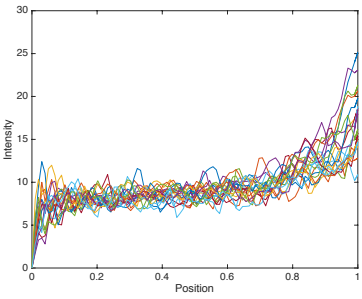

(a) HRK1_1

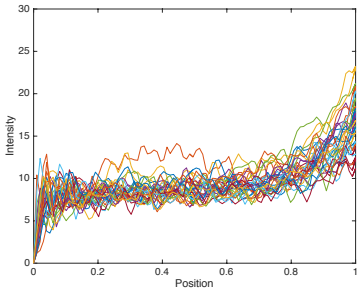

(b) HRK1_2

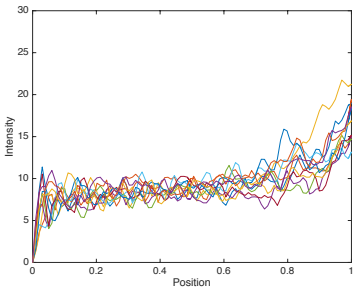

(c) HRK1_3

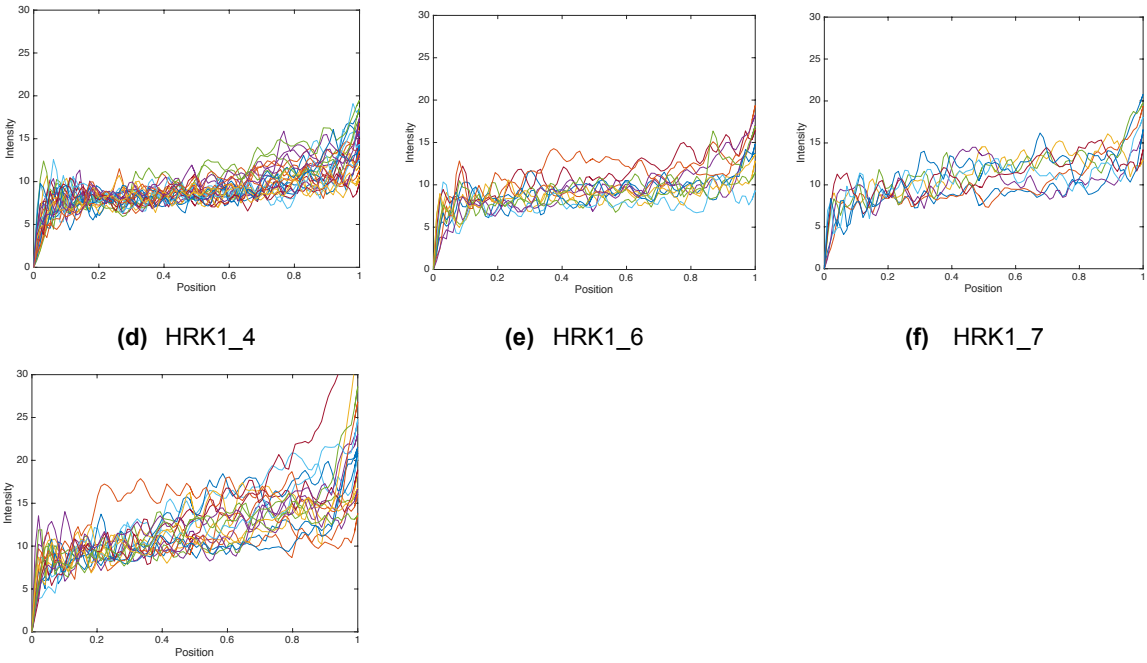

(d) HRK1_4 **(e)** HRK1_6 **(f)** HRK1_7

(g) HRK1_8

Figure A.72 – Standard Deviation Profiles for all replicas of *HRK1* strain after 1 hour in incubation in presence of acetic acid.

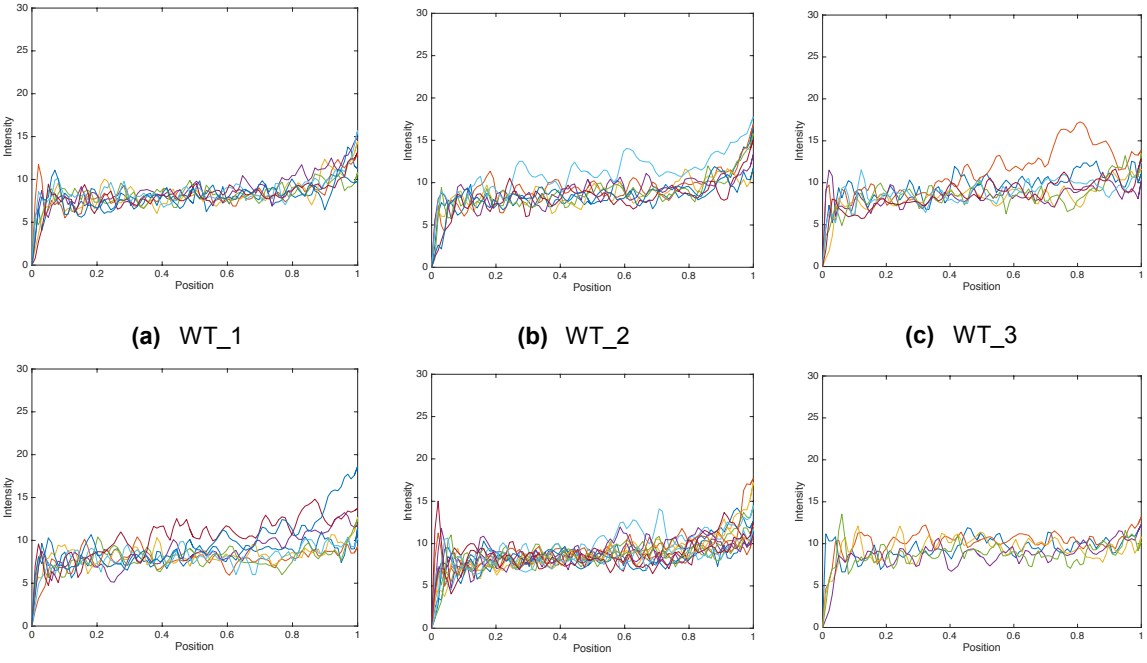

(a) WT_1 **(b)** WT_2 **(c)** WT_3

(d) WT_4 **(e)** WT_5 **(f)** WT_7

Figure A.73 – Standard Deviation Profiles for all replicas of *WT* strain after 2 hour in incubation in absence of acetic acid.

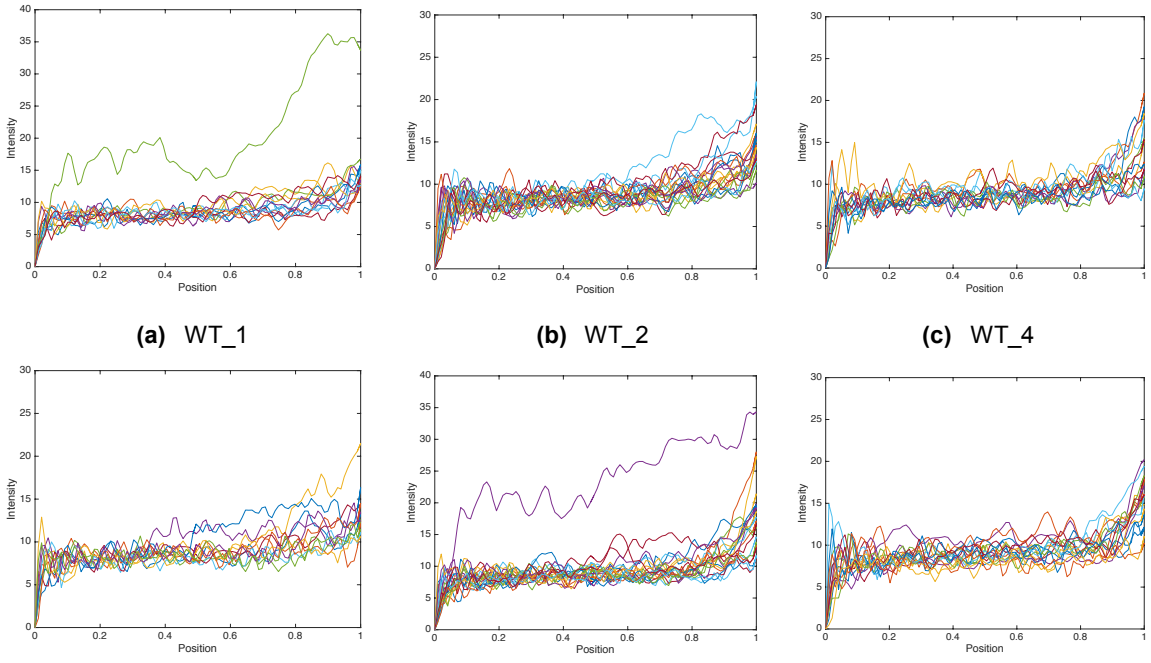

(a) WT_1 **(b)** WT_2 **(c)** WT_4

(d) WT_5 **(e)** WT_6 **(f)** WT_7

Figure A.74 – Standard Deviation Profiles for all replicas of *WT* strain after 2 hour in incubation in presence of acetic acid.

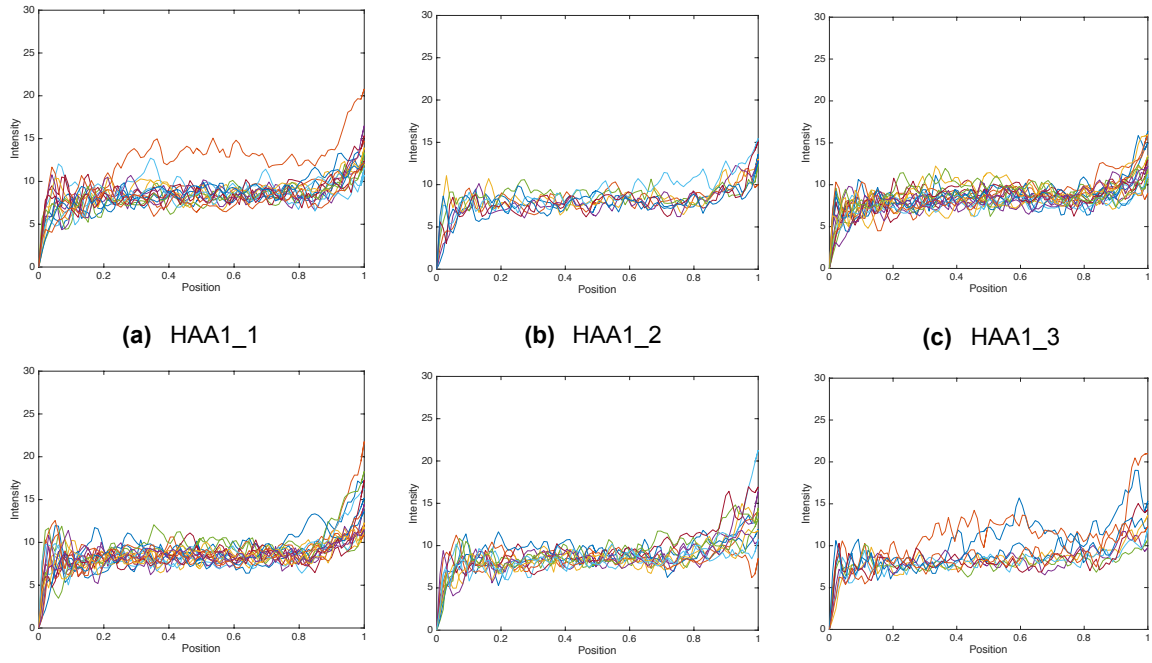

(a) HAA1_1 **(b)** HAA1_2 **(c)** HAA1_3

(d) HAA1_5 **(e)** HAA1_6 **(f)** HAA1_7

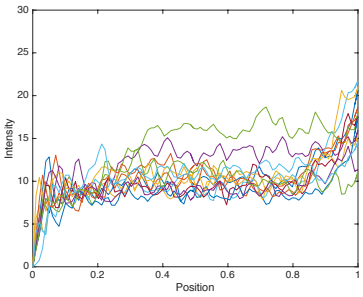

(g) HAA1_7

Figure A.75 – Standard Deviation Profiles for all replicas of *HAA1* strain after 2 hour in incubation in absence of acetic acid.

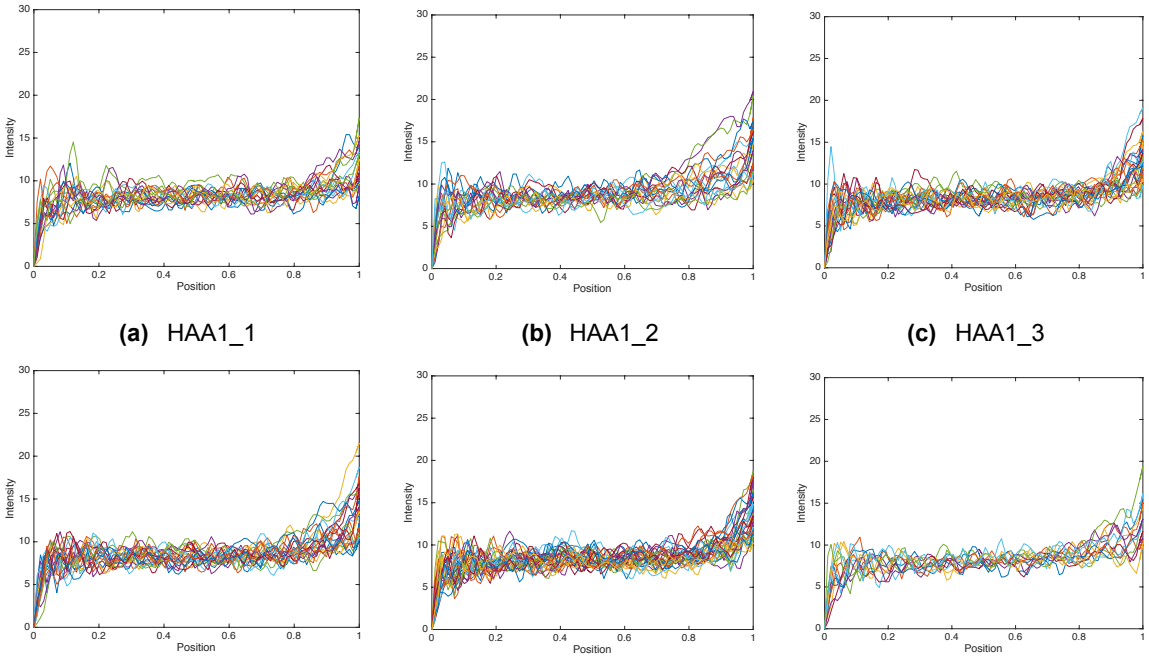

(a) HAA1_1 **(b)** HAA1_2 **(c)** HAA1_3

(d) HAA1_4 **(e)** HAA1_5 **(f)** HAA1_7

Figure A.76 – Standard Deviation Profiles for all replicas of *HAA1* strain after 2 hour in incubation in presence of acetic acid.

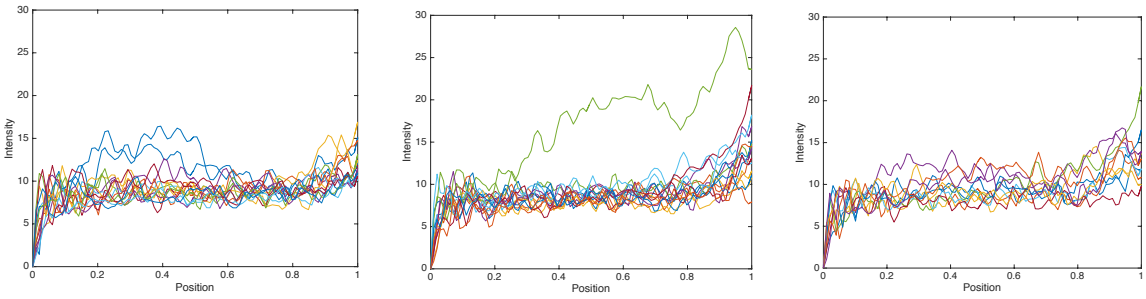

(a) HRK1_1 **(b)** HRK1_2 **(c)** HRK1_3

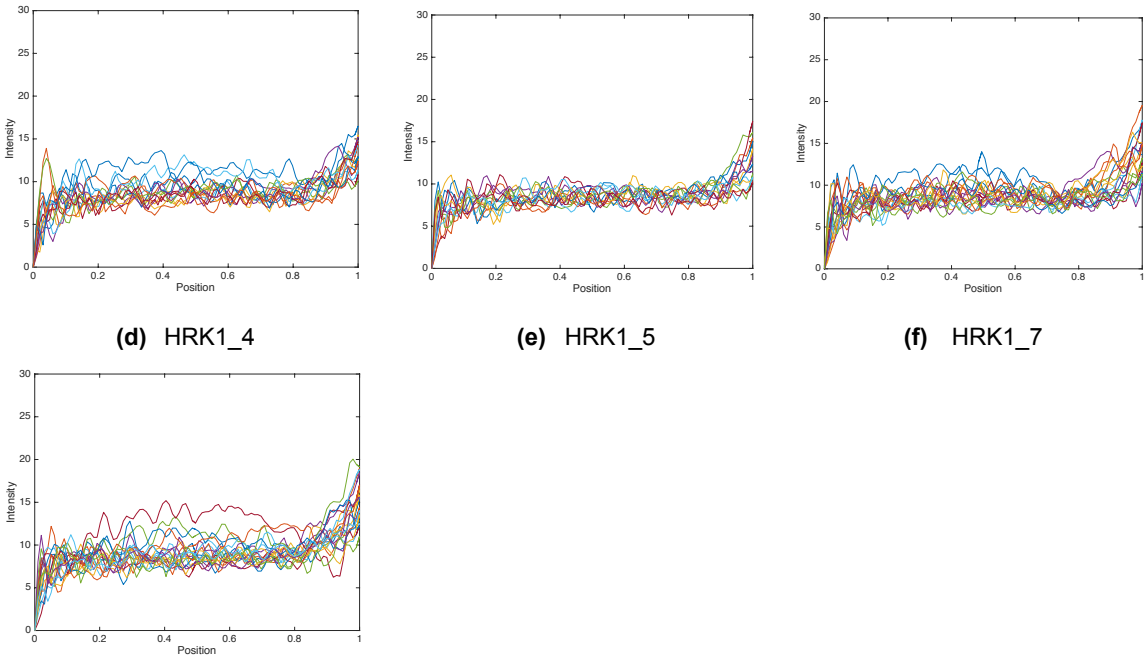

(d) HRK1_4 **(e)** HRK1_5 **(f)** HRK1_7

(g) HRK1_8

Figure A.77 – Standard Deviation Profiles for all replicas of *HRK1* strain after 2 hour in incubation in absence of acetic acid.

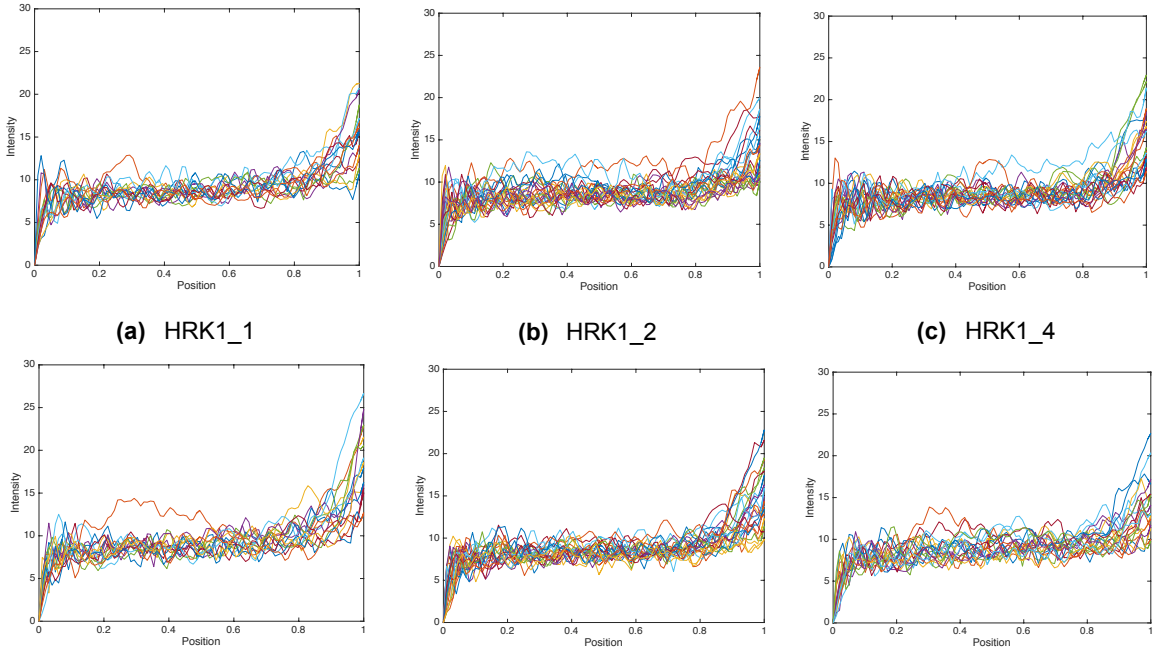

(a) HRK1_1 **(b)** HRK1_2 **(c)** HRK1_4

(d) HRK1_5 **(f)** HRK1_6 **(g)** HRK1_7

Figure A.78 – Standard Deviation Profiles for all replicas of *HRK1* strain after 2 hour in incubation in presence of acetic acid.

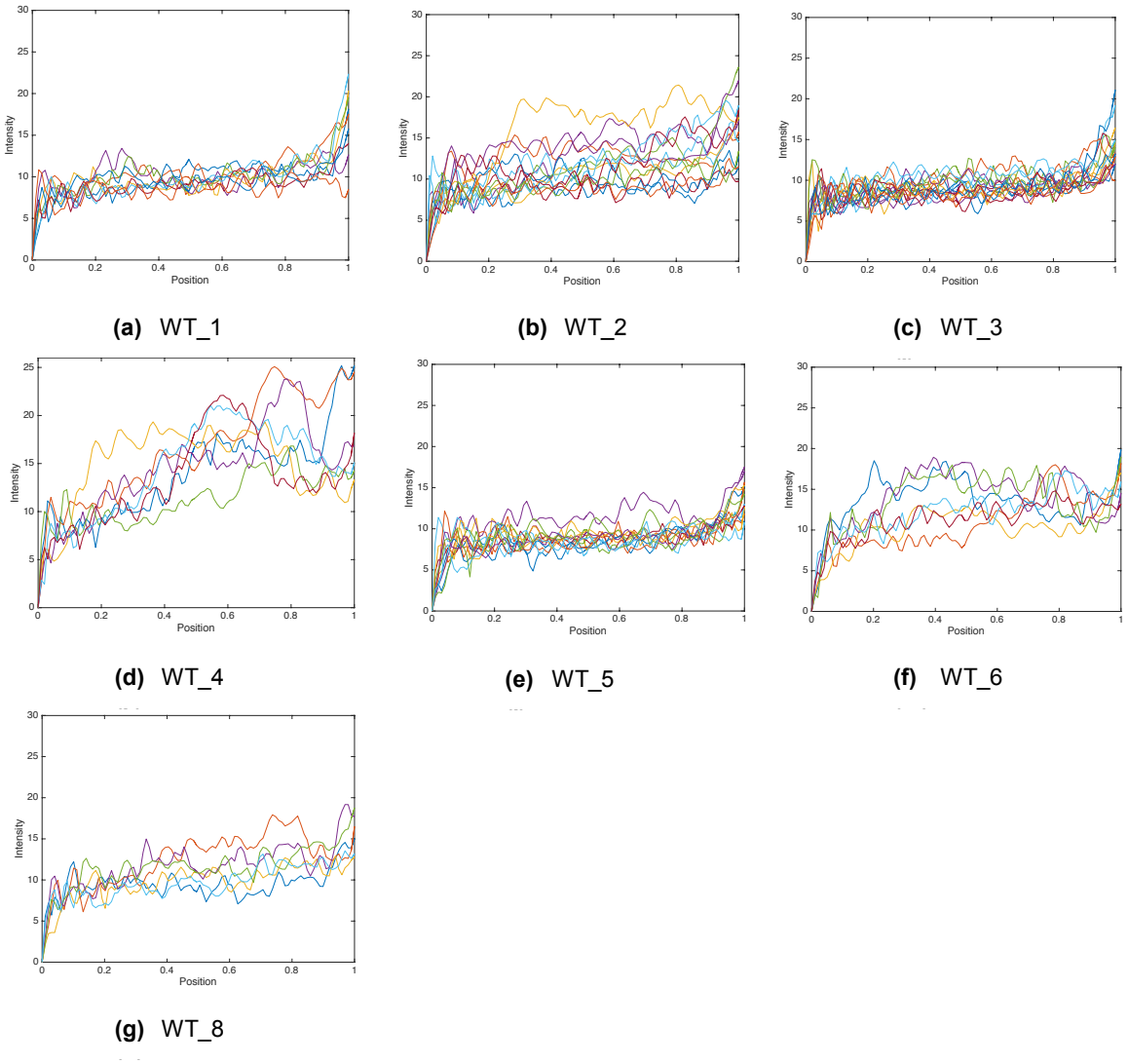

Figure A.79 – Standard Deviation Profiles for all replicas of *WT* strain after 4 hour in incubation in absence of acetic acid.

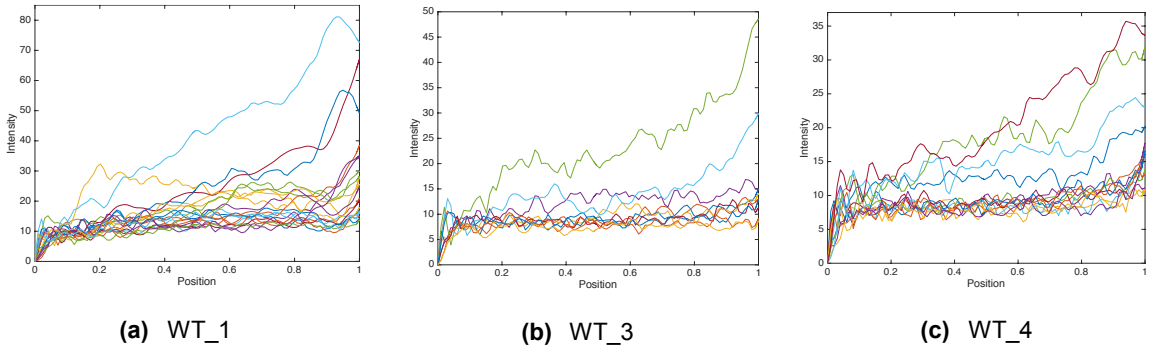

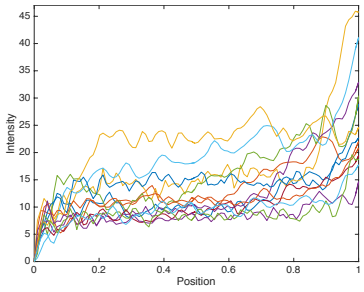

(d) WT_5

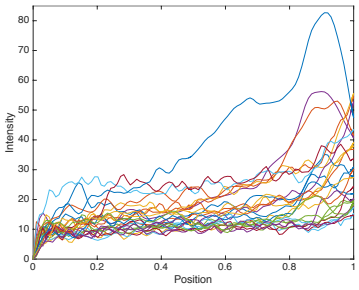

(e) WT_6

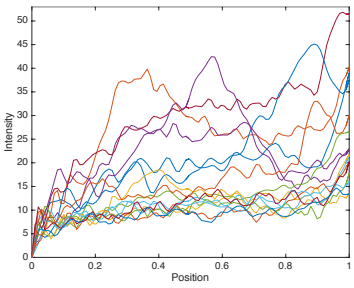

(f) WT_7

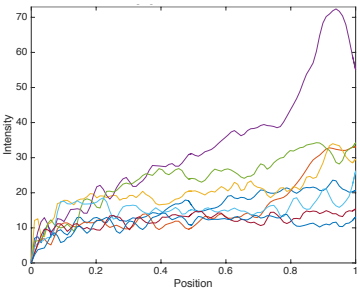

(g) WT_8

Figure A.80 – Standard Deviation Profiles for all replicas of *WT* strain after 4 hour in incubation in presence of acetic acid.

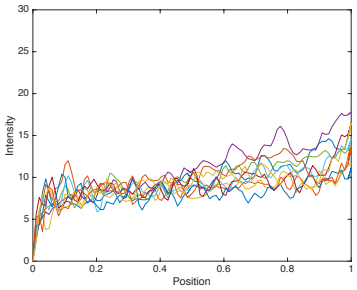

(a) HAA1_2

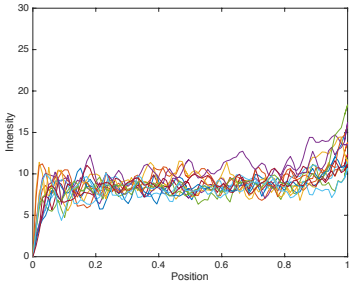

(b) HAA1_3

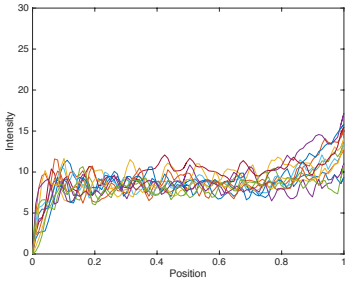

(c) HAA1_4

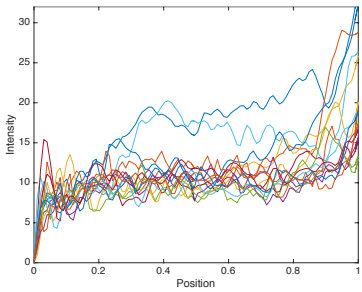

(d) HAA1_5

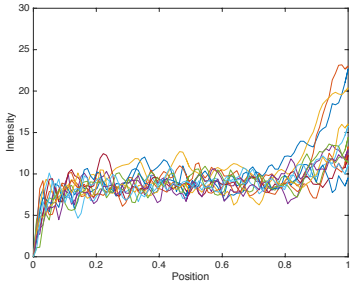

(e) HAA1_6

Figure A.81 – Standard Deviation Profiles for all replicas of *HAA1* strain after 4 hour in incubation in absence of acetic acid.

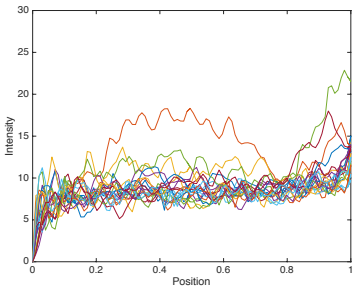

(a) HAA1_1

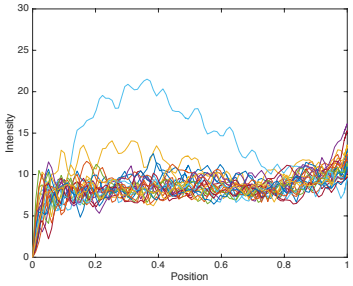

(b) HAA1_2

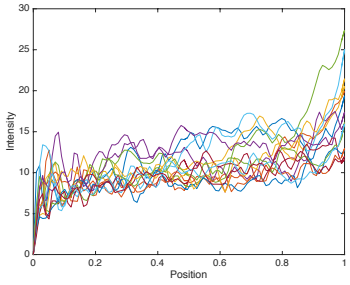

(c) HAA1_4

Figure A.82 – Standard Deviation Profiles for all replicas of *HAA1* strain after 4 hour in incubation in presence of acetic acid.

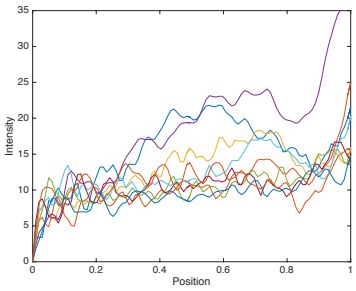

(a) HRK1_2

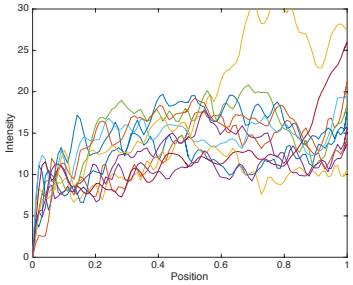

(b) HRK1_3

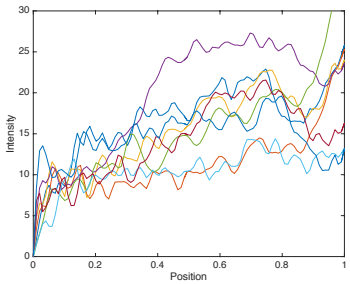

(c) HRK1_4

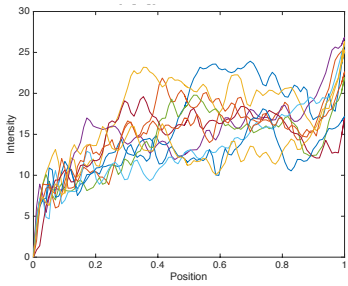

(d) HRK1_6

Figure A.83 – Standard Deviation Profiles for all replicas of *HRK1* strain after 4 hour in incubation in absence of acetic acid.

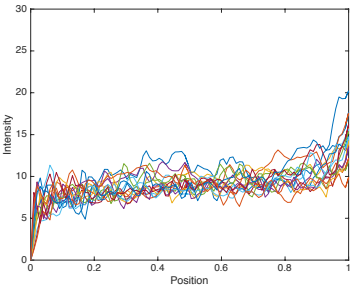

(a) HRK1_1

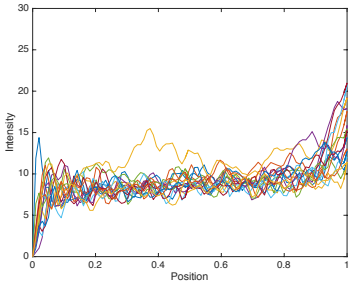

(b) HRK1_2

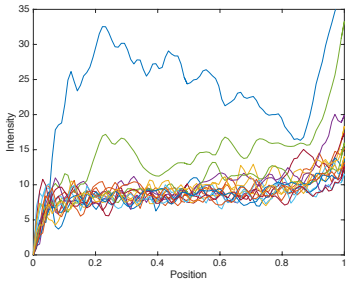

(c) HRK1_3

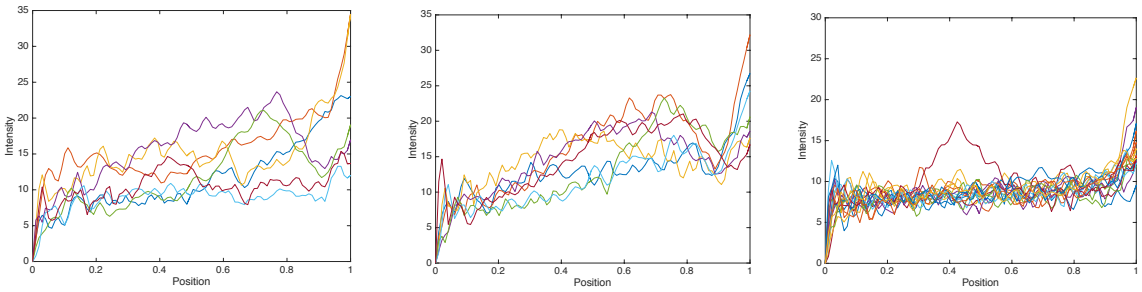

(d) HRK1_4 **(e)** HRK1_5 **(f)** HRK1_7

Figure A.84 – Standard Deviation Profiles for all replicas of *HRK1* strain after 4 hour in incubation in presence of acetic acid.